"*Transition metal modifications on TiO_2: Development of materials for the photocatalytic disinfection of water*"

CAMILO ANDRÉS CASTRO LÓPEZ

UNIVERSIDAD INDUSTRIAL DE SANTANDER
FACULTAD DE INGENIERÍAS FISICOQUÍMICAS
ESCUELA DE INGENIERÍA QUÍMICA
CENTRO DE INVESTIGACIONES EN CATÁLISIS (CICAT)
BUCARAMANGA. 2010

"*Transition metal modifications on TiO_2: Development of materials for the photocatalytic disinfection of water*"

CAMILO ANDRÉS CASTRO LÓPEZ

Tesis presentada como requisito para acceder al título de:
Doctor en Ingeniería Química

Directora:
Prof. Sonia Azucena Giraldo Duarte

Co-director:
Prof. Aristóbulo Centeno Hurtado

UNIVERSIDAD INDUSTRIAL DE SANTANDER
FACULTAD DE INGENIERÍAS FISICOQUÍMICAS
ESCUELA DE INGENIERÍA QUÍMICA
CENTRO DE INVESTIGACIONES EN CATÁLISIS (CICAT)
BUCARAMANGA. 2010

Dedicatoria

Creo firmemente en la gran riqueza de mi país y me sumo a la esperanza colectiva de tener una sociedad armoniosa, en donde la violencia no esté presente en nuestro diario vivir, en donde primen el valor moral y el respeto a la naturaleza.

Este trabajo de tesis es una pequeñísima hoja que cargué sobre mi espalda y llevé al hormiguero a donde otros santandereanos han llevado enormes piedras para la construcción de nuestra sociedad.

Dedico esta tesis a Javier Fernando Bohórquez, a mi madre Luz Marina López, a mi padre Faustino Castro, a mi familia y hermanos. Ustedes siempre han sido luz en mi camino.

Agradecimientos

No habría sido posible culminar esta tesis doctoral sin el financiamiento del Departamento administrativo de ciencia, tecnología e innovación de Colombia (COLCIENCIAS), de la UIS y de la Escuela Politécnica Federal de Lausanne, Suiza, (EPFL).

Expreso mis profundos agradecimientos a los profesores Sonia Giraldo y Aristóbulo Centeno quienes fueron siempre constantes en sus enseñanzas y su apoyo.

Por último agradezco a mis compañeros del CICAT, a la profesora Alba Arámbula de la escuela de Bacteriología, a Cesar Pulgarín y a mis compañeros en la EPFL por sus enseñanzas, risas y su valioso apoyo.

CONTENTS

List of Figures

ABSTRACT

TITLE: TRANSITION METAL MODIFICATIONS ON TiO_2; DEVELOPMENT OF MATERIALS FOR THE PHOTOCATALYTIC DISINFECTION OF WATER.*

AUTHOR: Camilo Andrés Castro López**

KEYWORDS: TiO_2, Photocatalytic disinfection, *E. coli*, Singlet oxygen, Hydroxyl radical, Fe, Ag.

Transition metal modifications on TiO_2 have been of research interest to achieve the increase in photoactivity of TiO2. Fe and Ag were chosen to modify the TiO_2 using the hydrothermal synthesis leading to different configurations of the synthesized photocatalysts. Photocatalysts were characterized by means of XRD, XPS, DRS and EPR analyses. Fe modifications revealed an interstitial location of Fe atoms and a possible replacement of Ti atoms in the TiO_2 matrix due to the similar ionic radii of both cationic species Fe^{3+} and Ti^{4+}. On the other hand, Ag was found to be located on the TiO_2 surface as metallic particles partially oxidized. Both metals, Fe and Ag, led to a remarkable increase of the light absorption capacity of visible light irradiation. However, Fe did not enhance the photoactivity under visible while Ag did significantly promote it. Several photooxidation reactions under different irradiation set-ups, such as, Ultraviolet (UV), Vis, and both combined using a solar light simulation system, were used to identify the mechanism of light activation and the role of the modifying metals in the photoactivity of the materials. Phenol degradation, as a hydroxyl radical mediated oxidation, evidenced the promotion of the recombination of the electron-hole pair in Fe-loaded TiO_2 under UV irradiation. However, Fe promoted the photosensitization of the TiO_2 under strict combination of both UV and Vis irradiation increasing its photoactivity towards the degradation of the azo dye Orange II. This suggests an increase in the electron caption capacity by the Fe embedded in the TiO_2. In contrast, Vis irradiation promoted the formation of singlet oxygen and hydroxyl radical in Ag-TiO_2 suspensions by injecting an e^- to the conduction band of TiO_2 due to the resonance of the Ag conduction band electrons with Vis light thus causing an efficient inactivation of *E. coli* in water.

---

* Thesis to obtain the degree of Doctor in Chemical Engineering.

** Faculty of Physical-chemical Engineering, Department of Chemical Engineering. Director: Prof. Sonia A. Giraldo, Ph. D Co-director: Prof Aristóbulo Centeno, Ph. D.

RESUMEN

TÍTULO: MODIFICACIÓN DEL TiO_2 CON METALES DE TRANSICIÓN: DESARROLLO DE MATERIALES PARA LA DESINFECCIÓN FOTOCATALITICA DE AGUA.

AUTOR: Camilo Andrés Castro López

PALABRAS CLAVE: TiO_2, Desinfección Fotocatalítica, *E. coli*, Oxígeno singulete, Radical hidroxilo, Fe, Ag.

Para incrementar la fotoactividad del TiO_2 se ha propuesto la modificación del TiO_2 con metales de transición. Los metales Fe y Ag fueron seleccionados en este trabajo para modificar el TiO_2 lo que conduce a diferentes configuraciones de los materiales sintetizados. Los fotocatalizadores fueron caracterizados con técnicas como XRD, XPS y DRS. Las especies reactivas de oxígeno producidas bajo irradiación Vis fueron detectadas usando EPR. En particular, la modificación con Fe mostraron una ubicación intersticial de los átomos de Fe y un reemplazo de átomos de Ti debido a la similitud de los radios iónicos de los cationes Fe^{3+} y Ti^{4+}. Por otra parte, se encontró la Ag localizada en la superficie como partículas parcialmente oxidadas. Ambos metales, Fe y Ag incrementaron considerablemente la absorción de luz Vis del TiO_2. Sin embargo, el Fe no incrementó la fotoactividad bajo luz Vis mientras que la Ag sí. Se usaron diferentes reacciones de oxidación y sistemas de irradiación como Ultravioleta (UV), Vis, y ambos tipos de luz combinados en una cámara de irradiación solar, para determinar los mecanismos de fotoactivación y el papel de los metales en la fotoactividad. La degradación de fenol, reacción de oxidación mediada por radicales hidroxilo, evidenció la recombinación de par electrón-hueco promovida por la presencia de Fe en el TiO_2 bajo irradiación UV. No obstante, se encontró que el Fe promueve la fotosensibilización del TiO_2 bajo estricta iluminación combinada UV y Vis, lo que incrementa la fotoactividad en la degradación del colorante azo Orange II. Ésto sugiere un incremento en la aceptación de electrones por el TiO_2 debida a la modificación con Fe. En contraste, la irradiación Vis promovió la formación de oxígeno singulete y radical hidroxilo en suspensiones de TiO_2 modificado con Ag irradiado con luz Vis responsables del incremento en la fotoinactivación de *E. coli*.

---

* Tesis para optar al título de Doctor en Ingeniería Química

** Facultad de Ingenierías Fisicoquímicas, Escuela de Ingeniería Química. Director: Prof. Sonia Giraldo, Ph. D. Co-director: Prof. Aristóbulo Centeno, Ph. D.

General Introduction

TiO_2 photocatalysis and its relevance nowadays

Human activities constantly increase the volume of wastewaters with contaminants recalcitrant to conventional degradation treatments. Such a developed world demands the development of powerful, clean, safe and revolutionary technologies for decontamination. Advanced oxidation processes, based on the action of highly oxidizing radicals, may be applied to water decontamination. Among these processes, titanium dioxide (TiO_2) photocatalysis has been extensively studied due to the use of light irradiation in the production of radicals with high oxidation potentials.

Since the discovery of the photoinduced process of the TiO_2 electrode on the electrolysis of water into H_2 and O_2, in the early 70's [1], TiO_2 photocatalysis has become a scientific interest to transform solar energy into useful chemical energy. The photoinduced process originates from the semiconductor band gap (E_g). The E_g in semiconductors is the forbidden energetic distance between the valence band (VB) and the conduction band (CB), in which, electrons are not allowed to be located. When photons have a higher energy than the E_g they are absorbed by the semiconductor and electrons are promoted to the CB, leaving a positive vacancy in the VB known as "hole" (Eq. (1)). The photogenerated electron – hole pair (e^- - h^+) can react with the reaction media and thus be involved in redox reactions.

As in heterogeneous catalysis, heterogeneous photocatalysis follows the 5-step process of chemical engineering [2]: i) transfer of the reactants in the fluid phase, ii) adsorption of the reactants at the surface of the catalyst, iii) reaction in the adsorbed phase, iv) desorption of the final products, and finally, v) removal of the final products into the fluid phase. The only difference resides in step iii, in which, the activation is attributed to light

absorption by the solid. Hence, step iii includes the absorption of photons, the creation of the e^- - h^+ pair and the subsequent charge transfer reactions.

TiO_2 has a forbidden gap of 3.2 eV thus absorbing energy of the near UV spectrum (UV-A ~ 480 nm) to form such e^- - h^+ pair. UV-A corresponds to 3-5% of the solar spectrum. When TiO_2 is irradiated with such energy the separation of the e^- - h^+ occurs (Eq. (1)) together with the reduction of O_2 (Eq. (2)) and the oxidation of H_2O (Eq. (3)) to form the well known reactive oxygen species (ROS), such as, superoxide ($O_2^{\bullet-}$) and hydroxyl radicals ($^{\bullet}OH$).

$$TiO_2 + h\nu(\lambda = 480\ nm) \rightarrow e^- + h^+ \quad (1)$$

$$O_2 + e^- \rightarrow O_2^{\bullet-} \quad (2)$$

$$H_2O + h^+ \rightarrow {}^{\bullet}OH + H^+ \quad (3)$$

Interactions of $O_2^{\bullet-}$ and $^{\bullet}OH$ radicals with the reaction media induce the formation of peroxide radical ($HO_2^{\bullet}$), and a low amount of hydrogen peroxide (H_2O_2); Eqs. (4)-(7).

$$O_2^{\bullet-} + H^+ \rightarrow HO_2^{\bullet-} \quad (4)$$

$$HO_2^{\bullet} + HO_2^{\bullet} \rightarrow H_2O_2 + O_2 \quad (5)$$

$$H_2O_2 + e^-_{CB} \rightarrow {}^{\bullet}OH + OH^- \quad (6)$$

$$H_2O_2 + O_2^{\bullet-} \rightarrow {}^{\bullet}OH + OH^- + O_2 \quad (7)$$

These radicals are useful for the degradation of recalcitrant water contaminants [3-5], and the deactivation of virus [6] and bacteria [7-9].

However, the efficiency of the photocatalytic degradation processes with TiO_2 is low due to the fast recombination of the e^- - h^+ pair [3], in addition to the poor absorption of solar light.

The efficiency of the photocatalytic process was observed by our group in a pilot-plant scale. The use of a compound parabolic collector for the solar photocatalytic degradation of organic azo dyes, with an effective illuminated area of 1 m^2, showed that

decontamination of 15 L of a 20 mg/L solution of the azo dye Orange II takes 120 min of exposure time using a concentration of photocatalyst of 0.25 g/L, under normal sunlight irradiation at noon in Bucaramanga, Colombia, of about 500-600 $W.m^{-2}$ [10]. Commercial TiO_2 (Evonik-Degussa P-25) was used in these experiments due to its well-known high photoactivity. From these results, it is possible to infer using rough calculations, that treating 15 L of a 300 mg/L solution of biorecalcitrant azo dyes, as in industrial wastewaters [11], it would be necessary to increase the irradiation period by more than ten times the time used in our experiments using the same TiO_2 concentration, or, to increase the exposed area in a similar ratio. Higher values would be obtained if calculations are made for real volumes of wastewaters. Such irradiation efficiencies imply irradiation during at least two consecutive days, or the use of enormous areas for exposure increasing costs in decontamination processes. Therefore, it is highly important to increase the activity of TiO_2 based photocatalyst in order to diminish times and areas of exposition to appropriate values for an effective and low cost photocatalytic decontamination process. Hopefully, the increasing amount of related scientific research, and thesis such as this study, could increase knowledge for future possibilities of industrial applications of TiO_2 photocatalysis.

Transition metal modifications on TiO_2; trapping electrons to increase photoactivity

One of the most studied ideas to increase the photoactivity of TiO_2 is doping the semiconductor with transition metals. TiO_2 particles can be simply substitutionally or interstitially doped with different cations forming mixed oxides or a mixture of oxides. The effect of metal ion dopants on the photocatalytic activity is a complex problem. Many controversial results are reported in literature since even the method of doping leads to different morphological and crystalline properties of the photocatalyst. Different methods, such as, Impregnation, coprecipitation, and sol-gel process are used to introduce metals in the TiO_2's structure.

The total induced alteration of the photocatalytic activity by the doping metals is made up from the sum of changes in: light absorption, the interfacial charge transfer rate, and the proximity of the target contaminant with the metal modified TiO_2's surface [3].

Choi *et al.* [12] doped TiO_2 in a systematic study with 21 different metallic ions to increase the optical response to the visible part of the spectrum. Metal ions can induce new energy levels in the TiO_2 electronic structure leading to interband e^- transitions by absorption of light with wavelengths of lower energy as those from the visible range. This absorption should increase the amount of e^- - h^+ separations increasing photoactivity. Among the studied metals by *Choi et al.*; Fe, Mo, Ru, Os, Re, V and Rh increased photoactivity, while Co and Al decreased it. Moreover, Xin *et al.* [13] could increase photoactivity doping with rare earth metals (La, Ce, Er, Pr, Gd, Nd, and Sm), with a special response in the visible region using Gd.

Metal ions (M^{n+}) can act as electron traps by being reduced, Eq. (8). Trapped electrons are expected to be easily transferred to oxygen adsorbed on the surface of the catalyst and the metallic ions to return to the original oxidation state. The prerequisite for an effective dopant involves the possibility of charge releasing and effective transfer to the adsorbed reactant.

$$M^{n+} + e^- \rightarrow M^{(n-1)+} \quad (8)$$

Noble metals have been suggested to act as traps for the photogenerated electron and increase charge transfer. Yu *et al.* [14] proposed that charge transfer dynamics of Ag doped TiO_2 imply the excitation of the TiO_2-CB e^- and its migration to Ag particles where reduction processes can take place. Au and Pt have been also proposed as bridges for electron transfer processes in modified TiO_2 [15-17]. However, it has been also proposed that silver particles, excited under visible light, inject electrons to TiO_2 [18], thus proposing a new mechanism of photoactivation for the metal modified photocatalyst. Excitation of silver particles on the surface of TiO_2 arises from the resonance of the collective oscillations of electrons in the metal CB with the incident

irradiation. This electromagnetic resonance, known as surface plasmon resonance (SPR), allows the migration of e^- to the semiconductor's CB. Such SPR effect has also been observed for Au, Pt and Cu [19, 20].

Therefore, two different mechanisms are accepted in recent literature for activation of the Ag modified TiO_2 photocatalyst. Consequently, there is plenty of work to do aiming to contribute to the conception of mechanisms of light activation of the TiO_2 and photoactivity of the modified TiO_2 with transition metals since, among others unsolved problems related to the surface structure and to the charge carriers, the photoactivation has not been totally understood [3].

Photocatalysts applied to the photocatalytic disinfection of water based on TiO_2 modified with transition metals

One of the important applications of TiO_2 photocatalysis is disinfection. Common processes for disinfection, such as, chlorination, UV irradiation, membrane filtration and ozonification have their advantages and disadvantages due to their costs and generation of collateral hazardous by-products. In particular, ozonification and UV irradiation lack of the residual effect since ozone has a short life-time, and, the UV effect is observed under strict illumination. Moreover, chlorination, as the most common technique for disinfection, presents a well-known residual effect. Nevertheless, it has been observed the generation of by-products from reactions between chlorine and the natural organic matter [21], molecules known as disinfection by-products (DBPs), with a highly harmful potential to human health [22].

TiO_2 photocatalysis is a technique that may contribute to solve such problems. The oxidative attack of ROS may be applied to the inactivation of bacteria and the degradation of DBPs. The effect of such attack generates disruption in the microorganisms' outer membrane [23] leading to cell death by lysis [24] and the total mineralization of the constituting components [25]. However, the described

disadvantages of TiO_2 are also applied in the photocatalytic disinfection of water since production of oxidative radicals does not vary with the application of the material.

One of the most studied topics in photocatytic disinfection kinetics is the modification of TiO_2 using metallic ions. Several metals, such as, Ag, Pd, Fe, Cu, and Pt have been inserted in TiO_2 to enhance photodisinfection activity [26-30]. Among them, silver has been of research interest due to its well-know bacteriostatic activity [31] which complements the photodisinfection effect of the Ag modified TiO_2 (Ag-TiO_2). Such bacteriostatic activity has also been observed using Cu [32] and Au [33].

Metallic silver nanoparticles in TiO_2 surface present the surface plasmon resonance effect under visible light irradiation enhancing the photodisinfection activity [28]. In addition, the Ag-TiO_2 antimicrobial photoactivity was found to depend on the microbial strain, the Ag content and the Ag reducing agent used in the synthesis of the material [34]. Moreover, it has been observed that Ag increases the adhesion of the photocatalyst to the bacteria reducing the interaction of the microorganism with the reaction media for metabolism processes [35]. However, the underlying mechanisms of light activation and photoactivity are topics of current discussion in literature.

Therefore, in the chemical engineering context, the photocatalytic disinfection process may be altered by the metal modifications of TiO_2 in two ways: i) the surface interaction bacteria-photocatalyst, and, ii) the charge transfer reactions for the production of the oxidative species.

The aims, methodology and scope of this study

As previously observed in this introduction, it is remarkably important to increase the production of ROS in TiO_2 irradiation for photocatalytic water disinfection. To accomplish the purpose it is necessary to widen the spectral response of TiO_2 into the visible part of the solar spectrum, which corresponds to 50% of the total irradiation. The chosen route in this study, to achieve an increase in the ROS production and the response in the visible spectra, was the modification of TiO_2 using transition metals: Fe y Ag, inserted during the synthesis process.

Escherichia coli was chosen as a representative contaminant of the microbial pollution of water. However, following the evolution of the concentration of bacteria, by standard plate counting, considerably takes more time than analysis of conventional photodegradation processes due to preparation of the required materials, incubation of the reaction samples and sterilization and disposal of the residues. Thus, in order to get faster results to analyze photoactivity of the materials it was used the photodegradation of different model contaminants, such as, dichloroacetic acid, phenol and the organic azo dye Orange II (Or-II).

Photocatalytic tests were made under different irradiation set-ups: ultraviolet irradiation (UV) was used to evaluate the effect on photoactivity of the generation of the e^- - h^+ pair. Visible light irradiation (Vis) was used to follow possible activation of the materials by electron transitions with light of lower energy levels due to the change in the synthesis processes and the insertion of Fe and Ag. In addition, a combination of UV and Vis irradiations was used in some cases, in a solar light simulation chamber, to study the efficiency of the materials under solar light irradiation.

Some preliminary results, using modified TiO_2 with a series of transition metals in SODIS[1] type systems (not shown here, but part of them available for lecture [36][2]), led to choose Fe-TiO_2 and Ag-TiO_2 between a series of photocatalysts. However, to achieve a significant increase in photoactivity it was necessary to study different methods of synthesis of the TiO_2, and subsequently choose among them a suitable process for insertion of the metal into the TiO_2's matrix.

Seeking this, different methods of wet synthesis of the TiO_2 were compared aiming to identify a suitable synthesis route of the photocatalyst. These results are discussed in chapter 1. The effect of different synthesis variables on the photoactivity and characteristics of the material, such as, the light absorption, the crystalline structure and the textural properties were studied. This chapter additionally presents the study of two different synthesis methods used to insert Fe in the TiO_2's structure. The discussion of the results showed that the hydrothermal synthesis is a suitable route to modify TiO_2 with transition metals. Furthermore, it was possible to distinguish a surface oxidation mode of the photocatalysts synthesized by the hydrothermal method.

Once identified an appropriate synthesis route, it was necessary to go further in analysis of the spectral response of the Fe-TiO_2 material, its characteristics, the main species enrolled in photoactivity and the new mechanisms of light activation and photoactivity towards Or-II photodegradation under strict simultaneous irradiation of UV and Vis irradiation, as described in chapter 2.

Chapter 3 presents a rigorous study of the photoactivity of the TiO_2 modified with Ag towards *E. coli* inactivation. This chapter includes, the identification of the Ag species involved in the photoinactivation of the material, as well as, the reactive oxygen species formed during visible light irradiation of the Ag-TiO_2 suspension. Moreover, it was possible to discuss the bactericidal activity of Ag ions under dark, and the regeneration

[1] SODIS: Solar Disinfection of water in PET bottles.
[2] doi:10.1612/inf.tecnol.4133it.08

of the photocatalyst due to reductive post-irradiation processes attributed to the dark contact with *E. coli*.

Finally, chapter 4 presents a review of the effects of the modifications of TiO_2, using Fe and Ag, on the TiO_2 light absorption and photoactivity features. Thus, it was possible to discuss the changes in spectral responses due to metal insertions in semiconductors. As a final point, some important parameters for photocatalyst engineering towards the photocatalytic inactivation of *E. coli* in water are discussed leading to the general conclusions of this thesis.

References

[1] A. Fujishima, K. Honda, *Electrochemical photolysis of water at a semiconductor electrode*, Nature, 238 (1972) 37-38.

[2] J.M. Herrman, *Photocatalysis fundamentals revisited to avoid several misconceptions*, Appl. Catal. B: Env., 99 (2010) 461-468.

[3] O. Carp, C.L. Huisman, A. Reller, *Photoinduced reactivity of titanium dioxide*, Prog. Solid State Chem., 32 (2004) 33-177.

[4] D.M. Blake, *Bibliography of work on the heterogeneous photocatalytic removal of hazardous compounds from water and air*, National renewable Energy Laboratory, Colorado, 2001.

[5] J.M. Herrmann, *Destrucción de contaminantes orgánicos por fotocatálisis heterogénea*, in Solar Safe Water, M. Blesa, J. Blanco, Eds., Escuela de Posgrados UNSAM, Buenos Aires, 2005.

[6] L. Zan, W. Fa, T. Peng, Z. Gong, *Photocatalysis effect of nanometer TiO_2 and TiO_2-coated ceramic plate on Hepatitis B*, J. Photochem. Photobiol., B: Biol. 86 (2007) 165-169.

[7] D. Gumy, C. Morais, P. Bowen, C. Pulgarín, S. Giraldo, R. Hajdu, J. Kiwi, *Catalytic activity of commercial TiO_2 powders for the abatement of the bacteria (E. coli) under*

solar simulated light: Influence of the isoelectric point, Appl. Catal. B: Env., 63 (2006) 76-84.

[8] A.G. Rincón, C. Pulgarin*, Photocatalytic inactivation of E. Coli: effect of (continous-intermittent) light intensity and of (suspended-fixed) TiO_2 concentration*, Appl. Catal. B: Env., 44 (2003) 263-284.

[9] P. Amézaga, G.V. Nevárez, E. Orrantia, M. Miki, *Photoinduced bactericidal activity against Pseudomonas aeruginosa by TiO_2 based thin films*, FEMS Microbiol. Lett., 211 (2002) 183-188.

[10] C. Gutiérrez, L. Robles, *Utilización de un colector parabólico compuesto CPC para la purificación de agua*, Ingeniería Química, UIS, Bucaramanga, 2009. Trabajo de grado.

[11] L.F. Garcés, G.A. Peñuela, *Tratamiento de aguas residuales de la industria textil por medio de la fotocatálisis*, P+L, 2 (2007) 18-29.

[12] W.Y. Choi, A. Termin, M.R. Hoffmann, *The role of metal ion dopants in quantum-sized TiO_2: correlation between photoreactivity and charge carrier recombination dynamics*, J. Phys. Chem., 98 (1994) 13669-13679.

[13] A.W. Xu, Y. Gao, H.Q. Liu, *The preparation characterization and their photocatalytic activities of rare-earth doped TiO_2 nanoparticles*, J. Catal., 207 (2002) 151-157.

[14] J. Yu, J. Xiong, B. Cheng, L. Liu, *Fabrication and characterization of Ag/TiO_2 multiphase nanocomposite thin films with enhanced photocatalytic activity*, Appl. Catal. B: Env., 60 (2005) 211-221.

[15] H.W. Chen, Y. Ku, Y.L. Kuo, *Effect of Pt/TiO_2 characteristics on temporal behavior of o-cresol decomposition by visible ligth-induced photocatalysis*, Water Res., 41 (2007) 2069-2078.

[16] L.H. Huang, C. Sun, Y.L. Liu, *Pt/N-codoped TiO_2 nanotubes and its photocatalytic activity under visible light*, Appl. Surf. Sci., 253 (2007) 7029-7035.

[17] Z. Du, C. Feng, Q. Li, Y. Zhao, X. Tai, *Photodegradation of NPE-10 surfactant by Au-doped nano-TiO_2*, Coll. Surf. A: Phys. Eng. Aspects, 135 (2008) 254-258.

[18] K. Naoi, Y. Ohko, T. Tatsuma, *TiO_2 Films loaded with silver nanoparticles: Control of multicolor photochromic behavior*, J. Am. Chem. Soc., 126 (2004) 3664-3668.

[19] T.A. El-Brolossy, T. Abdallah, M.B. Mohamed, S. Abdallah, K. Easawi, S. Negm, H. Talaat, *Shape and size dependence of the surface plasmon resonance of gold nanoparticles studied by photoacoustic technique*, Eur. Phys. J. Special Topics, 153 (2008) 361-364.

[20] R.C. Johnson, J. Li, T. Hupp, G.C. Schatz, *Hyper-Rayleigh scattering studies of silver, copper, and platinum nanoparticle suspensions*, Chem. Phys. Lett., 356 (2002) 534-540.

[21] W.W. Bunn, B.B. Haas, E.R. Deane, R.D. Kleopfer, *Formation of trihalomethanes by chlorination of surface water*, Environ. Lett., 10 (1975) 205-213.

[22] G.S. Wang, Y.C. Deng, T.F. Lin, *Cancer risk assessment from trihalomethanes in drinking water*, Sci. Total Environ., 387 (2007) 86-95.

[23] C.V. Nadtochenko, A.G. Rincón, S.E. Stanca, J. Kiwi, *Dynamics of E. coli cell wall membrane peroxidation during TiO_2 photocatalysis studied bye ATR-FTIR sepctroscopy and AFM microscopy*, J. Photochem. Photobiol. A: Chem., 169 (2005) 131-137.

[24] C. Ogino, M.F. Dadjour, K. Takaki, N. Shimizu, *Enhancement of sonocatalytic cell lysis of Escherichia coli in the presence of TiO_2*, Biochem. Eng. J., 32 (2006) 100-105.

[25] K. Sunada, T. Watanabe, K. Hashimoto, *Studies on photokilling of bacteria on TiO_2 thin film*, J. Photochem. Photobiol. A: Chem., 156 (2003) 227-233

[26] C.C. Trapalis, P. Keivanidis, G. Kordas, M. Zaharescu, M. Crisan, A. Szatnayi, M. Gartner, *TiO_2 (Fe^{3+}) nanostructured thin films with antibacterial properties*, Thin Solid Films, 433 (2003) 186-190.

[27] M. Pratap, A. Venugopal, M. Subrahmanyam, *Hydroxyapatite-supported Ag-TiO_2 as Escherichia coli disinfection photocatalyst*, Water Res., 41 (2007) 379-386.

[28] O. Akhavan, E. Gadheri, *Self-accumulated Ag nanoparticles on mesoporous TiO_2 thin film with high bactericidal activities*, Surf. Coat. Technol., 204 (2010) 3676-3683.

[29] E. Arkan, U. Bakir, G. Karakas, *Photocatalytic microbial inactivation over Pd doped SnO_2 and TiO_2 thin films*, J. Photochem. Photobiol. A: Chem, 184 (2006) 313-321.

[30] C. Karunakaran, G. Abiramasundari, P. Gomathisankar, G. Manikandan, V. Anandi, *Cu-doped TiO_2 nanoparticles for photocatalytic disinfection of bacteria under visible light*, J. Colloid Interface Sci., 352 (2010) 68-74.

[31] D.R. Monteiro, L.F. Gorup, A.S. Takamiya, A.C. Ruvollo, E. Rodrigues, D. Barros, *The growing interest of materials that prevent microbial adhesion: antimicrobial effect of medical devices containing silver*, Int. J. Antimicrob. Agents, 34 (2009) 103-110.

[32] C. Castro, R. Sanjines, C. Pulgarin, P. Osorio, S.A. Giraldo, J. Kiwi, *Structure-reactvity relations for DC-magnetron sputtered Cu-layers during E. coli inactivation in the dark and under light*, J. Photochem. Photobiol. A: Chem., 2010, doi: 10.1016/j.jphotochem.2010.06.030.

[33] Y.H. Gao, N.C. Zhang, Y.W. Zhong, H.H. Cai, Y.L. Liu, *Preparation and characterization of antibacterial Au/C core-shell composite*, Appl. Surf. Sci., 256 (2010) 6580-6585.

[34] A. Zielinska, E. Kowalska, J.W. Sobczak, I. Lacka, M. Gazda, B. Ohtani, J. Hupka, A. Zaleska, *Silver-doped TiO_2 prepared by microemulsion method: Surface properties, bio- and photoactivity*, Sep. Purif. Technol., 72 (2010) 309-318.

[35] M.R. Elahifrad, S. Rahimnejad, S. Haghighi, M.R. Gholami, *Apatite-coated Ag/AgBr/TiO_2 Visible-light photocatalyst for destruction of bacteria*, J. Am. Chem. Soc., 129 (2007) 9552-9553.

[36] C. A. Castro, A. Arámbula, A. Centeno, S.A. Giraldo, *Evaluación de la degradación heliofotocatalítica de E. coli con TiO_2 modificado en sistemas tipo SODIS*, Inf. Tecnol., 20 (2009) 29-36.

1. Effect of the synthesis variables on photoactivity and features of TiO_2 and Fe modified TiO_2 photocatalysts

Abstract

Photoactivity of TiO_2 based materials was analyzed using different synthesis methods to obtain the photocatalysts particles. TiO_2 and Fe-TiO_2 photocatalysts were synthesized by hydrolysis of titanium butoxide. Sol-gel process leads to less active Fe-TiO_2 particles than bare TiO_2; meanwhile, the hydrothermal synthesis of the Fe-TiO_2 seems to promote the stabilization of Fe^{3+} in the TiO_2 structure promoting the photooxidation activity of TiO_2 towards the degradation of azo dyes and the inactivation of *Escherichia coli* (*E. coli*) in water. Photocatalysts were characterized by X-ray diffraction (XRD), diffuse reflectance spectrophotometry (DRS), and N_2 adsorption-desorption. The TiO_2 synthesized by the hydrothermal synthesis (HT) reaches the TiO_2 Degussa P-25 photooxidation activity towards the degradation of Orange II (Or-II). Furthermore, Fe loading of TiO_2 in HT synthesis improves its photoactivity. The comparative performance of the photocatalysts towards the direct photooxidation of iodide, the photocatalytic degradation of Or-II and the photocatalytic disinfection of water infected with *E. coli* suggested different mechanisms of oxidation; a surface-hole-oxidation mode for HT particles and a homogeneous-phase-oxidation mode promoted by $^{\bullet}OH$ radicals produced in the TiO_2 P-25 surface.

1.1. Introduction

The photocatalytic oxidation is a recently proposed route for the production of drinking water, especially in zones with high solar irradiations and lack of efficient water supplies. In photocatalysis, the capacity of an UV-A activated photocatalyst, such as TiO_2, to produce highly oxidizing radicals is used to efficiently destroy a wide variety of organic molecules [1, 2] and deactivate bacteria [3, 4]. These radicals are produced by redox reactions of water and dissolved oxygen with the UV-A photogenerated charged species of TiO_2: the promoted conduction band electron (e^-) and its positive counterpart, the valence band hole (h^+). Among the oxidant radicals produced in TiO_2 illumination, the hydroxyl radical ($^{\bullet}OH$) is the responsible, in most of the cases, of the complete mineralization of the target molecule [5], as well as the complete inactivation of different bacteria [3].

Sol-gel method has been widely used for the synthesis of TiO_2 [2, 6] because it allows to tailor the conditions of synthesis in order to produce crystalline and highly specific surface area particles [6]. Sol-gel involves the hydrolysis of a Ti alcoxide precursor with water in the presence of an alcohol and a subsequent condensation where the Ti-O-Ti network is formed. Therefore, the condensation conducts to the formation of a gel, which is dried at low temperatures. Finally, powders are calcined at 400 – 600 ℃ to release organic residuals from the TiO_2 matrix. More recently, significant variations to the sol-gel process have been adopted to synthesize the TiO_2, such as the replacement of the calcination step by hydrothermal treatments under pressure. This pressure treatment promotes the formation of TiO_2 particles with high specific surface area, low grain size, and additionally a high cristallinity of the anatase phase [7].

Efficiency of TiO_2 is decreased when the UV-A promoted charged species recombinate, and, thus, the possibility to produce $^{\bullet}OH$ is diminished. Transition metals have been proposed as dopants capable of enhancing the photoactivity of the TiO_2 by trapping the e^-- h^+ pair [8, 9]. In particular, iron doping increases the $^{\bullet}OH$ production by its capacity to

act as h^+ traps, which reduces the recombination [9-14], and thus, the chance for the e^--h^+ to form oxidant radicals is improved. In order to modify the TiO_2 with Fe and achieve an increase in the photocatalytic activity, some synthesis methods in liquid phase have been used, such as sol-gel [11, 14, 15] and hydrothermal synthesis [12, 13, 16]. Nevertheless, when Fe is oxidized to Fe_2O_3 and embedded in the TiO_2 matrix, its photoactivity decreases because this oxide acts as a recombination center of the photogenerated charges [11], and thus, reducing photoactivity. Moreover, new insights recently found propose that interactions between Ln^{2+} doped TiO_2 or Fe doped TiO_2 and the target molecule may increase the photooxidation, such as, the photosensitization of TiO_2 by organic dye molecules [17], and the photo-leaching of Fe from the TiO_2 matrix [18]. Both processes are not related to the mechanism of recombination but increase the photooxidation of the target.

In addition, the coexistence of phases in TiO_2 has been suggested to reduce the recombination of the e^-- h^+ pair [19, 20]. Anatase phase, with a band gap (E_g) of 3.2 eV, is known as the most photoactive phase in TiO_2. However, an anatase to rutile phase (E_g of 3.0 eV) ratio of 3:1 shows the best photocatalytic activity of the commercial TiO_2 Degussa P-25 [19]. Such a difference in the E_g of the anatase and rutile phases serves as an energy gradient, which conducts the e^- from rutile to anatase, thus, avoiding the recombination. Similarly, a mixed phase TiO_2, constituted of anatase and brookite phases, has a higher performance towards the degradation of 2-chlorophenol than pure anatase TiO_2 [20]. Then, an increase in photoactivity seems to be correlated to the coexistence of phases anatase and rutile [19] or brookite in TiO_2 [21].

Therefore, the photocatalytic activity of the TiO_2 and Fe modified TiO_2 photocatalyst is hardly dependent on the phase structure and the state of Fe in the oxide matrix.

In this work, TiO_2 photocatalysts modified with Fe^{3+} were prepared using two different synthesis methods, sol-gel and hydrothermal synthesis using titanium butoxide. The physical properties and the photooxidation ability of the Fe doped TiO_2 photocatalysts

are correlated to elucidate the state of Fe in the matrix. The photocatalytic production of $^{\bullet}OH$ radicals was followed by means of the photocatalytic degradation of orange II (Or-II), an organic azo dye recalcitrant to conventional degradation treatments [22], and the deactivation of the *E. coli* strain ATCC 11229 used for disinfectant quality tests [23]. Additionally, the oxidative potential of the photogenerated holes was analyzed towards the direct oxidation of iodide to iodine by the photogenerated h^+ [24].

1.2. Experimental

1.2.1. Synthesis of Fe-TiO_2 photocatalysts

Two methods were chosen to synthesize the Fe-TiO_2 photocatalyst: sol-gel and hydrothermal synthesis. Fe-SG was synthesized by sol-gel synthesis as follows: titanium butoxide (Ti(O-But)$_4$; 97% Aldrich) was added dropwise to isopropanol (Isop-OH; Merck), as co-solvent, in a molar ratio Isop-OH/Ti(O-But)$_4$ = 55. Then, an adequate amount of $Fe(NO_3)_3$ was diluted in water and pH was adjusted to 1.5 with HNO_3 (65%, Merck). Fe aqueous solution was added dropwise to the Ti(O-But)$_4$-Isop-OH solution. The amount of water corresponds to a molar ratio H_2O/Ti(O-But)$_4$ = 1.5. Fe content was adjusted to a nominal molar percentage of 0.1 (%mol). The formed solution was stirred until gel was formed. Then, the stirring was stopped, and the gel was aged for 72 h, and immediately dried at 70℃ for 4 h. The obtained cry stals were grounded in a mortar, and the yellowish powders were calcined at 400℃ for 2 h. Bare TiO_2 sol-gel synthesized, labeled as SG, was obtained as described above without the addition of the Fe salt.

Fe-HT was hydrothermal synthesized by hydrolysis of Ti(O-But)$_4$ in aqueous media. In this case, the Ti(O-But)$_4$ was added dropwise to Isop-OH, as co-solvent, in a volume ratio Isop-OH/Ti(O-But)$_4$ = 10. Then, an adequate amount of $Fe(NO_3)_3$ was diluted in water and pH was adjusted to 1.5 with HNO_3. Then, the Fe aqueous solution was added dropwise to the Ti(O-But)$_4$-Isop-OH solution. The amount of water corresponds to a volume ratio H_2O/Ti(O-But)$_4$ = 25. The Fe content was nominally adjusted to 0.1 %mol.

The latter suspension was hydrothermally treated with water stream in an autoclave at 120℃ and ~ 144 KPa during 3 h. Then, water was extracted by evaporation and continuous stirring at 70℃. Finally, the obtained powders were grounded in a mortar. TiO_2 obtained by hydrothermal synthesis, as described above but with no Fe salt addition, was labeled as HT.

In the HT case, the effect of some synthesis variables on photoactivity was analyzed. Thus, the volumetric ratios: Isop-OH/Ti(O-But)$_4$ and H_2O/Ti(O-But)$_4$ were varied from 10 to 62.5, and, 1 to 5, respectively. In addition, instead of isop-OH linear alcohols, such as, ethanol and methanol were used as solvents.

All photocatalysts were named as Fe-Y, where Y stands for the synthesis route of the Fe-TiO_2 photocatalyst, SG for sol-gel synthesis, and HT for hydrothermal synthesis. TiO_2 P-25 from Evonik, previously known as Degussa, was used for comparison purposes.

1.2.2. Photocatalysts characterization

X-ray diffraction measurements

To analyze the phase structure of the photocatalysts, DRX patterns were collected using a D-Max IIIB Rigaku system at room temperature from angles 2θ of 2 to 70°. The diffractometer was operated at 40 kV and 80 mA with a monochromatic Cu Kα radiation.

Specific surface areas of photocatalyst were determined by the BET method. The N_2 adsorption-desorption isotherms were recorded on a Nova 1300 apparatus of Quantachrome.

Diffusive reflectance spectroscopy

UV-Vis diffusive reflectance spectra (DRS) were recorded on a UV-2401PC Shimadzu spectrophotometer with an ISR 240A integrating sphere accessory. $BaSO_4$ was used as a blank reference. The energy band gap widths of the samples were determined using the Kubelka-Munk phenomenological theory reported elsewhere [25]. The DRS can be

related to the absorbance by the *K/S* (where *K* = absorption and *S* scattering) ratio using the Kubelka-Munk relations ($F(R_\infty)$) (Eq. (1.1)), where the reflectance is noted as *R*. The reflectance is related to the absorption coefficient α and it is proportional to the absorbance *K*.

$$\frac{K}{S} = \frac{(1-R_\infty)^2}{2R_\infty} \equiv F(R_\infty) \qquad (1.1)$$

Where R_∞ is the ratio of the sample's reflectance over that of the $BaSO_4$ reference. The intercept of the major slope with the wavelength axis gives the value of the sample's E_g if transformed to energy data in eV.

1.2.3. Photocatalytic tests

Photocatalytic activity tests were performed in 50 mL borosilicate glass reactors illuminated in an ATLAS *Suntest* CPS+ system with external magnetic stirring. *Suntest* Xenon lamp's spectrum covers wavelengths from 300 to 800 nm, with 7% of the photons in the UV-A region. Irradiation and temperature were controlled at 400 $W.m^{-2}$ and 35℃ respectively.

Photocatalytic degradation of Orange II

The photocatalytic degradation of Or-II was carried out with a 20 ppm Or-II aqueous solution with 0.25 $g.L^{-1}$ of photocatalyst. This suspension was stirred 1 h under darkness prior to illumination. Samples were taken every 15 min for 1 h and centrifuged at 3000 rpm for 15 min. The concentration of Or-II in the supernatant was determined with a HP 8453 UV-Vis spectrophotometer at maximum wavelength absorption, 486 nm. Blank experiments were carried out to determine possible degradation by photolysis. The adsorption equilibrium concentration, reached after 1 h of stirring under darkness, was used as the initial value for the photodegradation efficiency calculations. To follow the degradation the obtained Or-II concentration data is presented as a relative

concentration during testing time: C/C_0, where C stands for the concentration at any given time and Co is the initial concentration.

Photocatalytic disinfection of water with E. coli ATCC 11229

E. coli ATCC 11229 was incubated for 10 h in 100 mL of Luria Bertani growth media (1% wt, Tryptone from Oxoid), 0.5% wt yeast extract from Oxoid, and 1% wt NaCl from Merck) under 120 rpm of stirring at 35 ± 2℃. A 2 m L aliquot was taken from the growth media for centrifugation at 3000 rpm for 15 min. The supernatant was discarded, and cell biomass pellet was washed twice with saline solution (0.85% NaCl); then, the pellet was suspended in sterilized distillated water and added to a 50 mL borosilicate glass reactor for photocatalytic disinfection. The reaction media consists of 50 mL of an *E. coli* cell suspension with 0.25 $g.L^{-1}$ of photocatalyst. Samples were taken from the reaction media every 15 min for 1 h and serially diluted in saline solution. To follow the concentration of survival *E. coli* 10 µL of the dilutions were plated onto plate count agar (Merck) and incubated for 24 h before growth colony counting. *E. coli* concentration data is presented as the average of 3 countings on plates as colony forming units per mL (CFU/mL) from independent experiments. Initial concentration of *E. coli* was adjusted to ~$1x10^7$ $CFU.mL^{-1}$. Blank experiments were carried out to determine any possible bactericidal activity under darkness labeled as dark, and the influence of simulated solar light to cause solar disinfection labeled as the photolysis blank.

Photocatalytic oxidation of iodide

The direct photooxidation of iodide (I^-) by the TiO_2 photogenerated hole (h^+) to produce iodine (I_2), Eq. (1.2) [24], was conducted using a $4.5x10^{-3}$ $mol.L^{-1}$ solution of KI with 0.25 $g.L^{-1}$ of photocatalyst. Samples were taken every 20 min for 1 h and centrifuged at 3000 rpm.

$$2I^- + h^+ \rightarrow I_2 \qquad (1.2)$$

The concentration of iodine in the supernatant was followed by complexation of I_2 with a 50 $g.L^{-1}$ starch suspension and determined by absorption at 620 nm in a UV-Vis spectrophotometer.

1.3. Results and Discussion

1.3.1. Characterization

The XRD patterns of the TiO_2 and the Fe modified TiO_2 particles are shown in Fig. 1.1. It can be seen that XRD patterns of all samples show an anatase-characteristic peak at 2θ=25.2°.

Fig. 1.1 XRD patterns of TiO_2 (HT, SG, P-25) and Fe-TiO_2 (Fe-HT, Fe-SG) samples. A: Anatase, B: Brookite, R: Rutile.

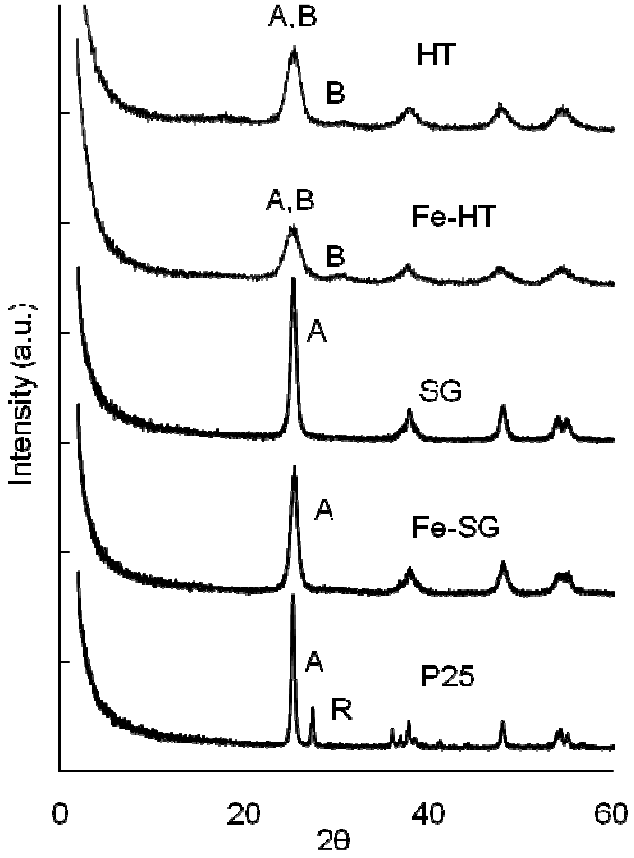

Source: The author.

No correspondent peaks to Fe phases were indentified, possibly due to the low Fe concentrations in the TiO_2 matrix. The ionic radius of Fe^{3+} and Ti^{4+} are very similar, 0.79 and 0.75 Å respectively for a coordination number of 6, thus, iron ions may substitute titanium on the TiO_2 matrix or be located interstitially forming a Fe-TiO_2 solid solution [16]. In hydrothermally synthesized photocatalysts; HT and Fe-HT, the main peak of anatase at 2θ = 25.2° overlaps with the diffraction peaks of broo kite phase at 2θ = 25.34 and 25.68°, which is usually found when both phases coexist in TiO_2 structure [20]. A characteristic peak of brookite is observed with a small diffraction at 2θ = 30.2° marked as B on Fig. 1.1. Fe-HT shows a slight distortion of the diffraction peaks indicating a reduction of crystallinity due to the presence of Fe. This result is in accordance with the fact that Fe^{3+} may be inserted in the TiO_2 matrix as a substituent for Ti^{4+} or interstitially located. In SG and Fe-SG cases, the anatase phase is notorious for both samples with a high crystallinity. This high crystallinity of anatase phase is related to a high photocatalytic activity of the TiO_2 [26]. A slight decrease in this crystallinity is observed when modifying SG with Fe, suggesting an insertion of Fe into the TiO_2 framework.

The DRS spectra of the TiO_2 and Fe-TiO_2 samples and their correspondent energy band gaps (E_g) are shown in Fig. 1.2. P-25 shows the highest absorption in the UV region of the spectrum (200-360 nm), while SG and Fe-SG present the lowest. When comparing the spectrum of bare TiO_2 samples, SG and HT to Fe modified TiO_2, Fe-SG and Fe-HT, a red-shift is notorious in the absorption to the visible region (> 400 nm).

Fig. 1.2 shows the E_g of the photocatalysts obtained by the Kubelka-Munk theory. The reduction in the band gap due to the presence of Fe may be explained since Fe induces new intra band gap states, giving to the TiO_2 the capacity to absorb light at lower energy levels [8], thus, promoting the absorption on the visible part of the spectrum. The excitation of 3d electrons of the Fe^{3+} transferring from the energy level of the dopant to the conduction band of the TiO_2 could effectively shift the absorption threshold into the visible region.

Fig. 1.2 DRS spectra and their correspondent calculated E_g for the TiO_2 (P-25, SG, HT) and Fe-TiO_2 (Fe-SG, Fe-HT) samples.

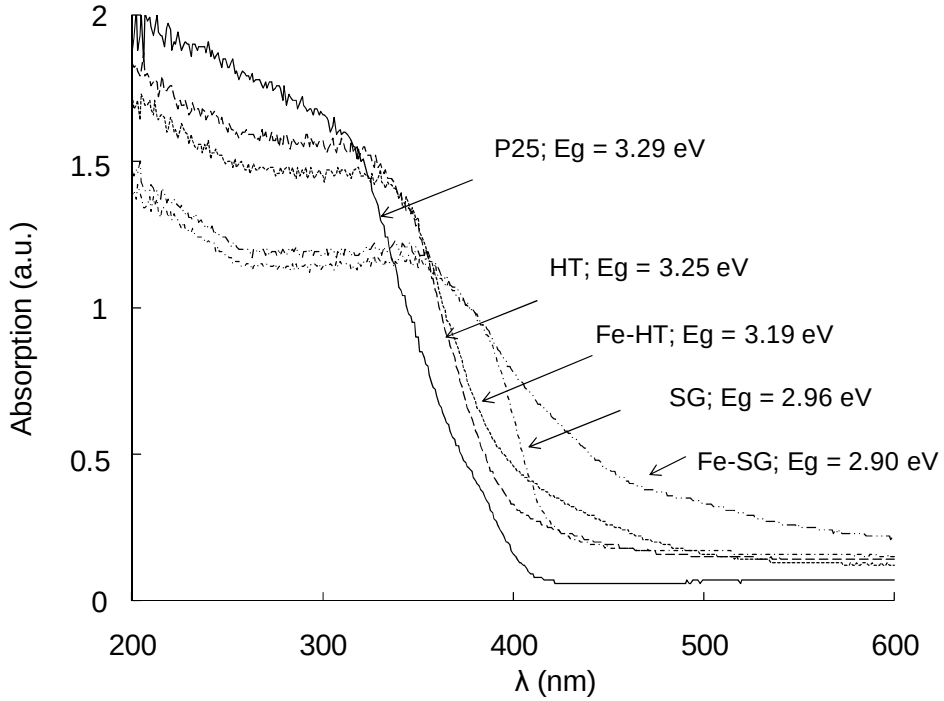

Source: The author.

The textural properties, the specific surface area (S_{BET}), and average pore diameter (D_A) of photocatalysts are shown in Table 1.1. From BET analysis, it is seen a decrease in surface area when modifying the TiO_2 with Fe loading in sol-gel (Fe-SG) and hydrothermal synthesis (Fe-HT). Hydrothermal synthesis leads to TiO_2 particles (HT) with higher surface and external area and similar average pore diameter than SG and P-25. No significant changes were observed when loading TiO_2 with Fe in Fe-SG and Fe-HT cases, due to the minimum concentrations used here. Nevertheless, it is important to note that in photocatalysis a higher external area exposed for light absorption is preferred to a higher surface area, since the effective area for photon absorption is the external area of the semiconductor.

Thus, for pores hidden to photon absorption no generation of oxidative radicals is expected inside since outer parts of the photocatalyst may screen and scatter light just

as when exceeding the concentration of photocatalyst in which light penetration is obstructed [27]. But of course, adsorption of the target molecule may be increased.

Table 1.1 Textural properties of TiO_2 and Fe modified TiO_2 samples.

Photocatalyst	HT	Fe-HT	SG	Fe-SG	P-25
S_{BET} ($m^2.g^{-1}$)	161	147	44	41	48
D_A(Å)	17	13	19	18	26

S_{BET}: specific surface area, D_A: average pore diameter, N.D: not determined. Source: The author.

1.3.2. Effect of the synthesis variables on TiO_2 photoactivity

Fig. 1.3 shows the photocatalytic degradation of Or-II using TiO_2 samples synthesized by the hydrothermal method using different volumetric ratios of Isop-OH/Ti(O-But)$_4$ (*Vi*) and H_2O/ Ti(O-But)$_4$ (*Vw*).

Fig. 1.3 Effect of Isop-OH/Ti(O-But)$_4$ (*Vi*) and H_2O/Ti(O-But)$_4$ (*Vw*) volumetric ratios used in the hydrothermal synthesis of the TiO_2 on the Orange II photocatalytic degradation.

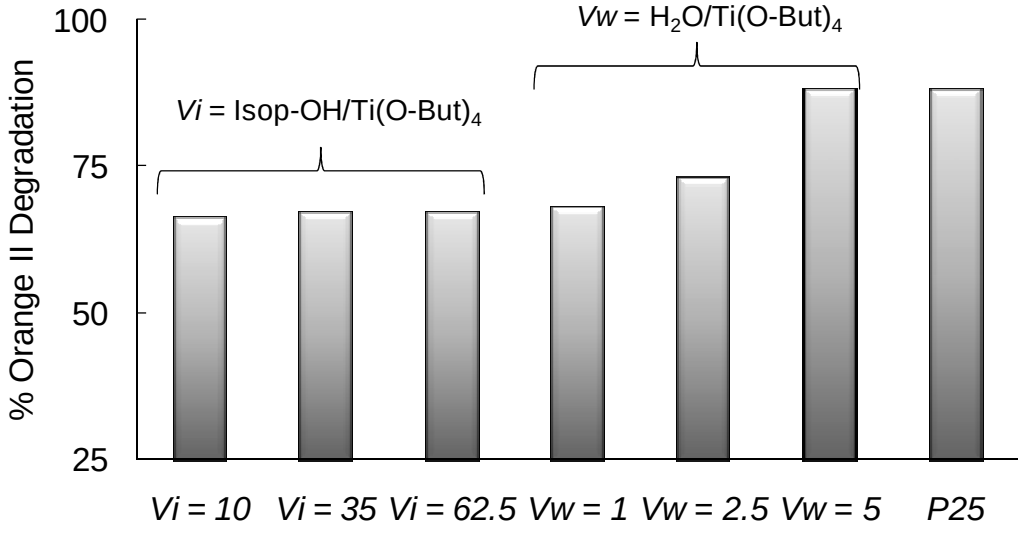

Source: The author.

The variation of the alcohol amount used in the hydrothermal synthesis analyzed here (*Vi* = 10-62.5) did not cause a relevant change in the photocatalytic activity of the HT sample. On the contrary, Xu *et al.* [7] reported that the increase in the alcohol

concentration during the synthesis reduces the photoactivity due to an increased amount of amorphous in the TiO_2 structure.

Nevertheless, the increase in H_2O amount, as shown in Fig. 1.4, increases the photoactivity. Possibly the decrease of Isop-OH concentration, caused by the increase in the concentration of water reduces the negative effect over the hydrolysis reaction due to the presence of Isop-OH; which slows down the reaction [7]. This reduce rate of hydrolysis leads to the formation of amorphous TiO_2 particles. The influence of the crystalline structure will be discussed in detail in the next section.

On the other hand, the effect of the alcohol type used during the hydrothermal synthesis is shown in Fig. 1.4.

Fig. 1.4 Effect the alcohol type used in the TiO_2 synthesis on the photocatalytic degradation of Orange II: ◊) methanol, □) ethanol, Δ) isopropanol.

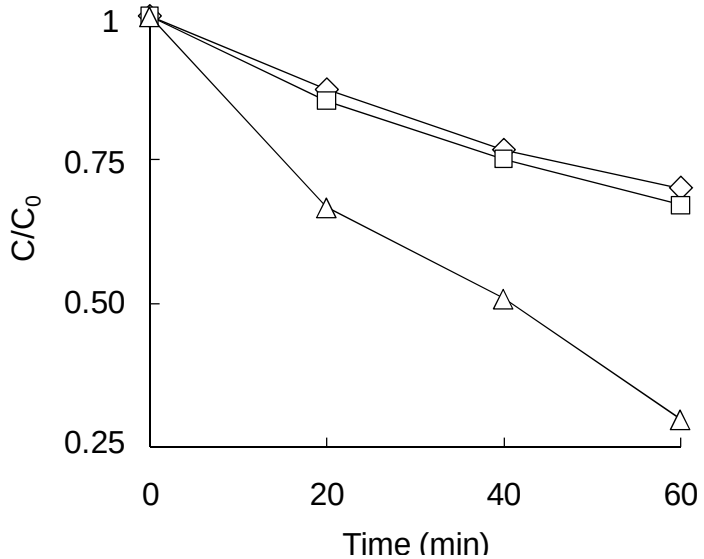

Source: The author.

The X-ray difractrograms of the samples (not shown here) are very similar to the HT sample (Fig. 1.1) and thus they are expected to have the same crystallite sizes. However, the photocatalytic activity is different. Possibly, the reduction of photoactivity caused by the use of short linear chain alcohols, such as, methanol and ethanol may be

due to the tendency of these to form hydrogen bonds with the surface hydroxyl groups reducing the amount of oxidation sites on the TiO_2 surface [28]. Moreover, the exchange of radicals between the Ti alcoxide and the alcohol may be affected by the use of linear alcohols such as methanol and ethanol, or branched type alcohols such as isopropanol. Therefore, the use of isopropanol may promote the formation of a more defective particle than linear alcohols [6], and thus, the surface area available for photon adsorption by TiO_2 is expected to increase, increasing the possibility to separate the electron and hole on the surface of the photocatalyst.

The S_{BET} for the HT synthesized samples with methanol, ethanol and isopropanol are 84, 95 and 147 $m^2.g^{-1}$ respectively. These results confirm that the use of branched alcohols increase the specific surface area during the hydrothermal synthesis of the TiO_2.

1.3.3. Photoactivity of Fe modified TiO_2 samples

Fig. 1.5 shows photocatalytic degradation of Or-II by the TiO_2 and Fe-TiO_2 photocatalysts under simulated solar light irradiation. Sol-gel synthesized samples, SG, and Fe-SG show the lowest performance in the photodegradation of Or-II. This poor photoactivity of sol-gel synthesized samples was not expected by means of crystallinity of the anatase phase since SG has high crystallinity. Then, it is not possible to establish a direct relationship between crystallinity of phases and the photoactivity of TiO_2 without comparing the whole set of properties of the samples. In addition, the sol-gel synthesized samples (SG and Fe-SG) showed the lowest absorption capacity in the UV region, which may explain their poor photoactivity (Fig. 1.2). P-25 and HT (using H_2O/Ti(O-But)$_4$ and Isop-OH/ Ti(O-But)$_4$ volumetric ratios of: 25 and 10, respectively) photocatalysts present almost the same photoactivity towards degradation of Or-II. Both crystalline structures of P-25 and HT show two phases. In the case of P-25, anatase and rutile are present in a mass ratio of 3 to 1, and in HT case, there exists a combination of anatase and brookite in an undetermined mass ratio. The well known photoactivity of P-

25 is ascribed to the coexistence of anatase and rutile [19] due to the difference in the band gap of these phases, which is an energy gradient that forces the rutile photogenerated e^- to an intra band gap energy state of anatase, avoiding its recombination with the h^+ [19]. Therefore, it is possible to assume that photoactivity of HT may be determined by the synergistic action of the conjunction of phases anatase and brookite, as suggested by Ardizzone *et al* [20].

However, light absorption capacity of HT in the UV region is lower than that one of P-25 (Fig. 1.2) suggesting a decrease in photoactivity for HT. This, in fact, seems a contradiction since P-25 and HT have similar Or-II phototodegradation activities. The textural properties of the samples may add new clues for comparison purposes. HT particles show a high photoactivity with the highest surface area. Thus, it is expected that HT particles with higher surface area may have a higher area exposed for light absorption. In this case, there should be a high possibility for more photons to produce more photogenerated charge species due to a higher surface extension in HT particles, and hence, the reduction in photoactivity caused by the lower light absorption of HT may be compensated and reach the activity of P-25. On the other hand, Fe alters the photocatalytic activity of the TiO_2. The concentration of Fe here used is in accordance with the optimal concentrations of Fe in the TiO_2 matrix found by Ghorai *et al* [10] and Tong *et al* [29]. However, Fe reduces the photoactivity of SG despite of the increase in absorption capacity in the visible region as seen in DRS analyses (Fig. 1.2). Contrarily, there is a remarkable increase in photoactivity in HT due to the presence of Fe in Fe-HT, which indeed promotes visible light absorption. Thus, it is not possible to correlate the photoactivity of Fe modified TiO_2 particles with the increased visible light absorption capacity. The direct photooxidation of iodine may give an explanation of the state of Fe in the TiO_2 network for the photocatalysts. The concentration of iodine reached by the TiO_2 and Fe modified TiO_2 photocatalysts is shown in Fig 1.6.

Fig. 1.5 Or-II degradation as relative concentration C/C_0 by: (■) Fe-SG; (□) SG; (○) P-25; (Δ) HT, and (▲) Fe-HT, during 60 min of 400 $W.m^{-2}$ of simulated solar light irradiation and (X) blank photolysis.

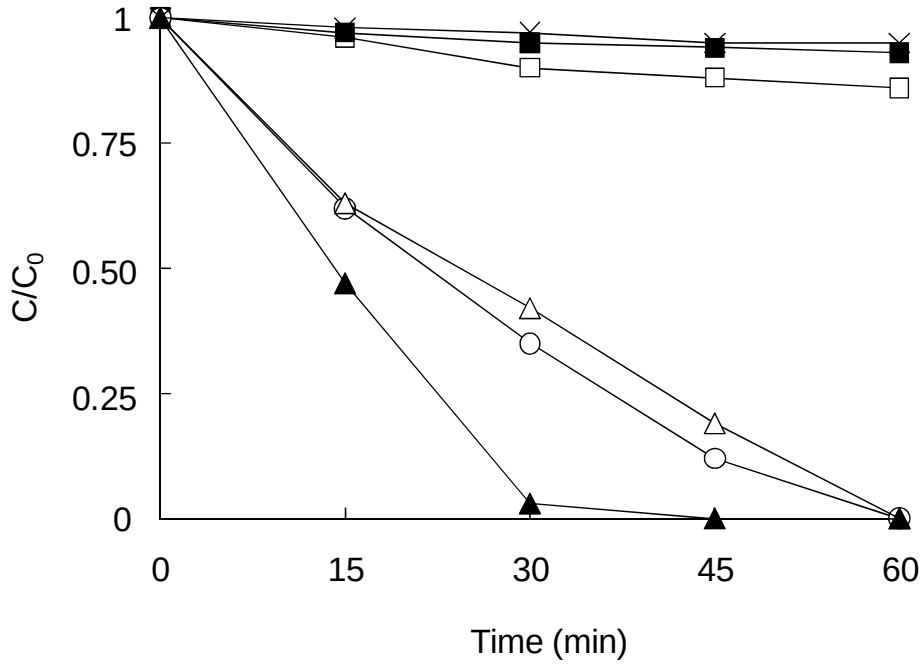

Source: The author.

The I_2 concentration reached by the SG sample is slightly higher than its correspondent Fe modified TiO_2 (Fe-SG), suggesting that Fe is acting as a recombination center for the e^--h^+ pair. For the Fe-HT sample there is not a significant increase of the performance of HT to suggest the action of Fe as a trap for the h^+. Such trap could avoid the recombination of the photogenerated charges and increase the direct oxidation of I^- to I_2 by the h^+ recombination [24]. Then, it is possible to assume that the chosen sol-gel route promotes Fe as a recombination center for the photogenerated charges in Fe-SG.

However, using the hydrothermal synthesis to modify TiO_2 with Fe it is possible to increase the photoactivity. Fe doping induces some extent deformation on the crystal lattice of the TiO_2 due to the different atomic sizes [29]. However, hydrothermal

treatment restrains grain growth, stabilizing particle formation [29], and possibly conducts iron to substitute Ti on the TiO_2 matrix, thus promoting photoactivity [13].

Adsorption of Or-II molecules on P-25 and SG surfaces in the dark agitation period prior to illumination is shorter than adsorption on HT surface indicating a strong interaction of this photocatalyst surface and Or-II. Or-II has a sulfonate functional group ($-SO_3^-$), negatively charged, that promotes its adsorption on positive surfaces [30].

Fig. 1.6 Concentration of Iodine achieved by: (▲) Fe-HT, (Δ) HT, (○) P-25, (□) SG and (■) Fe-SG during 40 min of 400 $W.m^{-2}$ of simulated solar light irradiation.

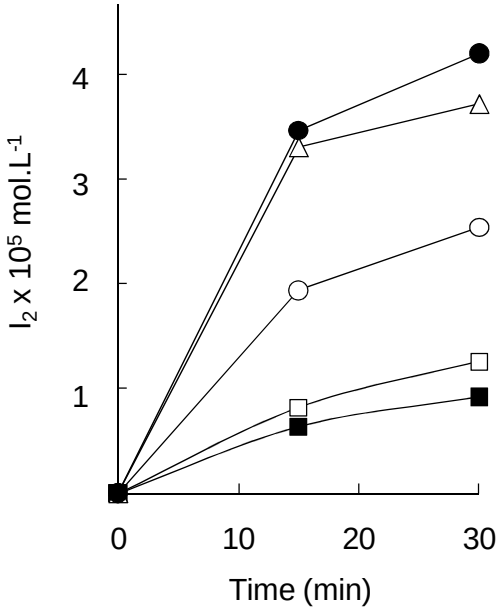

Source: The author.

TiO_2 has a point of zero charge at a pH about 6.5. Therefore, at pHs lower than this, as in our case with pHs of 5.7 to 6.1, the surface is positively charged. Then, it is possible to suggest a direct oxidation of Or-II in the surface of HT and Fe-HT; meanwhile P-25, with lower Or-II adsorption, may degrade the target molecule by oxidation due to the $^{\bullet}OH$ free radicals in homogeneous phase. This assumption is in agreement to the photooxidation of the I^- by the photocatalysts, since HT causes a higher direct oxidation of iodide than P-25. Kormali *et al* [31] have proposed that oxidation activity of TiO_2 is

mainly due to the action of $^{\bullet}OH$ radicals and to a lesser extent to holes. However, the nature of the photooxidation mode depends on the nature of the substrate [31]. Additionally, as it is known the e^{-}-h^{+} pair transfer to the media takes 100 ns to 1 ms, and the recombination takes 10 to 100 ns [2]. Then, it is more probable that surface oxidation by the photogenerated h^{+} on the surface of HT takes place faster than the homogeneous phase oxidation caused by $^{\bullet}OH$ homogenous phase free radicals produced on the surface of P-25. Indeed, homogeneous phase oxidation of P-25 may take an additional time for the $^{\bullet}OH$ to reach the Or-II molecules in solution.

In the case of Fe modified TiO_2 the photoactivity is attributed to the enhanced interactions of the surface and the Or-II molecule. Such interactions will be discussed in the following chapter of this thesis.

The performance of the photocatalyst in the photocatalytic disinfection of water supposes an aggressive test of their photooxidation activity, since *E. coli* is a 1-3 µm living cell with protection mechanisms to oxidative stress and 3.5 million macromolecules on its cell wall. The survival bacteria after 40 min of illumination for TiO_2 and Fe modified TiO_2 photocatalyst are shown in Fig 1.7. Blank experiments named as Dark and the photolysis blank indicate no bactericidal activity of the system under darkness and a small disinfection activity due to irradiation using the simulated solar light source during 40 min of test. The performance of the photocatalysts in the photocatalytic disinfection is comparable to their performance on the Or-II photocatalytic degradation, except for the activity of HT. Unlike the Or-II degradation, the *E. coli* inactivation by HT is lower than that of P-25.

These results neglect the assumption that HT sample has a similar oxidative power than that of the P-25. Nevertheless, when dealing with enormous complex systems like *E. coli*, compared to 1 nm Or-II molecule, interactions between the target and the photocatalyst become highly important. Gumy *et al* [4] found an important relation of the surface charge of the photocatalyst and the cell wall charge. *E. coli* cells have positive

and negative charged macromolecules on their surface with predominant negative groups. This implies that a more positive charged surface is preferred to increase the electrostatic attraction between the photocatalyst's surface and bacteria to be efficiently attacked and inactivated.

As proposed before, the oxidation activity of hydrothermally synthesized photocatalysts (HT and Fe-HT) seems to be promoted by a surface oxidation mode. Since Kormali *et al* [31] have proposed that the photooxidation mode of the photocatalyst depends on the nature of the substrate, and as it is well-known for P-25, the photocatalytic oxidation for the inactivation of *E. coli* in water is mainly caused by the attack of free $^{\bullet}OH$ radicals to the cell wall in the homogenous phase. This assumption on mechanisms may explain the difference in photocatalytic disinfection activities for HT and P-25 particles. It is possible to assume that HT particles have a high surface interaction with Or-II to promote the surface oxidation mode, but there is no such interaction between HT surface and *E. coli* to promote a similar $^{\bullet}OH$ radical mode oxidation as P-25 do.

Moreover, Fe slightly enhances the photoactivity of the HT sample towards the photocatalytic disinfection of water. Probably, surface Fe atoms may promote the interaction bacteria-photocatalyst thus increasing photoactivity.

The photocatalytic disinfection and photocatalytic detoxification activities seem to be related to the crystalline structure, the optical properties, and the interactions between the surface of the photocatalyst and the target. In this chapter is proposed a correlation of these characteristics by comparing the photocatalytic activity of two different Fe-TiO_2 samples synthesized by well-known wet chemical synthesis methods: sol-gel and hydrothermal synthesis. This correlation suggests that the synthesis route determines the activity of Fe modified TiO_2 since the chosen synthesis may promote the stabilization of Fe in the TiO_2 matrix enhancing the photoactivity.

Fig. 1.7 Survival *E. coli* ATCC 11229 after 40 min of 400 $W.m^{-2}$ of simulated solar light irradiation using TiO_2 (SG, P-25, HT) and Fe modified TiO_2 (Fe-SG, Fe-HT) photocatalysts.

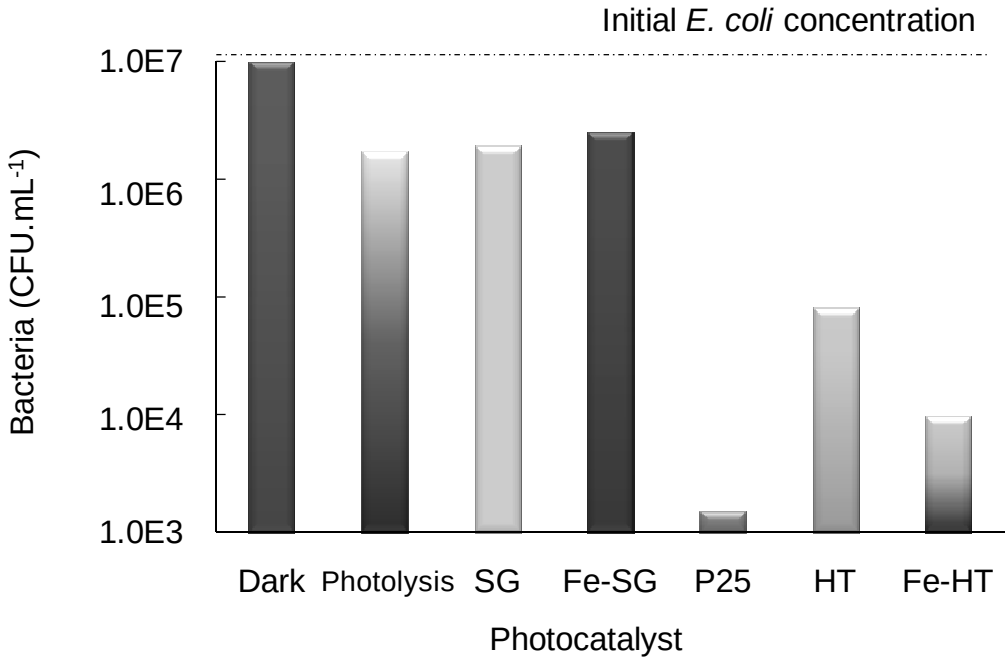

Source: The author.

Literature has reported that iron doping in TiO_2 increases photoactivity in the visible region due to the intra band gap states promoted by Fe^{3+} [32], but contrarily, Fe^{3+} may decrease photoactivity under UV-light irradiation [32, 33]. These differences in activities may conduct to lower activities under solar light irradiation where both ranges, UV and visible, are used. In this chapter, we present a synthesis route possibility to obtained Fe doped TiO_2 particles with enhanced photoactivity towards the degradation of the chosen targets under solar light irradiation.

1.4. Conclusions

TiO_2 and Fe modified TiO_2 particles were synthesized by hydrolysis of titanium butoxide in the presence of a Fe inorganic salt by the sol-gel and the hydrothermal synthesis. Hydrothermal synthesis leads to TiO_2 particles (HT) with higher photocatalytic oxidation

activity towards the degradation of Orange II than TiO_2 sol-gel synthesized particles (SG) and similar to that of the commercial TiO_2 P-25.

Results of characterization techniques indicate that there is no direct correlation of the photoactivity with the level of crystallinity of the anatase phase but to the presence of amorphous and the coexistence of anatase with one of two phases, rutile or brookite in the structure.

The water/alcoxide ratio and alcohol type used in the synthesis have a marked effect on the photoactivity of the HT sample, while the ratio alcohol/alcoxide does not significantly change the Or-II degradation photoactivity. The positive effect of the increased water/alcoxide ratio is possibly due to the increase in the alcohol dilution decreasing its negative effect towards the rate of the hydrolysis reaction. Moreover, the use of branched type alcohols, such as, isopropanol in the synthesis increase the activity of the photocatalyst, possibly due to the increase in the available area for UV light absorption.

Diffusive reflectance analyses of the samples show an increase in visible light absorption capacity due to the presence of Fe. However, sol-gel process promotes Fe as a recombination center of the photogenerated e^- - h^+ reducing photoactivity.

Additionally, it is possible to suggest that the mechanism of photooxidation for HT in the surface of the photocatalyst, since the photoactivity of the HT sample, in oxidative reactions promoted in the surface, was higher than that of the commercial TiO_2 used as reference, which action is known to be due to hydroxyl radicals ($^{\bullet}OH$) produced in the photocatalyst's surface but active in the homogeneous phase. Moreover, the photoactivity towards reactions attributed to $^{\bullet}OH$ was lower than that of the TiO_2 P-25, thus confirming the assumption of the surface mode oxidative pathway in the HT samples.

References

[1] J.M. Herrman*, Heterogeneous photocatalysis: fundamentals and applications to the removal of various types of aqueous pollutants*, Catal. Today, 53 (1999) 115-129.

[2] O. Carp, C.L. Huisman, A. Reller, *Photoinduced reactivity of titanium dioxide*, Prog. Solid State Chem., 32 (2004) 33-177.

[3] J. Blanco, P. Fernández, S. Malato, *Solar Photocatalytic Detoxification and Disinfection of Water: Recent Overview*, J. Sol. Energy Eng., 129 (2007) 4-15.

[4] D. Gumy, C. Morais, P. Bowen, C. Pulgarín, S. Giraldo, R. Hajdu, J. Kiwi, *Catalytic activity of commercial TiO_2 powders for the abatement of the bacteria (E. coli) under solar simulated light: Influence of the isoelectric point*, Appl. Catal. B: Env., 63 (2006) 76-84.

[5] M. Mahalaksmi, S.V. Priya, B. Arabindoo, M. Palanichamy, V. Murugesan, *Photocatalytic degradation of aqueous propoxur solution using TiO_2 and Hb Zeolite supported TiO_2*, J. Hazard. Mat., 161 (2009) 336-343.

[6] I.A. Montoya, T. Viveros, J.M. Dominguez, L.A. Canales, I. Schifter, *On the effects of the sol-gel synthesis parameters on textural and structural properties of TiO_2*, Catal. Lett., 15 (1992) 207-217.

[7] Y. Xu, W. Zheng, W. Liu, *Enhanced photocatalytic activity of supported TiO_2: dispersing effect of SiO_2*. J. Photochem. Photobiol. A: Chem., 122 (1999) 57-60.

[8] W.Y. Choi, A. Termin, M.R. Hoffmann, *The role of metal ion dopants in quantum-sized TiO_2: correlation between photoreactivity and charge carrier recombination dynamics*, J. Phys. Chem., 98 (1994) 13669-13679.

[9] M.I. Litter, J.A. Navío, *Photocatalytic properties of iron doped-titania semiconductors*, J. Photochem. Photobiol. A: Chem., 98 (1996) 171-181.

[10] T.K. Ghorai, S.K. Biswas, P. Pramanik, *Photooxidation of diferent organic dyes (RB, MO, TB, and BG) using Fe(III)-doped TiO_2 nano photocatalyst prepared by novel chemical method*, Appl. Surf. Sci., 254 (2008) 7498-7504.

[11] B. Xin, Z. Ren, P. Wang, J. Liu, L. Jing, H. Fu, *Study on the mechanisms of photoinduced carriers separation and recombination for the Fe^{3+}-TiO_2 photocatalysts*, Appl. Surf. Sci., 253 (2007) 4390-4395.

[12] M. Asiltürk, F. Sayilkan, E. Arpaç, *Effect of Fe^{3+} ion doping to TiO_2 on the photocatalytic degradation of Malachite green dye under UV and vis irradiation*, J. Photochem. Photobiol. A: Chem., 203 (2009) p. 64-71.

[13] M.A. Khan, S.I. Woo, O. Yang, *Hydrothermally stabilized Fe(III) doped titania active under visible light for water splitting reaction*, Int. J. Hydrogen Energy, 33 (2008) 5345-5351.

[14] S. Liu, Y. Chen, *Enhanced photocatalytic activity of TiO_2 powders doped by Fe unevenly,* Catal. Commun., 10 (2009) 894-899.

[15] C.C. Trapalis, P. Keivanidis, G. Kordas, M. Zaharescu, M. Crisan, A. Szatnayi, M. Gartner, *TiO_2 (Fe^{3+}) nanostructured thin films with antibacterial properties, Thin Solid Films*, 433 (2003) 186-190.

[16] C.Y. Wang, C. Bottcher, D.W. Bahneman, J.K. Dohrman, *A comparative study of nanometer size Fe(III)-doped TiO_2: photocatalysts: synthesis, characterization and activity*, J. Mater. Chem., 13 (2003) 2322-2325.

[17] Y. Xie, C. Yuan, X. Li, *Photosensitized and photocatalyzed degradation of azo dye using Ln^{n+}-TiO_2 sol in aqueous solution under visible light irradiation*, Mat. Sci. Eng. B., 117 (2005) 325-333.

[18] C. Adan, A. Martinez, S. Malato, A. Bahamonde, *New insights on solar photocatalytic degradation of phenol over Fe-TiO_2 catalysts: Photo-complex mechanism of iron lixiviates*, Appl. Catal. B: Env., 93 (2009) 96-105.

[19] D.C. Hurum, A.G. Agrios, K.A. Gray, T. Rajh, M.C. Thurnauer, *Explaining the enhanced photocatalytic activity of Degussa P-25 mixed phase oxide TiO_2 using EPR*, J. Phys. Chem., 107 (2003) 4545-4549.

[20] S. Ardizzone, C. Bianchi, G. Cappelletti, S. Gialanella, C. Pirola, V. Ragaini, *Tailored Anatase/Brookite Nanocrsytalline TiO_2. The optimal Particle Features for Liquid and Gas-Phase Photocatalytic Reactions*, J. Phys. Chem. C, 111 (2007) 13222-13231.

[21] A. Paola, G. Cufalo, M. Addamo, M. Bellardita, R. Campostrini, M. Ischia, R. Ceccato, L. Palmisano, *Photocatalytic activity of nanocrystalline TiO_2 (brookite, rutile, and brookite-based) powders prepared by thermohydrolysis of $TiCl_4$ in aqueus chloride solutions*, Colloids Surf. A: Physicochem. Eng. Aspects, 317 (2008) 366-376.

[22] P. Pitter, J. Chudoba, *Biodegradability of organic substances in the aquatic environment*, CRC Press, Boca Raton, 1990.

[23] G.P. Anipsitakis, T.P. Tufano, D. Dionysiou, *Chemical and microbial decontamination of pool water using activated potassium peroxymonosulfate*, Water Res., 42 (2008) 2899-2910.

[24] C. Karunakaran, P. Anilkumar, *Semiconductor-catalyzed solar photooxidation of idodide ion*, J. Mol. Catal. A. Chem., 265 (2007) 153-158.

[25] N. Todorova, T. Giannakopoulou, G. Romanos, T. Vaimakis, J. Yu, C.C. Trapalis, *Preparation of fluorine-Doped TiO_2 photocatalysts with controlled crystalline structure*, Int. J. Photoener., 2008 (2008) 1-9.

[26] K.Y. Jung, S.B. Park, *Anatase-phase titania: preparation by embedding silica and photocatalytic activity for the decomposition of trichloroethylene*, J. Photochem. Photobiol. A: Chem., 127 (1999) 117-122.

[27] I.K. Konstantinou, T.A. Albanis, *TiO_2-assisted photocatalytic degradation of azo dyes in aqueous solution: kinetic and mechanistic investigations*, A review. Appl. Catal. B: Env., 49 (2004) 1-14.

[28] E. Alonso, I. Montequi, M.J. Cocero, *Effect of synthesis conditions on photocatalytic activity of TiO_2 powders synthesized in supercritical CO_2*, J. Supercritic. Fluids, 49 (2009) 233-238.

[29] T. Tong, J. Zhang, B. Tian, F. Chen, D. He, *Preparation of Fe^{3+}-doped TiO_2 catalyst by controlled hydrolisis of titanium alcoxide and study on their photocatalytic activity for methyl orange degradation*, J. Hazard. Mat., 155 (2008) 572-579.

[30] C. Guillard, H. Lachheb, A. Houas, M. Ksibi, E. Elaloui, J.M. Herrman, *Influence of chemical structure of dyes, of pH and inorganic salts on their photocatalytic degradation by TiO_2 comparison of the efficiency of powder and supported TiO_2*, J. Photochem. Photobiol. A: Chem., 158 (2003) 27-36.

[31] P. Kormali, T. Triantis, D. Dimotikali, A. Hiskia, E. Papaconstantinou, *On the Photooxidative behavior of TiO_2 and $PW_{12}O_{40}^{3-}$: $^{\bullet}OH$ radicals versus holes*, Appl. Catal. B: Env., 68 (2006) 139-146.

[32] Y. Wu, J. Zhang, L. Xiao, F. Chen, *Preparation and characterization of TiO_2 photocatalyst by Fe^{3+} doping together with Au deposition for the degradation of organic pollutants*, Appl. Catal. B: Env., 88 (2008) 525-532.

[33] Z. Li, W. Shen, W. He, X. Zu, *Effect of Fe-doped TiO_2 nanoparticle derived from modified hydrothermal process on the photocatalytic degradation performance on methylene blue*, J. Hazard. Mat., 155 (2008) 590-594.

2. Iron promotion of the TiO_2 photosensitization process towards the photocatalytic oxidation of azo dyes under solar-simulated light irradiation

Abstract

The photocatalytic activity of Fe loaded TiO_2 was studied towards the photocatalytic oxidation of the azo dye Orange II (Or-II) under ultraviolet (UV) and solar-simulated light (UV-Vis) irradiations. In XPS analyses Fe_2O_3 was identified on the photocatalyst's surface inducing Vis light absorption of TiO_2 as observed in diffusive reflectance spectroscopy. Moreover, X-ray diffractograms evidence a reduction of the anatase phase crystallinity due to Fe_2O_3 presence. Fe modification enhanced the TiO_2 photocatalytic activity towards Or-II photodegradation under strict simultaneous irradiation of UV and Vis light. Even so, the performance of the Fe-TiO_2 samples towards the photodegradation of phenol, under UV irradiation, was lower than TiO_2 suggesting the recombination of the UV photogenerated electron - hole pair. Therefore, results evidence the Or-II photooxidation under UV-Vis irradiation by losing energy in electron transferring processes to sensitize TiO_2, and, the formation of reactive oxygen species promoted by the transferred electron.

Introduction

Among the different methodologies used in order to increase the TiO_2 photoactivity the doping with transition metal ions has been extensively used, but the understanding of the mechanisms of the photocatalytic process have turned into a controversy [1-3]. The metallic ions into the TiO_2 matrix may act as traps for the photogenerated charges: electron and hole (e^--h^+). This e^--h^+ pair is the responsible for the generation of radicals useful with high oxidation potentials [4-6]. Therefore, it is expected that charge traps may reduce the recombination of the e^--h^+ pair enhancing the production of oxidative radicals.

In particular, Fe doping has been a research interest in synthesis, characterization, optical features, recombination and photocatalytic activity of the TiO_2 [2, 7-10]. The presence of Fe in the TiO_2 increase visible (Vis) light absorption [2, 11] which indeed may generate an increase in the photocatalytic activity of the material when irradiated with light of $\lambda > 400$ nm [11]. Nevertheless, it has been proved a decrease in photoactivity under irradiation with light of higher energy, such as, UV-A type irradiation ($\lambda < 400$ nm) [2, 11]. In addition, Fe^{3+} ions may act as either electron or hole traps [12], but, even if the photogenerated pair is “trapped”, these traps may interact and promote the recombination [11] turning into a decrease in photoactivity.

As a result of the exposed, it is possible to predict a competition of negative and positive effects under simultaneous irradiation of UV and Vis. The aim of this work is to analyze the action of Fe in loaded TiO_2 particles towards the photocatalytic degradation of the azo-dye Orange-II (Or-II). Moreover, the photoactivity of the materials was also analyzed towards the photooxidation of phenol which does not photosensitize the TiO_2, thus, allowing the establishment of the action of the modifying metal in the subsequent processes after photogeneration of the electron-hole pair, such as, recombination or trapping.

The analyses of the results of the photooxidation of Or-II and phenol under several light irradiation set-ups such as ultraviolet and UV-Vis using a solar light simulation chamber, in addition to the characterization of the materials, led to the understanding of the possible mechanisms of photocatalytic and photodynamic degradation of the chosen molecules as an effect of the type of light source by the Fe-TiO_2 photocatalysts.

2.1. Experimental

2.1.1. Fe-TiO_2 Photocatalysts Synthesis

The TiO_2 sample was obtained using the hydrothermal synthesis. In this case, a volume of titanium butoxide ($Ti(O\text{-}But)_4$, Sigma) was added dropwise to isopropanol (Isop-OH, Merck) under vigorous magnetic stirring in a volumetric ratio Isop-OH/$Ti(O\text{-}But)_4$ = 5. Then, 3 µL of HNO_3 (65%, Merck) per each 2 mL of $Ti(O\text{-}But)_4$ were added to the previous solution. Immediately after, water was added dropwise to the reaction in a volumetric ratio H_2O/$Ti(O\text{-}But)_4$ = 1. The formed gel was pressure treated using an autoclave for 3 h at 120℃ and ~ 144 kPa. The obtained crystals were manually grounded in mortar, followed by a washing step in which the powders were twice suspended in water with an intermediate centrifugation. Finally, water was extracted in an oven at 70℃ for 12 h.

To synthesize the Fe modified TiO_2 sample the procedure described above was used but instead of water it was added an aqueous solution of $Fe(NO_3)_3.9H_2O$ (Merck), in an appropriate amount to obtained a nominal molar percentage (mol%) of 1, 2, 3, and 10. Photocatalysts are labeled as Fe(x)-TiO_2, where x corresponds to the mol%.

2.1.2. Photocatalysts Characterization

X-ray diffraction patterns and UV-Vis diffusive reflectance spectra were collected using the equipment and procedures described in chapter 2. The energy band gap widths of the samples were determined using the Kubelka-Munk phenomenological theory [13].

X-ray photoelectron spectroscopy measurements

XPS analyses were carried out on an AXIS NOVA photoelectron spectrometer (Kratos analytical, Manchester, UK) equipped with a monochromatic AlKα (*hv* = 1486.6 eV) anode. The kinetic energy of the photoelectrons was determined with the hemispheric analyzer set to the pass energy of 160 eV for wide-scan spectra and 20 eV for the case of high resolution spectra. Electrostatic charge effect of the sample was overcompensated by means of the low-energy electron source working in combination with a magnetic immersion lens. The carbon C 1s line with position at 284.6 eV was used as a reference to correct the charging effect. The spectra were decomposed using the casaXPS program (Casa Software Ltd., UK) with a Gaussian/Lorentzian (70/30) product function after subtraction of a linear baseline. The assignation of different Ti peaks in Ti 2p spectra were restricted by distances between Ti peaks of 5.7 eV [14] and 13.6 eV for Fe 2p peaks [15].

2.1.3. Photocatalytic Tests

The photocatalytic degradation of Or-II and phenol follows procedures described in chapter 2. The illumination of the suspensions was made using three different set-ups: i) 400 $W.m^{-2}$ of solar-simulated light irradiation using a suntest system model CPS+ from ATLAS, with temperature and irradiation power control, and a xenon lamp emitting light with wavelengths of 300 y 800 nm, and 5% of the irradiation corresponds to UV-A. ii) 38 $W.m^{-2}$ of UV light irradiation using a closed chamber with a set of 5 TLD 18 W BLB Phillips lamps with an emission spectra of 330-400 nm, or , iii) 60 $W.m^{-2}$ of Vis light irradiation using a closed chamber with 5 TLD 18 W Blue Phillips lamps with an emission spectra of 400-500 nm. The radiant flux was monitored with a Kipp & Zonen (CM3) power meter (Omni instruments Ltd., Dundee, UK). Or-II photodegradation was followed by UV-Vis spectrophotometry and Total organic carbon (TOC) measurements that were done in order to analyze its mineralization. The equipment used was a Shimadzu 500 instrument provided with an auto-sampler. Phenol oxidation was followed

by HPLC using a Hewlett–Packard series 1100 equipment with a reverse phase Spherisorb silica column (Macherey–Nageland) and a Diode Array Detector. Phenol detection was carried out at 220 nm. As mobile phase a mixture of acetonitrile and water in a volume ratio of 60/40 was used.

2.2. Results and Discussion

2.2.1. Fe-TiO_2 photocatalyst features

Fig. 2.1a shows the Ti 2p XPS spectra of the Fe(3)-TiO_2 and the TiO_2 samples. The Ti 2p spectrum is constituted by two peaks at: 458.9 eV and 464.55 eV, assigned to Ti $2p_{3/2}$ and Ti $2p_{1/2}$, respectively, indicating a predominant state of Ti^{4+} in the surface of bare and Fe loaded samples [14].

Fig. 2.1 XPS spectra of a) Ti 2p, and, b) Fe 2p of the Fe-TiO_2 and TiO_2 samples.

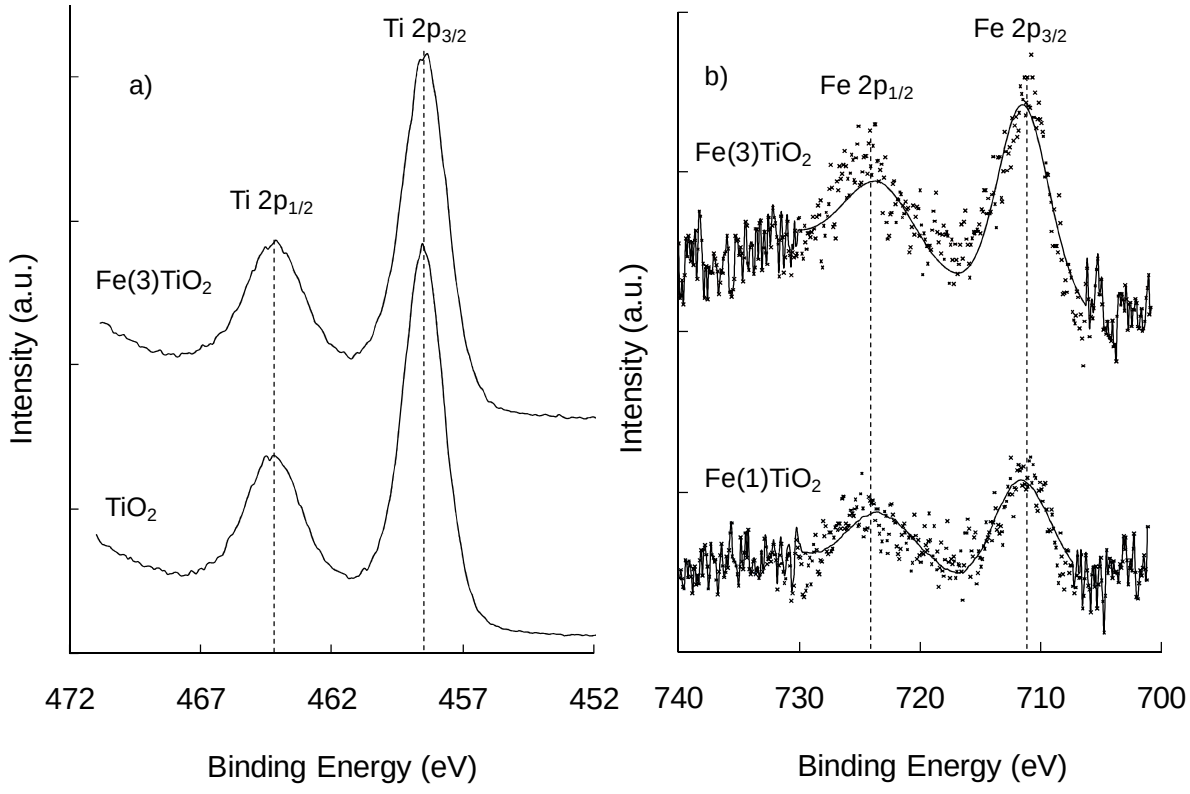

Source: The author.

No additional peaks could be assigned following constraints and restrictions suggested by Biesinger *et al.* [14]. Moreover, no shift was found for Ti 2p in Fe loaded TiO_2 sample's spectrum suggesting the absence of chemical bonds between Fe and Ti. Fig. 2.1b Shows the Fe 2p XPS spectra of the samples: Fe(1)-TiO_2 and Fe(3)-TiO_2. These spectra are constituted by Fe peaks at 711.1 and 724.4 eV for Fe $2p_{3/2}$ and Fe $2p_{1/2}$, respectively, assigned to Fe^{3+} in Fe_2O_3 [15]. As expected, the increase in concentration leads to an increase in the signal intensity due to the enrichment of surface atomic layers with Fe. Therefore, it is possible to suggest that Fe is interstitially located as cationic Fe^{3+} aggregates and/or Fe_2O_3.

The X-ray diffractograms of the synthesized photocatalysts are show in Fig. 2.2.

Fig. 2.2 X-ray Diffractograms of: a) TiO_2 and the Fe(X)-TiO_2 samples with X (mol%) of: b) 1, c) 3, d) 10. A: Anatase, B: Brookite.

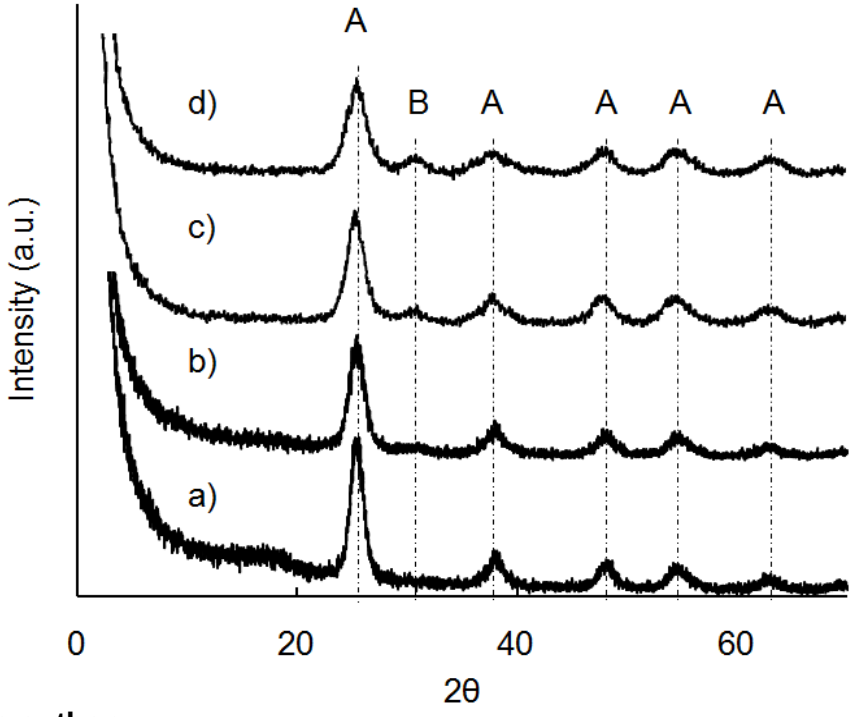

Source: The author.

In all cases, there is presence of the anatase phase at 2θ = 25.2°. The presence of Fe causes a decrease in the crystallization in sample Fe(1)-TiO_2 which is possibly due to: i) the restriction to the formation of the crystallites by the interstitially located cationic Fe^{3+}cationic aggregates or iron oxide, and ii) the net distortion caused by the location of Fe atoms in the TiO_2 matrix [2, 16]. No additional phases for Fe were observed indicating: i) the presence of an amorphous phase, and ii) the dispersion of the modifying metal in the TiO_2's structure [16].

Fig. 2.3 shows the DRS spectra of the TiO_2 and Fe-TiO_2 samples with different Fe concentrations.

Fig. 2.3 DRS spectra for the Fe(x)-TiO_2 samples (x = 3, 2, 1 and 0 nominal mol% of Fe). In the inset, the effect of x on the E_g calculated value using the Kubelka-Munk theory.

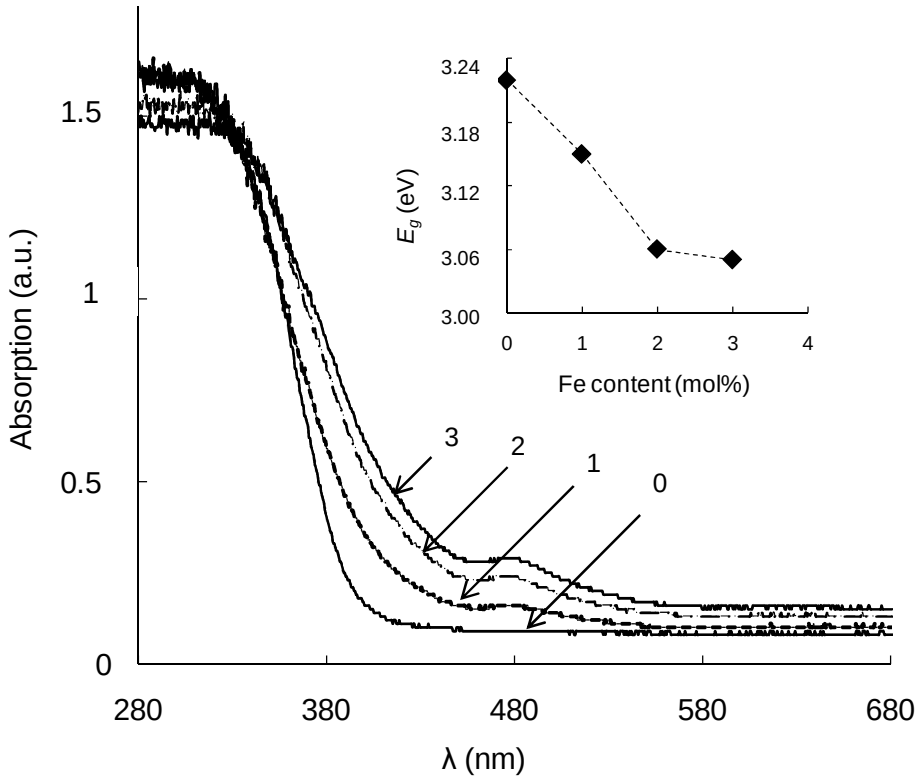

Source: The author.

The inset shows the decrease in the energy band gap due to the increased nominal concentration of Fe_2O_3 in the TiO_2's network. These spectra show an effective increase in the visible light (Vis) absorption capacity of TiO_2 that increases with Fe_2O_3 nominal concentration. As a consequence, calculated E_g values show a decrease with increasing Fe concentration. Furthermore, the spectra show an absorption shoulder-like peak at ~ 480 nm for the Fe modified samples. Jeong *et al.* [17] discussed such peaks in DRS spectra, for Fe-Cr codoped TiO_2, as absorption bands of new energy states in the photocatalyst related to d-d transition of Fe and Cr electrons.

Such effect has also been observed when modifying TiO_2 with Co or Cr [18]. Therefore, in our case the shoulder-like peak is attributed to the Vis light absorption promoting electron transitions in Fe^{3+}/Fe_2O_3 aggregates.

2.2.2. Effect of Fe on the photooxidation activity of TiO_2

The Or-II degradation under simulated solar light using the TiO_2 and the Fe-TiO_2 samples is shown in Figs. 2.4 and 2.5. Fig. 4 shows the Or-II photodegradation followed by UV-Vis spectrophotometry.

As observed, photoactivity of TiO_2 is increased due to the presence of Fe. The increase in Fe concentration increases the TiO_2's photoactivity up to 1 mol%, after which, there is a decrease in the photodegradation of Or-II. Higher concentrations of Fe result in the promotion of recombination centers for the photogenerated charges [19, 20].

The evolution of TOC concentration during the photocatalytic degradation of Or-II under solar light irradiation is shown in Fig. 2.5. In accordance to this, Fe enhances the photooxidation activity of the TiO_2 sample. When comparing velocities of Figs. 2.4 and 2.5

Fig. 2.4 Photocatalytic degradation of Or-II under UV-Vis light irradiation by: (○) TiO_2, and Fe(x)-TiO_2 with x = (■) 0.5, (▲) 1, (♦) 2, and (x) 3 nominal mol% of Fe. (◊) The photolysis blank.

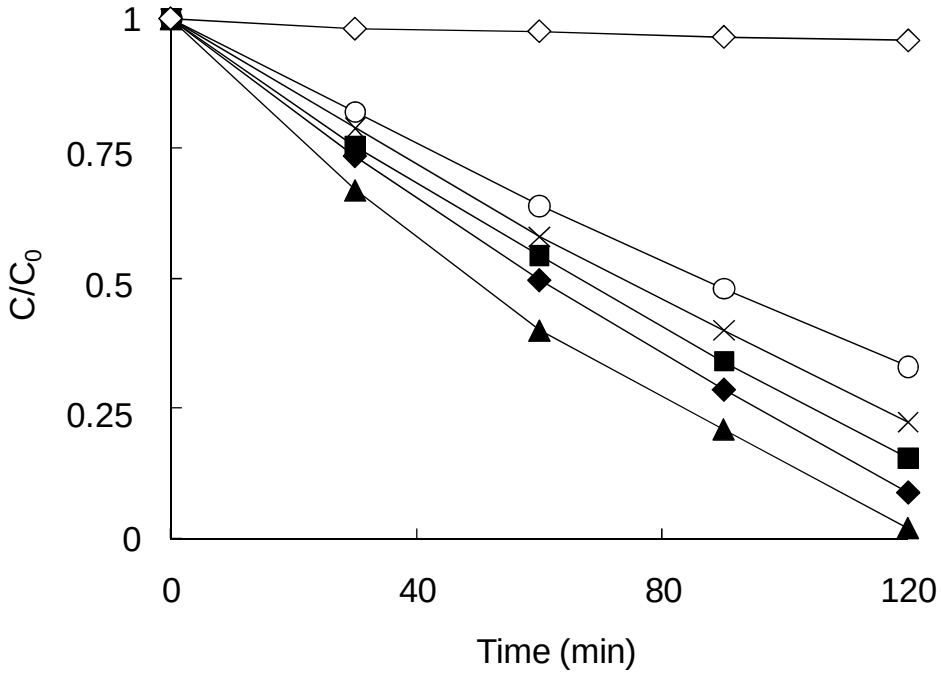

Source: The author.

it is seen that discoloration is faster than mineralization as observed in TOC decay analyses. This is due to mineralization of Or-II by reactive oxygen species that undergoes through attack of the N=N bond as first step, thus decreasing absorption at 486 nm. Then, a subsequent destruction of aromatic compounds occurs, such as hydrazine, and finally, the oxidation process ends with the formation of carboxylic acids, CO_2 and nitrogen by products as NOx [21].

However, the TOC evolution of the photocatalytic degradation of Or-II under UV irradiation shows contrary results as presented in Fig. 2.6. In this case, the performance of the Fe modified TiO_2 samples was opposite to the obtained results under simulated-solar light. This implies that under UV-Vis light there possibly is a beneficial effect of Vis irradiation for the photooxidation of the dye.

Fig. 2.5 TOC evolution during the photocatalytic degradation of Or-II under UV-Vis irradiation using the (○) TiO_2, and, Fe(x)-TiO_2 x = (▲) 1, and, (X) 3 nominal mol% of Fe.

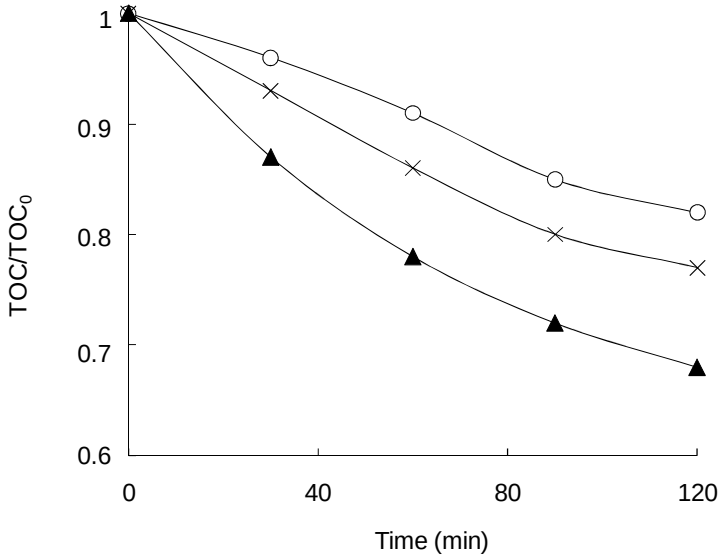

Source: The author.

Fig. 2.6 Or-II photocatalytic mineralization under UV irradiation followed by TOC evolution using the (○) TiO_2, and, Fe(x)-TiO_2 samples, x = Fe nominal mol% of: (■) 0.5, (▲) 1, and, (x) 3.

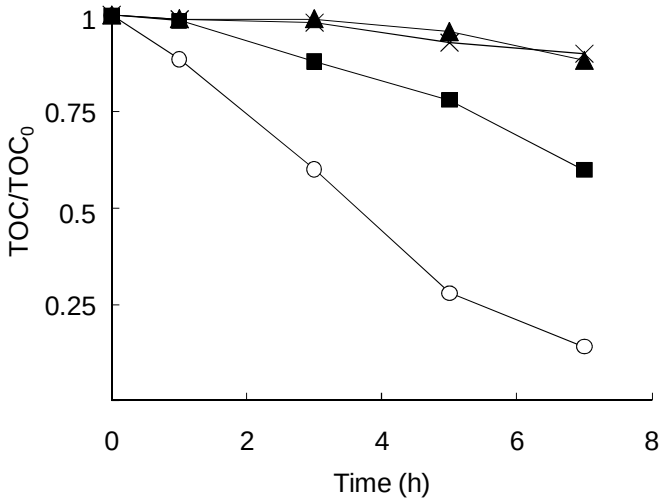

Source: The author.

This effect is not due to the promotion of e^- to the TiO_2 conduction band since this would increase the photoactivity which by the contrary is diminished. Moreover, for the Or-II

photooxidation tests it was also used a set of visible light emitting lamps. Results (not presented) showed no significant activity for all of the photocatalysts during 6 h of visible light irradiation.

In addition, it is possible to reject any given interaction of the dye with leached Fe^{3+} that could promote oxidation of Or-II. Such possibility arises from the Fe^{3+} complexing capacity with organic compounds in solution under UV irradiation [22]. However, that possible leaching did not increase the dye oxidation under the different light irradiation systems used here. Therefore, the photooxidation pathway of the Fe-TiO_2 photocatalyst is due to a photodynamic effect in which Or-II photosensitizes Fe-TiO_2 particles; process promoted by the presence of Fe.

2.2.3. Fe promoted electron caption mechanism under UV-Vis irradiation

To understand the photooxidation mechanism it is important to evaluate the recombination of the photogenerated charges and its interaction with Fe. The photocatalytic oxidation of phenol using TiO_2 has been proved to be due to the indirect oxidation with $^{\bullet}OH$ radicals [23-25]. Therefore, it is possible to get indirect information of the recombination when degrading phenol since $^{\bullet}OH$ is directly related to the photoproduction of “holes”.

Fig. 2.7 shows the photocatalytic degradation of phenol after 2 h of UV by the Fe-TiO_2 and TiO_2 samples. In this case Fe insertion in the TiO_2 matrix decreases photoactivity, thus, under UV irradiations there is a negative main effect of the Fe in the TiO_2 matrix. Consequently, after the TiO_2 excitation by UV light, Fe ions may act as traps for the photogenerated e^- - h^+ (Eqs. (2.1) and (2.2)) and interact promoting the recombination (Eq. (2.3)) decreasing the TiO_2 photoactivity.

Furthermore, the performance of the photocatalysts towards phenol photooxidation under 6 h of Vis light irradiation (data not shown) was almost zero, suggesting no activation of the photocatalyst by this type of irradiation.

$Fe^{3+} + h^+ \rightarrow Fe^{4+}$ (2.1)

$Fe^{3+} + e^- \rightarrow Fe^{2+}$ (2.2)

$Fe^{2+} + Fe^{4+} \rightarrow (e^- - h^+) + Fe^{3+}$ (2.3)

In addition, possible Fe^{3+} leaching did not promote the phenol degradation in Fenton like reactions promoted by H_2O_2 production during TiO_2 irradiation. Therefore, these results also discard the effect of leached Fe in the photocatalytic process.

Fig. 2.7 Photocatalytic degradation of phenol during 2 h of UV irradiation by the (○) TiO_2, and, Fe(x)-TiO_2 samples, x = Fe nominal mol% of: (■) 0.5, (▲) 1, and, (x) 3.

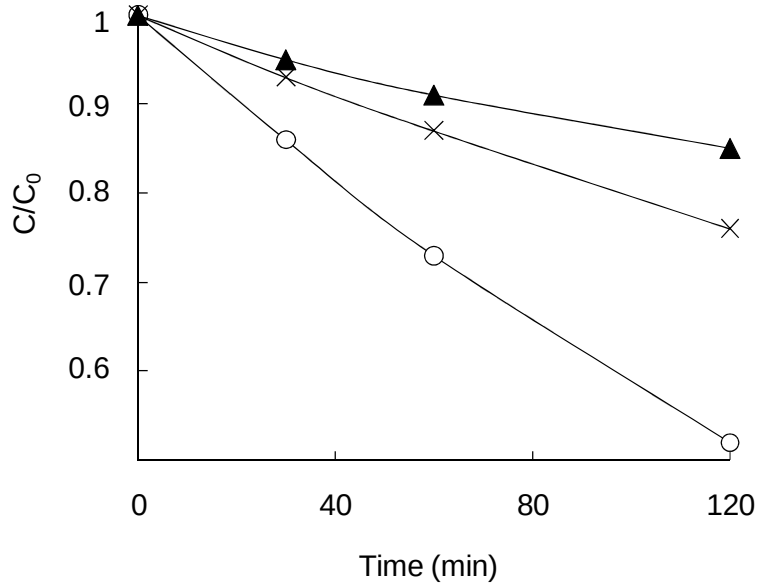

Source: the Author.

As observed above, in contrast to the diminished activity of Fe-TiO_2 towards the phenol degradation, there was an increase in photoactivity of the Fe modified TiO_2 samples towards the photodegradation of Or-II under UV-Vis light irradiation, therefore suggesting that photoactivity is due to the simultaneous irradiation of the system under Vis and UV irradiation. This assumption implies a possible photodynamic mechanism of photooxidation in which there is an interaction between the Or-II molecule and the Fe-TiO_2 surface. In DRS and XPS analyses it was suggested the presence of Fe_2O_3.

Therefore, Fe_2O_3 increase the TiO_2's electron caption capacity from photosensitizers. Hence, Vis-light-photoexcited Or-II (Or-II*; LUMO state) injects an e^- to the Fe-TiO_2 particles promoting the formation of reactive oxygen species, such as, superoxide radical ($O_2^{\bullet-}$) to efficiently oxidize the Or-II molecule. Hence, the photooxidation of Or-II is due to a double oxidation pathway: i) the selfdegradation of the molecule due to the loss of energy in the injection of the e^- to the TiO_2, and ii) the oxidation caused by the photoproduced oxidative species in the Or-II photosensitization promoted by Fe in the TiO_2 photocatalyst.

Fig. 2.8 shows a scheme of the double oxidation pathway proposed for the photodegradation of the Or-II due to UV-Vis irradiation of the Fe-TiO_2 photocatalyst.

Fig. 2.8 The energy band diagram for the suggested mechanism of oxidation of Or-II involving the iron species: Fe^{3+}/Fe_2O_3 and TiO_2 under solar light irradiation.

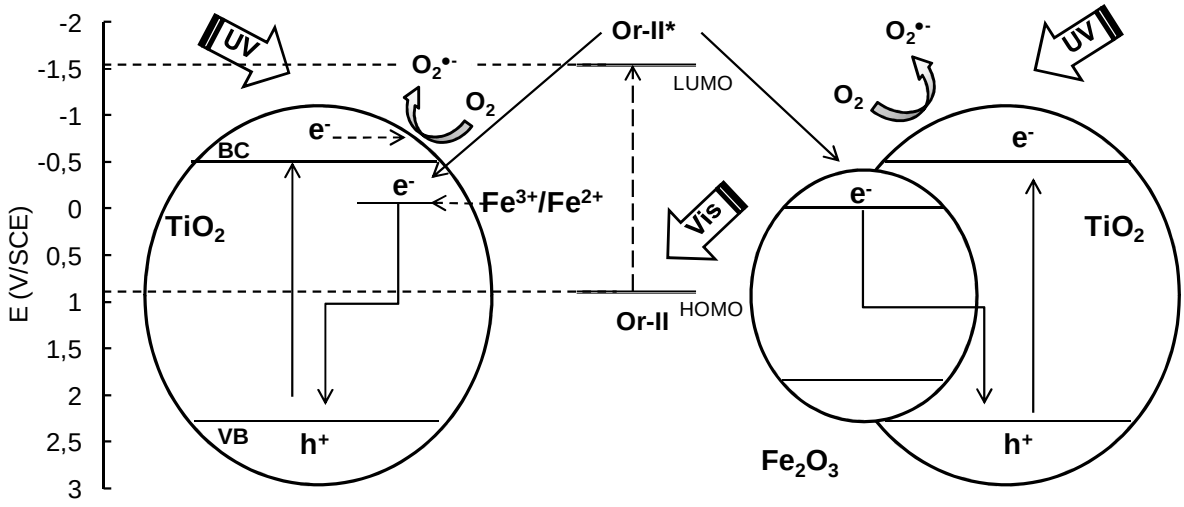

Source: The author.

Thermodinamics dictate that Fe_2O_3, or the Fe^{3+}/Fe^{2+}, cannot reduce O_2 to form $O_2^{\bullet-}$ since the $O_2/O_2^{\bullet-}$ redox potential lies at ~ -0.51 V vs SCE[3] (Standard Chalomel Electrode) above the conduction band of Fe_2O_3 at ~ 0.3 V vs SCE [26]. Therefore, Or-II's LUMO state, positioned at ~ -1.5 V vs SCE [27], can inject one electron to the Fe_2O_3

[3] The SCE is commonly used as a reference for the electrochemical measurements of redox potentials.

conduction band or the new energy state promoted by Fe^{3+}; e^- not related to the formation of oxidative radicals. Then, this e^- may stabilize the photogenerated hole (h^+) in the TiO_2's valence band. This process leaves free the photogenerated e^- in the TiO_2's conduction band to effectively reduce O_2 to form $O_2^{\bullet-}$, thus also involving a photocatalytic process. This process could explain that simultaneous irradiation of UV and Vis is strictly necessary to promote the photoactivity of Fe-TiO_2 since the Or-II excitation occurs under visible light, while photogeneration of the TiO_2's e^-_{CB} is possible under UV irradiation.

As a result, these materials have a potential as heterogeneous photocatalysts in the degradation of azo dyes, or to promote an electron flux in dye photosensitized TiO_2 for artificial photosynthesis due to its increased electron caption capacity.

2.3. Conclusions

The chosen hydrothermal synthesis route leads to the formation of TiO_2 particles constituted of anatase phase, with Fe species:Fe^{3+}/ Fe_2O_3. Iron effectively promotes visible light absorption of TiO_2, even so, enhancing the recombination of the photogenerated electron – hole pair, as observed in the photocatalytic degradation of phenol under UV irradiation.

However, the analysis of the mineralization of the Orange II (Or-II) dye by Fe-TiO_2 photocatalysts, under different illumination set-ups, suggested the Fe promotion of the electron caption in TiO_2 photosensitization by Or-II under solar-simulated light irradiation. Such interaction leads to a double oxidation pathway of the Or-II molecule: i) the selfdegradation due to the charge injection to the TiO_2 from its excited state, and ii) the oxidation caused by oxidative species produced in the photosensitization of the Fe-TiO_2 photocatalyst.

References

[1] O. Carp, C.L. Huisman, A. Reller, *Photoinduced reactivity of titanium dioxide*, Progress in Solid State Chemistry, 32 (2004) 33-177.

[2] Z. Li, W. Shen, W. He, X. Zu, *Effect of Fe-doped TiO_2 nanoparticle derived from modified hydrothermal process on the photocatalytic degradation performance on methylene blue*, J. Hazard. Mat., 155 (2008) 590-594.

[3] C. Hu, Y. Lan, J. Qu, X. Hu, A. Wang, *Ag/AgBr/TiO_2 Visible light photocatalyst for the destruction of azodyes and bacteria*, J. Phys. Chem. B, 110 (2006) 4066-4072.

[4] D. Gumy, C. Morais, P. Bowen, C. Pulgarín, S.A. Giraldo, R. Hajdu, J. Kiwi, *Catalytic activity of commercial TiO_2 powders for the abatement of the bacteria (E. coli) under solar simulated light: Influence of the isoelectric point*, Appl. Catal. B: Env., 63 (2006) 76-84.

[5] A.G. Rincón, C. Pulgarin, *Photocatalytic inactivation of E. Coli: effect of (continous-intermittent) light intensity and of (suspended-fixed) TiO_2 concentration*, Appl. Catal. B: Env., 44 (2003) 263-284.

[6] L. Zan, W. Fa, T. Peng, Z. Gong, *Photocatalysis effect of nanometer TiO_2 and TiO_2-coated ceramic plate on Hepatitis B*, J. Photochem. Photobiol. B: Biol., 86 (2007) 165-169.

[7] M.I. Litter, J.A. Navío, *Photocatalytic properties of iron doped-titania semiconductors*, J. Photochem. Photobiol. A: Chem., 98 (1996) 171-181.

[8] M.A. Khan, S.I. Woo, O. Yang, *Hydrothermally stabilized Fe(III) doped titania active under visible light for water splitting reaction*, Int. J. Hydrogen Energy, 33 (2008) 5345-5351.

[9] S. Liu, Y. Chen, *Enhanced photocatalytic activity of TiO_2 powders doped by Fe unevenly*, Catal. Commun., 10 (2009) 894-899.

[10] E. Piera, M.I. Tejedor, M.E. Zorn, M.A. Anderson, *Relationship concerning the nature and concentration of Fe(III) species on the surface of TiO_2 particles and photocatalytic activity of the catalyst*, Appl. Catal. B: Env., 46 (2003) 671-685.

[11] Y. Wu, J. Zhang, L. Xiao, F. Chen, *Preparation and characterization of TiO_2 photocatalyst by Fe^{3+} doping together with Au deposition for the degradation of organic pollutants*, Appl. Catal. B: Env., 88 (2008) 525-532.

[12] K. Mizushima, M. Tanaka, S. Lida*, Energy levels of iron group impurities in TiO_2*, J. Phys. Soc. Jpn., 32 (1972) 1519-1524.

[13] N. Todorova, T. Giannakopoulou, G. Romanos, T. Vaimakis, J. Yu, C. Trapalis, *Preparation of fluorine-Doped TiO_2 Photocatalysts with Controlled Crystalline Structure*, Int. J. Photoener., 2008 (2008) p. 1-9.

[14] M.C. Biesinger, L.W. Lau., A.R. Gerson, R.S. Smart, *Resolving surface chemical states in XPS analysis of first row transition metals oxides and hydroxides: Sc, Ti, V, Cu and Zn*, Appl. Surf. Sci., 2010, doi: 10.1016/j.apsusc.2010.07.086

[15] K.M. Parida, G.K. Pradhan, *Sol-gel synthesis and characterization of mesoporous iron-titanium mixed oxide for catalytic application*, Mat. Chem. Phys., 123 (2010) 427-433.

[16] Z. Ambrus, N. Balázs, T. Alapi, G. Wittmann, P. Sipos, A. Dombi, K. Mogyorósi, *Synthesis, structure and photocatalytic properties of Fe(III)-doped TiO_2 prepared from $TiCl_3$*, Appl. Catal. B: Env., 81 (2008) 27-37.

[17] E.D. Jeong, P.H. Borse, J.S. Jang, J.S. Lee, O.S. Jung, H. Chang, J.S. Jin, M.S. Won, H.G. Kim, *Hydrothermal syntehsis of Cr and Fe co-doped TiO_2 nanoparticle photocatalyst*, J. Ceram. Process. Res., 9 (2008) 250-253.

[18] S.W. Bae, P.H. Borse, S.J. Hong, J.S. Jang, J.S. Lee, E.D. Jeong, T.E. Hong, J.H. Yoon, H.G. Kim, *Photophysical properties of nanosized metal-doped TiO_2 photocatalyst working undeer visible light*, J. Korean Phys. Soc., 51 (2007) S22-S26.

[19] J. Li, J. Xu, W.L. Dai, K. Fan, *Direct hydro-alcohol thermal synthesis of special core-shell structured Fe-doped titania microspheres with extended visible light response and enhanced photoactivity*, Appl. Catal. B: Env., 85 (2009) 162-170.

[20] B. Xin, Z. Ren, H. Hu, X. Zhang, C. Dong, K. Shi, L. Jing, H. Fu, *Photocatalytic activity and interfacial carrier transfer of Ag-TiO_2 nanoparticle films*, Appl. Surf. Sci., 252 (2005) 2050-2055.

[21] J. Bandara, J. Kiwi, *Fast kinetic spectroscopy, decoloration and production of H_2O_2 induced by visible light in oxygenated solutions of the azo dye Orange II*, New J. Chem., 23 (1999) 717-724.

[22] W. Du, Y. Xu, Y. Wang, *Photoinduced Degradation of Orange II on different Iron (Hydr)oxides in aqueous suspension: Rate Enhancement on addition of Hydrogen Peroxide, Silver Nitrate and Sodium Fluoride*, Langmuir, 24 (2008) 175-181.

[23] A. Sobczynski, L. Duczman, W. Zmudzinsky, *Phenol destruction by photocatalysis on TiO_2: an attempt to solve the reaction mechanism*, J. Mol. Catal. A, 213 (2004) 225-230.

[24] P. Górska, A. Zaleska, J. Hupka, *Photodegradation of phenol by UV/TiO_2 and Vis/N,C-TiO_2 processes: comparative mechanistic and kinetic studies*, Sep. Purif. Technol., 68 (2009) 90-96.

[25] C.M. Miller, R.L. Valentine, *Mechanistic studies of surface catalyzed H_2O_2 decomposition and contaminant degradation in the presence of sand*, Water Res., 33 (1999) 2805-2816.

[26] M. Gratzel, *Energy resources through photochemistry and catalysis*, First ed., Academic Press Inc., New York, 1983.

[27] N. Helaïli, Y. Bessekhouad, A. Bouguelia, M. Trari, *Visible light degradation of Orange II using xCu_yO_z/TiO_2 heterojuncions*, J. Hazard. Mat., 168 (2009) 484-492.

3. Role of silver in the mechanisms of light excitation and Ag-TiO_2 performance towards the photoinactivation of *E. coli* in water

Abstract

Ag loaded TiO_2 was applied in the photocatalytic inactivation of *Escherichia coli* under ultraviolet (UV) and visible (Vis) light irradiations. Ag loading of TiO_2 enhanced the photocatalytic disinfecting effect under visible light irradiation by promoting the formation of ROS, such as, singlet oxygen ($^1O_2$), superoxide ($O_2^{\bullet-}$) and hydroxyl ($^{\bullet}OH$) radicals, as identified by electron paramagnetic resonance spectroscopy (EPR) measurements using the spin trap probe TMP-OH, and also, the detection of the by-product TEMPONE. Ag species undergo an oxidation process in the TiO_2 matrix under irradiation of UV or Vis light, as observed in XPS analyses. UV pre-irradiation of the material totally diminished the photodisinfection activity under subsequent Vis light irradiation. Under UV irradiation, the degradation of dichloroacetic acid (DCA), directly related to the photoproduced holes in TiO_2, was inhibited by the presence of Ag suggesting that oxidation of Ag^0 to Ag^+/Ag^{2+} is faster than the oxidative path of the TiO_2's holes on DCA molecules. Furthermore, the photoassisted increased Ag^+ concentration on TiO_2's surface enhances the bacteriostatic activity of the material in dark periods. Moreover, the latter dark contact of the Ag^+-TiO_2 material and *E. coli* seems to recover Ag-TiO_2 and its bactericidal photoactivity under visible light irradiation suggesting a reductive "bioregeneration" of the photocatalyst.

3.1. Introduction

TiO_2 photocatalysis has been subject of research interest in the last two decades as a promising technique to solve environmental problems such as water disinfection and organic pollutants degradation [1-4]. Silver doping has been used to prop up the absorption of visible light, as well as, the photoactivity of TiO_2 [5-7]. Light absorption of Ag loaded TiO_2 (Ag-TiO_2) covers a wider spectral range than TiO_2, ranging from UV to visible wavelengths up to 600 nm [5, 6, 8]. Such increase in absorption arises from a recently proposed phenomena in which the incident light excites the conduction band electrons promoting collective oscillations [9] and the enhancement of the local electric field of the particles [6], known as the surface plasmon resonance (SPR) of metallic nanoparticles. SPR directly depends on the geometry and composition of the metallic particle [9].

These interactions of Ag metallic particles and the incident light irradiation enhance the photoactivity of TiO_2 towards the photocatalytic inactivation of *E. coli* [8, 10]. Akhavan *et al.* have proposed a decrease in the recombination of the TiO_2 photogenerated charges that enhances the photocatalytic inactivation of *E. coli* [8]. Moreover, the antimicrobial activity of Ag-TiO_2 was found to depend on the microbial strain, the Ag content and the Ag reducing agent used in the synthesis [10] of the photocatalyst. In addition, there has been a growing interest in development of antimicrobial devices containing silver for medical applications due to its well-known bacteriostatic activity [11, 12].

Furthermore, interesting optic characteristics of the Ag-TiO_2 photocatalyst has been observed in multicolor photochromism, in which, electron transitions involving Ag and TiO_2 induce reductions and oxidations of the contained silver atoms [13] thus promoting different colors on the surface of the photocatalyst's particles [14, 15]. Such electrons may also be transferred to molecular oxygen [14], thus leading to a more efficient ROS production and to the higher photoactivity. However, the underlying mechanisms of such enhanced photoactivity are still under debate.

The aim of this study was to investigate the photocatalytic features of Ag-TiO_2 towards the photocatalytic disinfection of *E. coli* in water suspensions. Ultraviolet and visible light were used to suggest the mechanisms of light activation and photoactivity. Ag loading was found to remarkably increase the photoactivity of TiO_2 under visible light, which is related to the generation of singlet oxygen ($^1O_2$), superoxide ($O_2^{\bullet-}$) and hydroxyl ($^{\bullet}OH$) radicals. To understand the mechanisms of photoactivity of the Ag modified TiO_2 samples it was necessary to evaluate the effect of pre-irradiation, using different light set-ups, on the photoactivity and XPS spectra of the samples. The mechanisms were complemented by ROS detection using electron paramagnetic resonance spectroscopy (EPR) using the spin trap probe 2,2,6,6-tetramethyl-4-piperidinol (TMP-OH) in D_2O and standard water suspensions. In addition, post-irradiation experiments evidenced the increase in the bacteriostatic activity of the Ag-TiO_2 photocatalyst due to the increase in the content of surface Ag oxidized states.

3.2. Experimental

3.2.1. Photocatalysts Synthesis

The photocatalysts were synthesized using the hydrothermal synthesis as follows: 3.8 mL of titanium isopropoxide (Fluka) was added dropwise to 19 mL of isopropanol (Merck). Then, an adequate amount of $AgNO_3$ (Merck) was diluted in 2 mL of water at pH of 1.5 adjusted with HNO_3 (65%, Merck). Ag aqueous solution was added dropwise to the isopropoxide-isopropanol solution. The Ag content was adjusted to a nominal molar percentage of 0.5, 2 and 4 (mol%). Then, the formed gel was steam pressure treated using an autoclave for 3 h at 120℃ and ~14 4 KPa. The TiO_2 sample was obtained following the described procedure, but in this case, without the addition of $AgNO_3$ in the water for hydrolysis. The obtained wet crystals were manually ground in mortar, dried in oven at 60℃ for 12 h, and finally kept in dark to avoid surface oxidation of the samples. Photocatalyst were labeled using the nomenclature: Ag(x)-TiO_2, where x corresponds to the Ag mol%.

3.2.2. Photocatalysts Characterization

DRS and XRD analyses of the Ag(x)-TiO_2 samples were recorded using the same procedure and equipment described in chapter 2.

X-ray photoelectron spectroscopy measurements

Photocatalysts were XPS analyzed to determine the species involved in the photocatalytic activity of the fresh Ag loaded TiO_2 and the unloaded TiO_2 samples. In addition, in order to follow the Ag states in the Ag-TiO_2 sample after a typical photocatalytic test two 1 $g.L^{-1}$ suspensions of Ag(2)-TiO_2 samples, without the addition of *E. coli*, were submitted to Vis and UV irradiation for 2 h, filtered and dried in oven at 60℃. Subsequently, the pre-irradiated samples were further XPS analyzed. Analyses were carried out using procedures described in chapter 4. However, in this case the assignation of different Ag states in Ag 3d and Ti states in Ti 2p spectra were restricted by distances between Ag peaks of 6 eV [8] and 5.7 eV between peaks of Ti [16].

Electron paramagnetic Resonance Spectroscopy (EPR) - Reactive scavenging of ROS

2 mL of 0.3 $g.L^{-1}$ Ag(2)-TiO_2 suspension and $5x10^{-2}$ $mol.L^{-1}$ of the diamagnetic singlet oxygen scavenger 2,2,6,6-tetramethyl-4-piperidinol (TMP-OH, Fluka), was prepared in ultrapure H_2O, as well as, in D_2O (99.9% atomic purity from Aldrich). The suspensions were ultrasound treated for 1 min prior to illumination. Then, 1 mL aliquot of the suspension was transferred into a 5 mL Pyrex beaker and exposed to illumination under constant magnetic stirring with a white light halogen spot source of 150 W from OSRAM reference Gx5.3 (93638) emitting visible light. After subsequent time exposures, aliquots of ca. 7 µL of the illuminated suspensions were transferred into glass capillary tubes 0.7 mm ID and 0.87 mm OD, from VitroCom, NJ, USA. Tubes were sealed on both ends with Cha-Seal™ tube sealing compound (Medex International, Inc. USA). To maximize the sample volume in the active zone of the ESR cavity, assemblies consisting of seven of tightly packed capillaries were positioned in a wider quartz capillary (standard ESR

tube, 2.9 mm ID and 4 mm OD, Wilmad LabGlass, Vineland, NJ, USA). Such setup resulted in ca. 65 µL sample volume in the active zone of the ESR cavity, thus markedly improving the overall sensitivity of measurements [17].

EPR experiments were carried out at room temperature using an ESR300 spectrometer (Bruker BioSpin GmbH), equipped with standard rectangular mode TE_{102} cavity. Routinely, for each experimental point five-scan field-swept ESR spectra were recorded. The typical instrumental setting parameters were: microwave frequency: 9.38 GHz, microwave power: 2.0 mW, sweep width: 120 G, modulation frequency: 100 kHz, modulation amplitude: 0.5 G, receiver gain: $4x10^{-4}$, time constant: 20.48 ms, conversion time: 40.96 ms, and time per single scan: 41.9 s. The acquired EPR traces correspond to the second derivative of the sample´s paramagnetic absorption. A calibration point was made to correlate the double integrated signal, corresponding to the concentration, using a suspension of 100 µmol.L^{-1} of fresh solution of the stable nitroxide radical, 4-Hydroxy-2,2,6,6-tetramethylpiperidine 1-oxyl (TEMPOL, Sigma-Aldrich).

3.2.3. Photocatalytic activity tests

Photocatalytic tests were carried out using cylindrical Pyrex bottles (50 mL) with an aqueous suspension of the target contaminant (*E. coli* or dichloroacetic acid) and 1 g.L^{-1} of TiO_2. Irradiations set ups were: the described solar simulator *Suntest* chamber and the Vis and UV irradiation boxes.

Photocatalytic disinfection of water with E. coli K 12

The photocatalytic bactericidal activity was measured by sampling *E. coli* strain K 12 MG 1655 from the photoreactor. Before the experiment, bacteria were inoculated into Luria Bertani growth media (1% wt, Tryptone from Oxoid, 0.5% wt yeast extract from Oxoid, and 1% wt NaCl from Merck) and grown during 8 h at 37℃. During the stationary growth phase, bacteria were harvested by centrifugation at 5000 rpm for 10 min at 4℃. The obtained bacterial pellet was then washed three times with a saline solution (8 g.L^{-1}

NaCl and 0.8 $g.L^{-1}$ KCl in Milli-Q water, pH 7 by addition of HCl or NaOH). A suitable cell concentration (10^7 colony forming units (CFU) per mL) was inoculated in the reactor's saline solution. Then, a suitable amount of photocatalyst was added to obtain a 1 $g.L^{-1}$ concentration. Subsequently, the suspensions were illuminated during 2 h and samples (1 mL) were taken at different time intervals. Serial dilutions were performed in saline solution and 10 µL samples were inoculated 4 times in plate count agar (PCA, Merck). The number of colonies was counted after 24 h of incubation at 37℃.

Pre and Post-irradiation experiments

Pre-irradiation experiments were carried out to understand the effect of a previous process of irradiation on the photocatalytic activity of the samples. In this case, two Ag(2)-TiO_2 suspensions of 1 $g.L^{-1}$ were irradiated one under Vis, and the other one under UV during 4 h. Immediately after, a suitable aliquot of the harvested *E. coli* suspension, described above, was added to the suspension and subsequently irradiated under visible light for 2 h. Samples were taken at different time intervals.

Two different post-irradiation experiments were made, one after the other. The Ag(4)-TiO_2 sample was used in order to increase the Ag concentration on the photocatalyst surface to analyze the bacteriostatic activity of the sample under dark-contact processes with *E. coli*. First, in order to evaluate the effect of UV pre-irradiation on the bacteriostatic activity of the photocatalyst an experiment in dark was done, in which, *E. coli* was added to an aqueous suspension of a Ag(4)-TiO_2 sample that was UV pre-irradiated for 10 h. This suspension (*E. coli* + UV preirradiated Ag(4)-TiO_2) was constantly stirred during another 10 h and samples were taken in time intervals of 2 h. This used photocatalyst suspension will be referred as "used-in-dark". For comparison purposes a fresh Ag(4)-TiO_2 sample was suspended and evaluated in dark using the same procedure described above. Second, in order to evaluate possible changes in the photoactivity due to the described dark processes the used-in-dark suspension was evaluated towards the *E. coli* photocatalytic inactivation under visible light irradiation. In

this case, *E. coli* was added to the used-in-dark Ag(4)-TiO_2 suspension after the described 10 h dark process and was further submitted to Vis irradiation for 3 h. Samples were taken at different time intervals. The correspondent blank experiment using the used-in-dark Ag(4)-TiO_2 was made under dark to evaluate the remain bacteriostatic activity after the dark process.

Photocatalytic degradation of dichloroacetic acid (DCA)

A DCA solution containing $1x10^{-3}$ $mol.L^{-1}$ and 1 $g.L^{-1}$ of the Ag(2)-TiO_2 sample was added to the Pyrex glass reactors . Samples were taken and filtered by 0.2 µm membranes. DCA concentration was followed by HPLC analysis with a Hewlett Packard series 1100 equipment using a column Supelcogel H at 60℃. H_2SO_4 solution 5.10^{-3} $mol.L^{-1}$ was used as mobile phase. Detection was done by a refractive index detector.

Data hereby reported is expressed as C/C_0, where C stands for the molar concentration of DCA. The initial concentration (C_0) is the concentration reached in the suspension of TiO_2 and DCA after 1 h of stirring prior to the illumination.

3.3. Results

3.3.1. Photocatalyst characterization before and after UV and Vis light irradiations

Fig. 3.1 shows the Ag 3d high resolution XPS spectra of the fresh and the UV and Vis irradiated Ag(2)-TiO_2 samples. The spectra of the fresh Ag(2)-TiO_2 sample (Fig. 3.1a) consists of two individuals peaks at 374.6 and 368.6 eV assigned to Ag $3d_{5/2}$ and Ag $3d_{3/2}$ respectively. Furthermore, after peak deconvolution it is observed the presence of two different chemical states of Ag; the peak at 368.4 eV can be assigned to Ag^+ species [8, 18], while the peak 368.7 eV is attributed to Ag^0 [8, 19]. These results suggest the coexistence of Ag_2O and metallic Ag in the TiO_2 matrix. Since the precursor Ag solution is constituted by Ag^+ ions, silver may be partially reduced by action of isopropanol [20] forming the metallic species, thus, explaining the coexistence of both chemical states.

Fig. 3.1 XPS Ag 3d spectra of the: a) fresh, b) UV, and, c) Vis irradiated Ag(2)-TiO_2 samples.

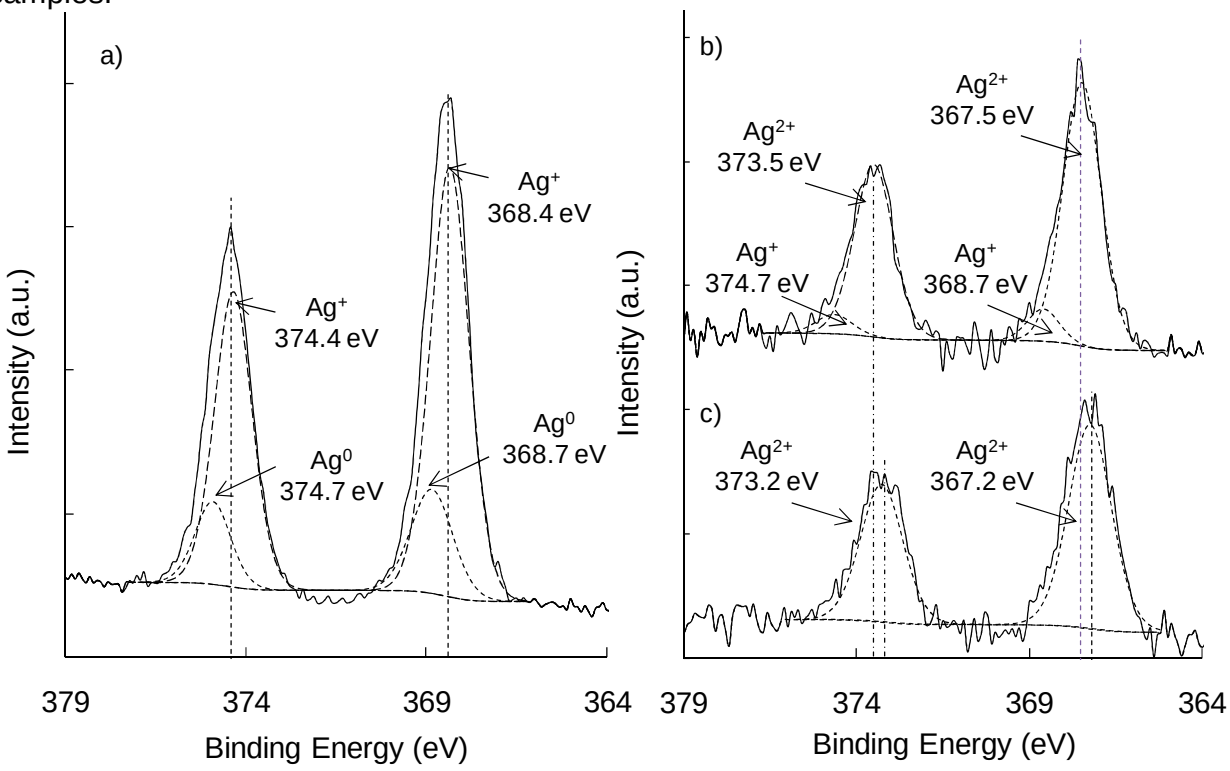

Source: The author.

The Vis (Fig. 3.1b) and UV (Fig. 3.1c) irradiated samples' spectra show a positive shift of 1.1 and 1.4 eV, respectively, positioning Ag $3d_{5/2}$ at 367.5 eV, Ag $3d_{3/2}$ at 373.5, for the Vis irradiated sample, and Ag $3d_{5/2}$ at 367.2 eV and Ag $3d_{3/2}$ at 373.2 eV, for the UV irradiated one. This suggests a decrease of the reduced Ag species, for the Vis irradiated sample, and the formation of new oxidized ones that can be related to Ag^+ in Ag_2O and Ag^{2+} in AgO as observed in XPS studies of mixed Ag compounds by Kaushik [21]. For the UV irradiated sample it was not possible to assign a peak for Ag^+ following constraints and restrictions suggested by Akhavan *et al.* [8]. Instead, it is observed a peak assigned to Ag^{2+} at 367.2 eV. Hence, it is possible to suggest that concentration of Ag metallic species has remarkably decreased during irradiation of the Ag(2)-TiO_2

sample increasing the signals of the Ag oxidized states with a more notorious oxidative effect due to UV irradiation.

Fig. 3.2 shows the Ti 2p XPS of the TiO_2 (Fig. 3.2a) and the Ag(2)TiO_2 (Fig. 3.2b) samples. The Ti 2p spectrum is constituted by two peaks at: 458.9 eV and 464.55 eV, assigned to Ti $2p_{3/2}$ and Ti $2p_{1/2}$, respectively, indicating a predominant state of Ti^{4+} in the surface of bare and Ag loaded samples [16, 22].

Fig. 3.2 XPS Ti 2p spectra of the: a) TiO_2 and b) fresh, c) UV, d) Vis irradiated Ag(2)TiO_2 samples.

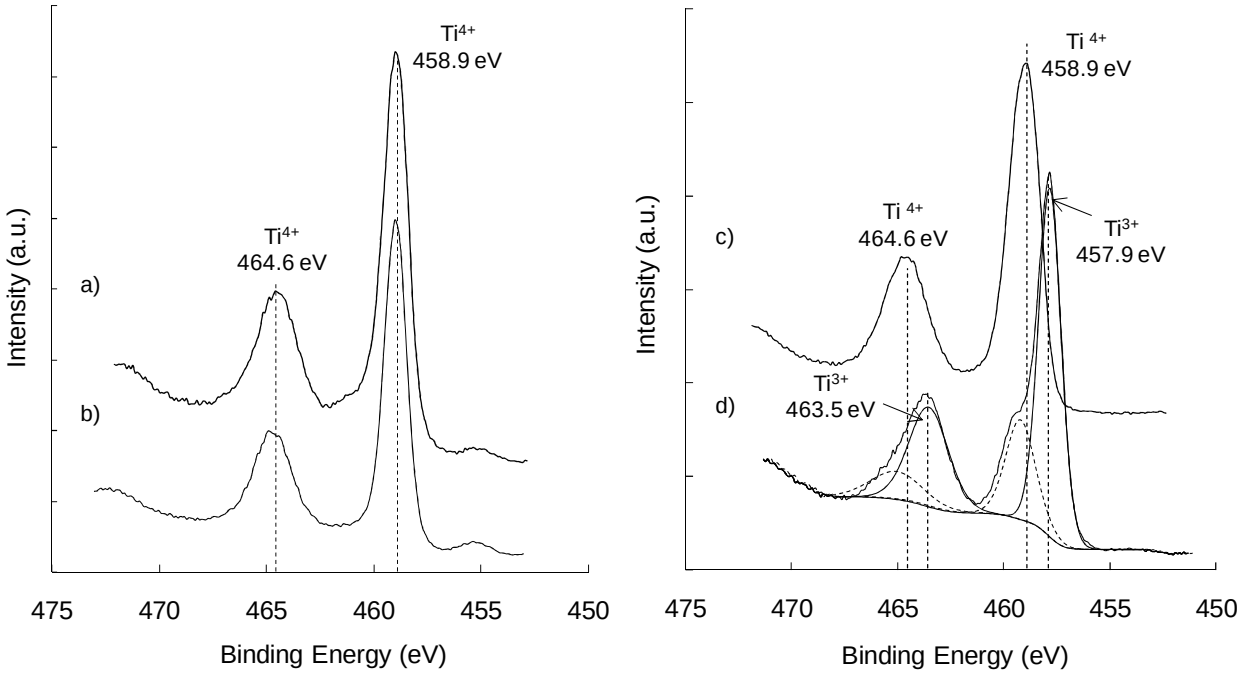

Source: The author.

No additional peaks could be assigned following constraints and restrictions suggested by Biesinger *et al.* [16]. Moreover, no shift was found for Ti 2p in Ag loaded TiO_2 sample's spectrum suggesting the absence of chemical bonds between Ag and Ti. In addition, as observed in Fig. 3.2c, visible light irradiation did not change the spectrum of the fresh Ag(2)-TiO_2 sample while UV (Fig. 2d) induced the reduction of the intensity of Ti^{4+} at 458.9 eV signal and the formation of a second peak at 457.9 eV assigned to Ti^{3+}

species in Ti_2O_3 [23]. The formation of the new signal is accompanied by a shift of the Ti $2p_{1/2}$ peak by 1.1 eV, also, due to the formation of a second Ti^{3+} peak (not shown) that corresponds to the Ti 2p doublet. Therefore, UV irradiation induces dramatic changes in the surface chemical composition of the Ag(2)-TiO_2 sample that are expected to have an important effect on the photoactivity of the photocatalyst.

On the other hand, XRD analyses confirmed anatase as the primary phase constituting the crystalline structure of Ag modified and unmodified TiO_2 (data not shown). In addition, a slight signal of Ag_2O was detected in Ag(2)-TiO_2, and no signal was found for Ag metallic particles. As observed in XPS analyses Ag^+ exceeds in intensity the signal of Ag^0, then Ag metallic species concentration is low avoiding its detection in XRD analysis.

Fig. 3.3 shows the DRS spectra obtained by UV-Vis absorption data *vs* the wavelength of the light source in nm for the bare TiO_2 and the Ag(x)-TiO_2 samples with different Ag nominal concentrations of 0.5, 2 and 4%. An interesting light response was found for Ag loaded TiO_2 samples.The increase in Ag concentration induces a shift in the light absorption capacity to the visible region for wavelengths up to 800 nm. The Ag(4)-TiO_2 sample exhibits an absorption peak at around 470 nm. Such increase in visible light absorption could arise from a localized surface plasmon resonance (SPR) effect of Ag particles on the surface of TiO_2, which is confirmed by the characteristic shoulder in the absorption spectra. This is an indicative of the formation of nanometer sized and semispherical silver metallic particles corresponding to a size of approximately 4-30 nm [8, 24, 25].

These silver metallic particles can easily disperse into the TiO_2 matrix [5]. Probably, the formation of such particles allows the detection of a silver phase in the crystalline structure of the Ag(x)-TiO_2 sample as observed in XRD analyses not shown here.

Fig. 3.3 DRS spectra for the Ag(x)-TiO_2 samples, x = nominal molar percentages (mol%) of Ag in the TiO_2 matrix.

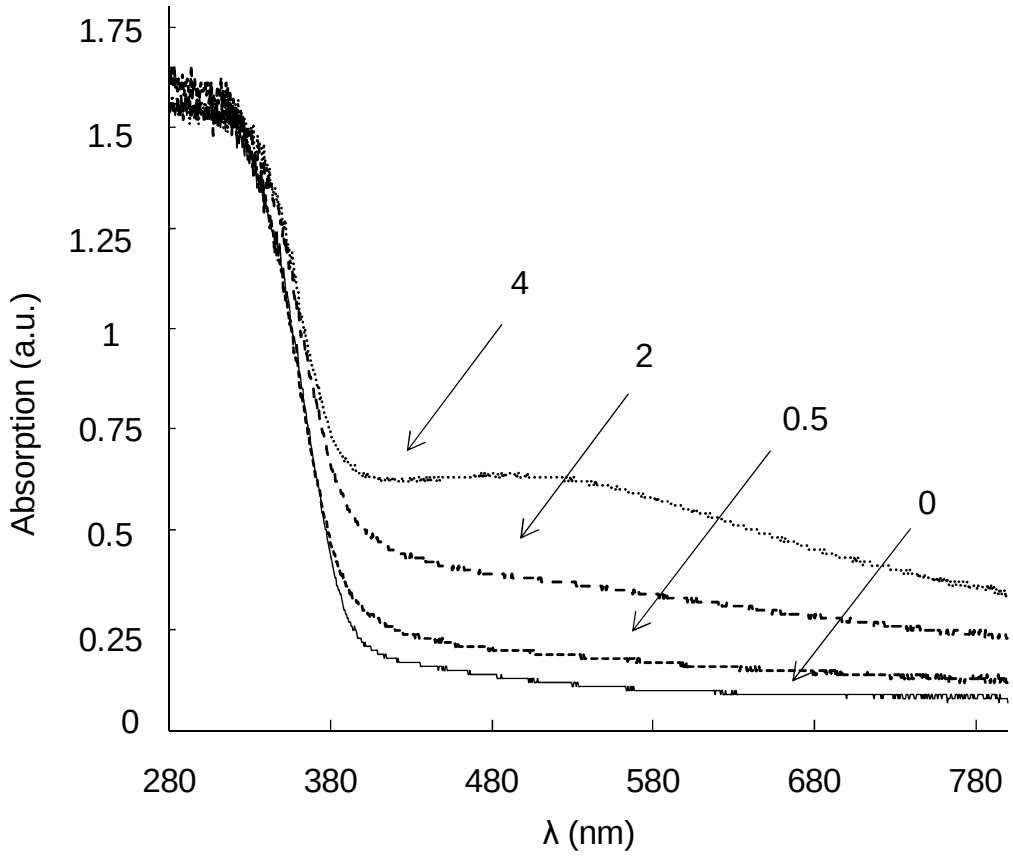

Source: The author.

3.3.2. Photocatalytic inactivation of *E. coli*

Fig. 3.4 shows the photocatalytic disinfection of water using the Ag loaded and bare TiO_2 samples under visible light, the insert shows the required time for total disinfection using different Ag nominal concentrations of 0.5, 2 and 4 mol% in the TiO_2's matrix. The Ag(2)-TiO_2 sample completes total *E. coli* inactivation within the first 60 min. of visible light irradiation while TiO_2 has a lower disinfection activity. Blank experiments using the Ag-TiO_2 sample under dark, and without photocatalyst under Vis irradiation, suggest the absence of: i) toxicity of the photocatalyst, and, ii) disinfection activity of the Vis light

alone during the testing time. In addition, as observed in the insert of Fig. 3.4 there is an increase in the visible light photoactivity of TiO_2 when increasing the Ag nominal concentration up to 2 mol%, after which there seems to be no increase in the photoactivity. Xin *et al.* observed a decrease in photoactivity with increasing Ag concentration after 5 mol% loading and proposed that silver particles in excess act as recombination centers, as well as, decrease in TiO_2's light absorption [7].

Fig. 3.4 Photocatalytic inactivation of *E. coli* under visible light by: (Δ) Ag(2)-TiO_2, (●) TiO_2, (x) Light blank, and, (♦) Ag(2)-TiO_2 under dark. In the insert, the time needed for total inactivation by the Ag(x)-TiO_2 photocatalysts.

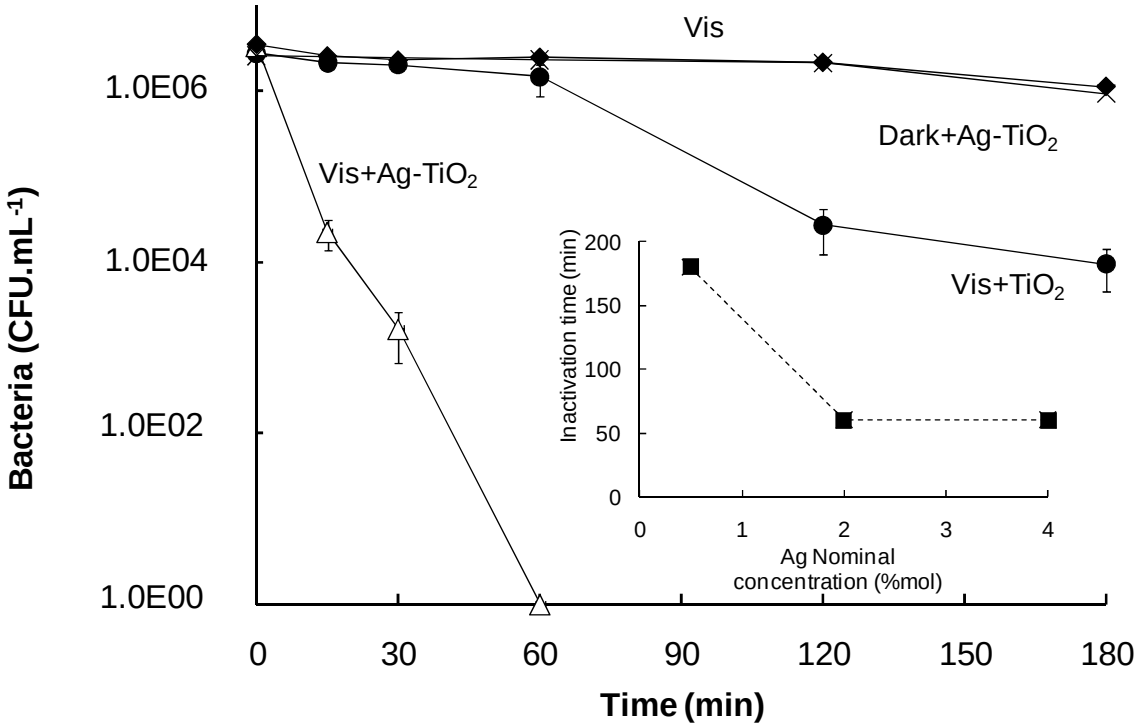

Source: The author.

Fig. 3.5 shows the disinfection performance of the photocatalysts under UV irradiation. In this case, the performance of the Ag(2)-TiO_2 sample was similar to that of the bare sample.

Fig. 3.5 Photocatalytic inactivation of *E. coli* under ultraviolet irradiation using the: (▲) Ag(2)-TiO_2, and, (●) TiO_2 samples.

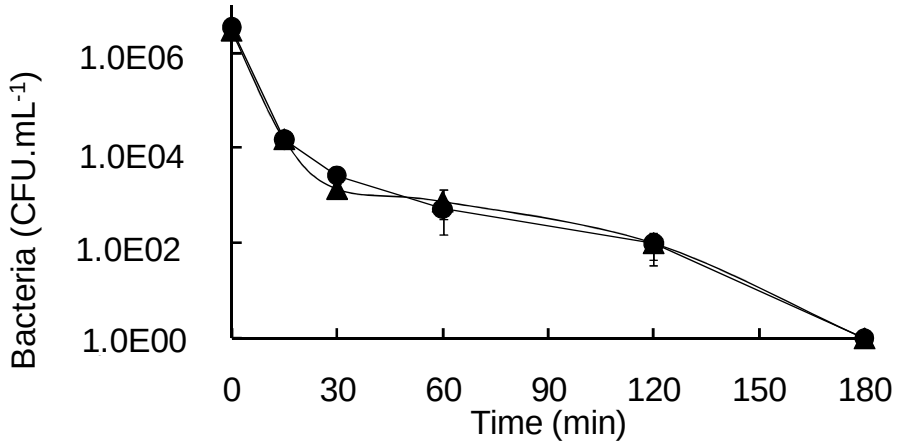

Source: The author.

Hence, UV irradiation does not photoactivate the Ag-TiO_2 photocatalyst to promote the inactivation of *E. coli* in water suspensions; this suggests different photoactivation mechanisms for Ag-TiO_2 and bare TiO_2.

Fig. 3.6 shows the photocatalytic disinfection activity under visible light irradiation of the Ag(2)-TiO_2 samples that were pre-irradiated for 2 h under: Vis (trace Δ), UV (trace O), and for comparison purposes; the fresh sample (trace x).

Fig. 3.6 Photocatalytic inactivation of *E. coli* under visible light using the fresh Ag(2)-TiO_2 (x), and Ag(2)-TiO_2 pre-irradiated samples under visible (Δ) and ultraviolet irradiation (○).

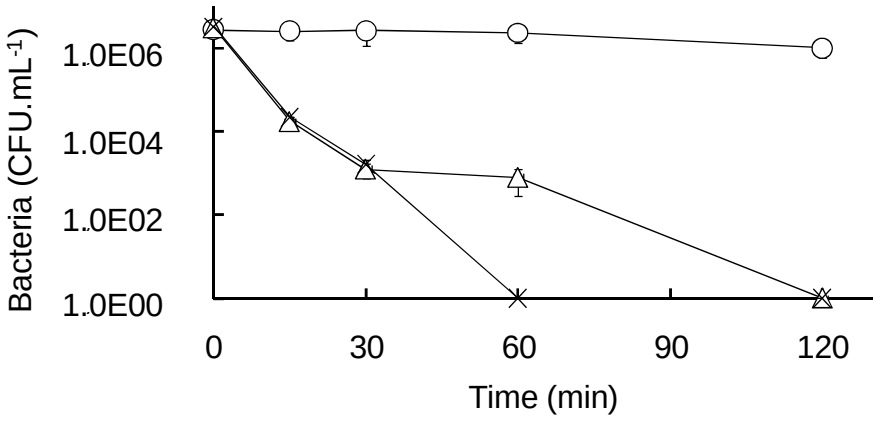

Source: The author.

The sample UV pre-irradiated has totally diminished its photocatalytic disinfecting activity under Vis. On the other side, the sample irradiated under Vis has a similar performance to that of the fresh sample.

3.3.3. Photocatalytic degradation of Dichloroacetic acid (DCA)

Fig. 3.7 shows the performance of the photocatalysts (Ag(2)-TiO_2 and TiO_2) in the photocatalytic degradation of DCA under Vis and UV irradiation. Vis light irradiation did not induce the photocatalytic degradation of the DCA using either of the samples.

Fig. 3.7 DCA Photocatalytic degradation using Ag(2)-TiO_2: under visible (Δ) and ultraviolet (▲) irradiations, and TiO_2 under visible (○) and ultraviolet (●) irradiations.

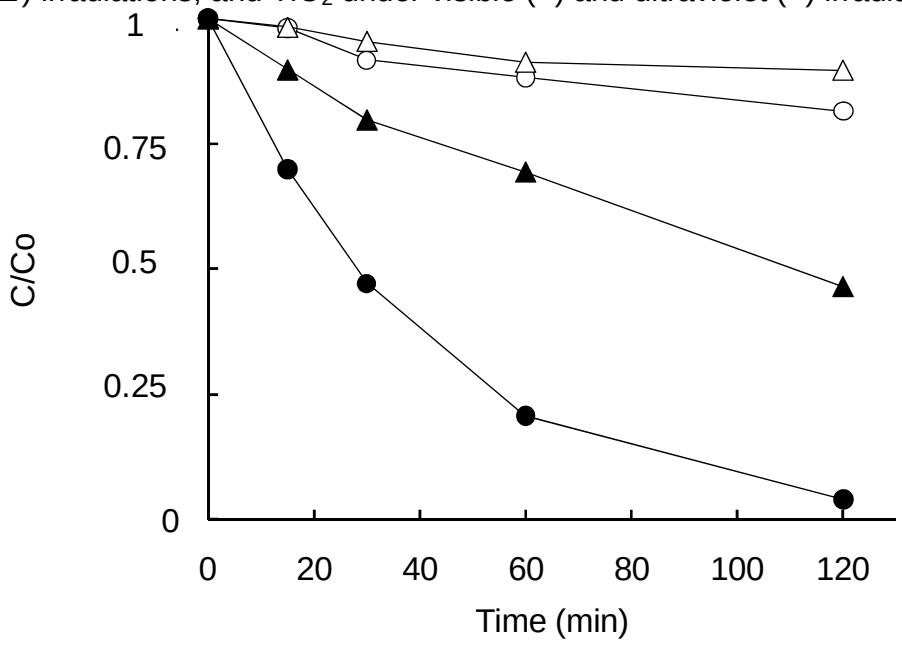

Source: The author.

On the other hand, under UV irradiation TiO_2 has a better performance than the Ag(2)-TiO_2 sample indicating a reduction in photoactivity due to the presence of Ag in the TiO_2's matrix.

3.3.4. Identification of ROS produced under Vis light irradiation of Ag(2)-TiO_2

The formation of reactive oxygen species (ROS), such as, singlet oxygen ($^1O_2$) and hydroxyl ($^{\bullet}OH$) radicals was monitored by electron paramagnetic resonance spectroscopy (EPR). It is well known that non-paramagnetic TMP-OH (nitroxide precursor) reacts with $^1O_2$, thus forming the paramagnetic product TEMPOL, which can easily be followed by ESR detection [26, 27]. Fig. 3.8 shows the concentration of TEMPOL reached after 100 min of visible light irradiation of suspensions of TiO_2 and Ag(2)-TiO_2 in D_2O.

Fig. 3.8 Photocatalytic productions of TEMPOL detected by EPR spin trapping using the (■) Ag(2)-TiO_2, and, (♦) TiO_2 samples. In the insert; the characteristic triplet signal obtained for the formation of TEMPOL using the Ag(2)-TiO_2 irradiated for 100 min under visible light.

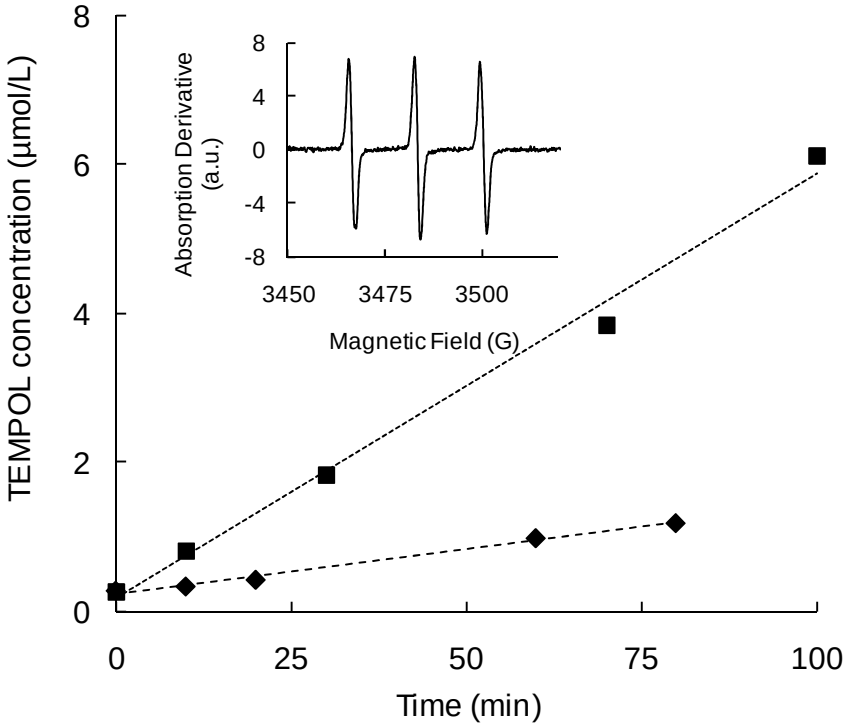

Source: The author.

Singlet oxygen formation was clearly evidenced for the irradiated suspension of Ag(2)-TiO_2 by observation of a characteristic 1:1:1 triplet signal of TEMPOL (spectral parameters. $\boldsymbol{D}$H=1.58 G, $\boldsymbol{a}_N$ =16.9 G, and $\boldsymbol{g}$=2.0066) as depicted in the inset to Fig 3.8. The Ag doped sample revealed an increase in the production of singlet oxygen formation in comparison to that of bare TiO_2. Moreover, new ROS were detected using standard water as solvent in EPR experiments. Fig. 3.9 shows the EPR signal obtained after 120 min of visible light irradiation of Ag(2)-TiO_2 suspensions using D_2O and H_2O as solvents.

Fig. 3.9 EPR spectra of the Ag(2)-TiO_2 sample and TMP-OH in aqueous and deuterium suspensions after 120 min of visible light irradiation. In the insert; a magnification of the absorption derivative signal between 3462 and 3474 Gauss.

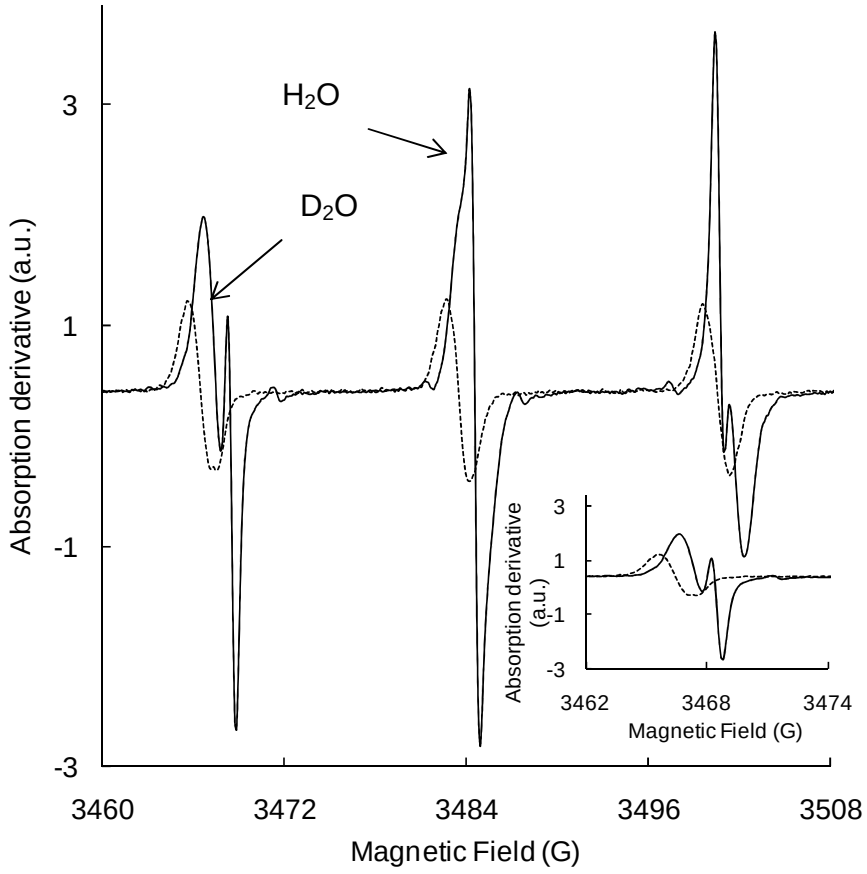

Source: The author.

The insert shows in detail the difference between the signals obtained using different solvents. A higher intensity of the triplet signal was observed for Ag(2)-TiO_2 than that obtained with TiO_2 both irradiated with Vis light in aqueous suspension.

It is well known that the lifetime of singlet oxygen increases in D_2O suspensions, which usually leads to reaction rate enhancement of singlet oxygen-mediated processes. Therefore, in the context of reactive scavenging of singlet oxygen with TMP-OH, such D_2O isotope effect results in increasing the EPR-detected TEMPOL signal. [26-28]. Though, in our case, there was a reversed isotopic effect. In particular, after 120 min of visible light irradiation, the EPR signal recorded in standard water increased by a factor of 3.2 in comparison to that obtained using D_2O.

Furthermore, an additional ESR signal, with spectral parameters ΔH=0.47 G, a_N =15.9 G, g=2.0065, was observed. This additional signal, overlapping with the signal of TEMPOL for the irradiated aqueous suspension of Ag(2)-TiO_2, corresponds to another nitroxide radical, TEMPONE. TEMPONE is a product of the attack of $^{\bullet}OH$ radicals on TEMPOL [29].The overall reduced rate of TEMPOL formation in D_2O is probably due to the lower quantum efficiency of the photocatalytic oxidation of the solvent for the formation of radicals, such as, "*deuteroxyl radicals*" ($^{\bullet}OD$), on the TiO_2's surface [30].

3.3.5. Post-irradiation events in dark and under light of the Ag-TiO_2 photocatalyst and *E. coli*

Fig. 3.10a shows the behavior of *E. coli* in dark contact with two samples of Ag(4)-TiO_2; the UV pre-irradiated sample for 10 h (trace ●), and, the fresh sample (trace ▲). The fresh Ag(4)-TiO_2 sample did not reduce the *E. coli* concentration during 10 h of dark suspension.

Fig. 3.10 Post-irradiation events using the Ag(4)-TiO_2 sample in contact with *E. coli* suspensions. a) under dark using: (▲) fresh, and, (●) UV pre-irradiated; b) The photocatalytic activity of the used-in-dark under: (●) visible irradiation, and, (■) dark as blank reference.

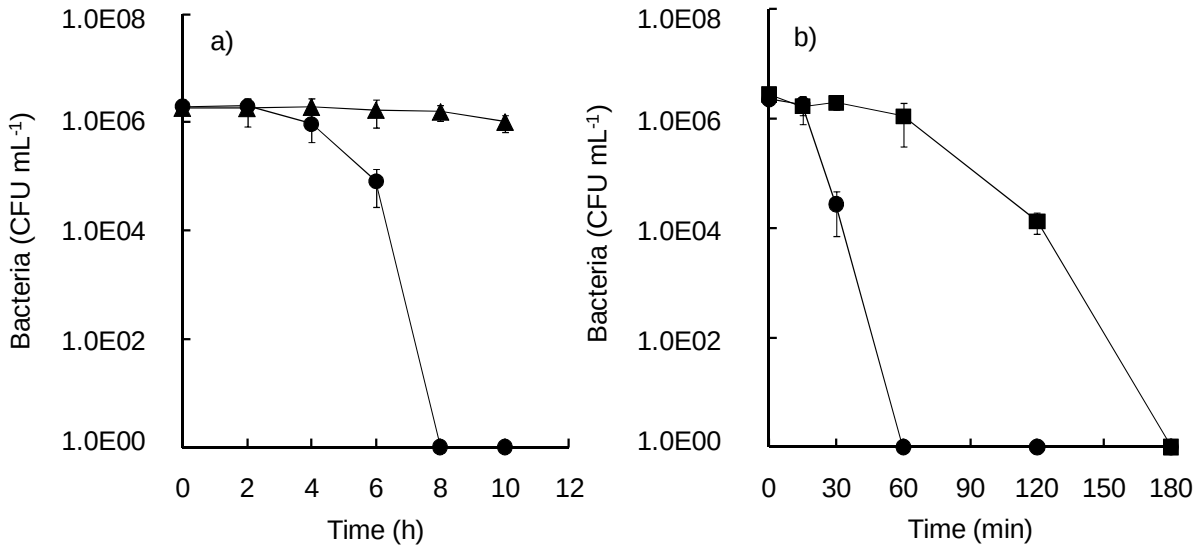

Source: The author.

On the contrary, the UV pre-irradiated Ag(4)-TiO_2 sample could initiate an effective disinfection after 4 h of dark suspension leading to a total decrease in the bacterial concentration in 8 h. Fig. 3.10b shows the performance of the used-in-dark Ag(4)-TiO_2 sample towards the Vis light photocatalytic *E. coli* inactivation (trace ●). In contrast, it was observed in Fig. 6 that UV irradiation led to the total decrease of the photoactivity. In this case, after a dark period, in dark contact with *E. coli*, the used-in-dark UV treated sample did recover part of its photoactivity since under visible light irradiation there was a total photocatalytic inactivation of *E. coli* within the first 60 min. In addition, the Ag(4)-TiO_2 remained its bacteriostatic activity and totally decreased bacteria concentration in 3 h as observed in Fig. 3.10 b (trace ■).

3.4. Discussion

3.4.1. Effect of Ag loading on the photocatalytic activity of TiO_2 under UV and Vis light irradiation

Results of characterization showed that Ag-TiO_2 is constituted by a TiO_2 matrix with Ag particles on the surface of the photocatalyst as observed in XPS analysis in Fig. 3.1. Such particles are formed by oxidized and reduced Ag species forming a AgO structure, as a minor crystalline phase, mixed with anatase as the major constituent as determined in XRD analysis. Moreover, DRS analysis showed an increase in Vis light absorption with a shoulder-peak at ~470 nm, which is characteristic of surface Ag particles with a special geometry suitable for the resonance of the Ag conduction band electrons with the incident visible light. This phenomenon is known as the SPR effect. In addition, this special configuration of the photocatalyst remarkably enhanced the photoactivity.

Ag(2)-TiO_2 sample with Ag^0 and Ag^+ species showed an increase in the visible light photoactivity towards *E. coli* inactivation. However, under UV irradiation the performance of the Ag(2)-TiO_2 sample was similar to that of TiO_2. Such features seem to be determined by the Ag chemical states: Ag^0 and Ag^+ in the Ag-(2)TiO_2's surface. UV pre-irradiation remarkably decreased concentration of the Ag reduced species and increased the presence of Ti^{3+} species observed in XPS analysis in Figs. 3.1 y 3.2. These dramatic changes on the surface's sample are related to a total decrease in photoactivity as observed in Fig. 3.6. Hence, results point the interaction between Ag^0 and TiO_2, promoted under visible light, as a determinant process in the photocatalytic activity of the material. In addition, XPS analysis showed a reduction of Ti^{4+} to Ti^{3+} species, suggesting the reduction of this beneficial interaction during UV irradiation.

Analysis of the photocatalytic degradation of DCA in Fig. 3.7 showed contrary results in the photoactivity of the Ag(2)-TiO_2 sample. It is customarily accepted that, after adsorption on the TiO_2's surface, DCA oxidation occurs due to photoproduced holes

(h^+_{VB}) by excitation of UV light [31, 32]. In our case, visible light did not promote DCA degradation using any of the samples. Probably, Ag could not promote the charge separation under visible light, and thus, there were no available photoproduced holes to oxidize DCA. In addition, under UV irradiation there was a decrease in photoactivity due to Ag loading. It is possible that photoproduced holes (h^+_{VB}) (Eq. 3.1) are being hindered from their oxidative action on DCA by the presence of Ag species on the photocatalyst's surface, thus, TiO_2's holes oxidize more rapidly the silver metallic species Ag^0 to Ag^+/Ag^{2+} (Eq. 3.2-3.3) than the DCA adsorbed molecules.

On the other hand, stabilized holes leave free the UV photogenerated electrons that may be responsible of the photoactivity of the Ag(2)-TiO_2 sample towards *E. coli* inactivation under UV irradiation, inducing the formation of ROS, thus, reaching the photoactivity of the TiO_2 sample as observed in Fig. 5.

$$TiO_2 + h\nu\ (\lambda < 400\ nm) \rightarrow h^+_{VB} \quad (3.1)$$

$$Ag^0 + h^+_{VB} \rightarrow Ag^+ \quad (3.2)$$

$$Ag^+ + h^+_{VB} \rightarrow Ag^{2+} \quad (3.3)$$

Ag^0 oxidation by TiO_2 in Ag-TiO_2 photocatalysts has been reported. The increased thickness of a Ag_2O film by oxidation of metallic Ag was suggested to be induced under irradiation in the interface of a TiO_2-Ag^0 thin film [33]. Moreover, photochromism of Ag-TiO_2 particles has been attributed to photooxidation of Ag^0 to Ag^+/Ag^{2+} in the TiO_2 matrix [14, 15]. It is important to note that electrons released from oxidation of the Ag metallic species, by UV photoproduced h^+_{VB}, induce the reduction of Ti^{4+} to form Ti^{3+} species as observed in XPS analysis in Fig. 3.2.

Therefore, since Vis irradiation did not increase the photoactivity towards DCA degradation of the Ag(2)-TiO_2 (Fig. 3.7), the silver metallic particles activated under visible light seem not to be related to the charge separation but to an increase in photoactivity towards *E. coli* inactivation. However, before proposing a mechanism of

light activation and generation of oxidative radicals mediated by Ag^0 loaded in a TiO_2 matrix it was necessary to follow the formations of ROS by EPR.

3.4.2. Mechanism of production of reactive oxygen species during the visible light irradiation of the Ag-TiO_2 photocatalyst

Zhang *et al.* [34] have proposed the formation of singlet oxygen by Rose Bengal enhanced by a surface plasmon resonance effect induced in the surface of silver particles. In addition, it was reported by Shcherbakov *et al.* [35] a mechanism in which metal oxides embedded in a semiconductor matrix, such as, V_2O_5/SiO_2 and MoO_3/SiO_2 photogenerated certain amounts of singlet oxygen when irradiated with a mercury lamp at room temperature. In this mechanism the illumination of the oxide generates an intermediate metallic oxide complex, $(Mo^{5+}\text{-}O^-)^*$, that promotes the photogeneration of $^1O_2$ in the presence of molecular oxygen (O_2) (Eq. 3.4), and a further regeneration of the initial chemical state of molybdenum.

$$(Mo^{6+} = O^{2-}) + h\nu \rightarrow (Mo^{5-}O^-) \rightarrow (Mo^{5+}\text{-}O^-)^* + O_2 \rightarrow (Mo^{6+} = O^{2-}) + {}^1O_2 \qquad (3.4)$$

However, in their study Shcherbakov *et al.* did not evidence the chemical states of the irradiated sample to confirm the return of the initial state of the metallic ion. Therefore, in our case it is possible to suggest the formation of $^1O_2$ is promoted by a plasmon resonance effect of silver particles on the surface of TiO_2 in which visible light excites Ag^0 (Eq. 3.5), thus, promoting electrons to the conduction band of TiO_2 and the formation of Ag^+ species. And finally, the conduction band electron is transferred to adsorbed O_2 molecules on TiO_2 surface promoting the singlet oxygen ($^1O_2$) generation, Eq. 3.6. Such energy transfer to oxygen has also been suggested using a hypocrellin B-chelated TiO_2 by Xu *et al.* [36].

$$Ag^0\text{-}TiO_2 + h\nu\ (\lambda > 400\ nm) \rightarrow Ag^+\text{-}TiO_2(e^-_{CB}) \qquad (3.5)$$

$$Ag^+\text{-}TiO_2(e^-_{CB}) + O_2 \rightarrow {}^1O_2 \qquad (3.6)$$

Singlet oxygen was found to be produced in non-equilibrium processes, which are related to electric fields created by extrinsic metal ions in semiconductors [37]. Such type of electric fields, produced by light irradiation, has been found to prop up electron excitation [19], thus, promoting photoactivity in Ag-TiO_2. Then, the formation of singlet oxygen is probably related to the interaction of the Vis-light-excited plasmonic Ag^0 particles on the surface of TiO_2 promoting energy transfer to O_2. Further investigations should be made to understand this phenomenon.

The production of $^1O_2$ by Ag^0-TiO_2 explains the enhanced photocatalytic activity towards *E. coli* inactivation. With a lifetime on the order of 3-5 μs in water, the diffusion of $^1O_2$ from its generation point is restricted to potential targets within a path length of approximately 0.1 μm [38], which may be enough for *E. coli* inactivation in aqueous suspensions under constant stirring as in our case. Virtually, a vast majority of cell types, from prokaryotic to mammalian cells, undergo irreversible damage leading to cell death by exposure to $^1O_2$ [27, 39, 40]. In addition, It has been proposed that generation of $^1O_2$ on TiO_2 surfaces could be enhanced in the microenvironment of the phospholipid membrane producing lipid peroxidation reactions leading to cell abatement [41]. Consequently, singlet oxygen may be responsible for *E. coli* inactivation in aqueous suspended Ag-TiO_2 irradiated with visible light.

Nevertheless, hydroxyl radical was found to be produced in EPR experiments during Vis irradiation as observed in Fig. 3.9. Probably, $^{\bullet}OH$ formation in standard H_2O may be induced by electron transferring processes between the excited Ag^0 particles and the conduction band of TiO_2 in water suspensions, as a consequence of the SPR effect. A possible route for $^{\bullet}OH$ formation is through chain reactions (Eqs. (3.7)-(3.11)) that may be started by the formation of superoxide radical ($O_2^{\bullet-}$) [1] involving O_2 and the TiO_2 conduction band promoted electron, Eq. 6.

$$O_2 + e^-_{CB} \rightarrow O_2^{\bullet-} \qquad (3.7)$$

Then, $O_2^{\bullet-}$ dismutation promotes the formation of H_2O_2,

$$O_2^{\bullet-} + H^+ \rightarrow HO_2^{\bullet-} \qquad pK_a = 4.88 \tag{3.8}$$

$$HO_2^{\bullet} + HO_2^{\bullet} \rightarrow H_2O_2 + O_2 \tag{3.9}$$

$$H_2O_2 + e^-_{CB} \rightarrow {}^{\bullet}OH + OH^- \tag{3.10}$$

$$H_2O_2 + O_2^{\bullet-} \rightarrow {}^{\bullet}OH + OH^- + O_2 \tag{3.11}$$

$O_2^{\bullet-}$ production may be enhanced by the e^- transfer from the excite Ag^0 particles to the TiO_2 conduction band. However, for $HO_2^{\bullet}$ formation a pH higher than the pK_a leads to an inversion of the reaction. A lack of $HO_2^{\bullet}$ inhibits the formation of H_2O_2 [1]. pH of the Ag-TiO_2 suspension is 6.5. Thus, it seems not to be possible the formation of $^{\bullet}OH$ through dismutation of $O_2^{\bullet-}$. Even so, Okuno *et al.* reported the enhanced $^{\bullet}OH$ formation from $O_2^{\bullet-}$ using organic selenium compounds in a buffered media at pH = 7.4 [42]. In this case, the selenium compounds act as electron donors in a dismutation reaction forming H_2O_2 from $O_2^{\bullet-}$. Then, the availability of e^- on the surface of Vis irradiated Ag-TiO_2 would probably induce dismutation of $O_2^{\bullet-}$, thus explaining the formation of $^{\bullet}OH$ radicals.

3.4.3. Effect of the increase of Ag oxidized states content and the regeneration of the photocatalyst

The production of ROS capable of inactivate *E. coli* was related to the oxidation of Ag^0 that led to the formation of Ag^+ and Ag^{2+} species, such ions are related to the bacteriostatic activity of silver [12]. Post-irradiation experiments showed an interesting performance of the Ag-TiO_2 sample in dark contact with *E. coli*. As observed, the UV treated Ag-TiO_2 sample increased its bacteriostatic activity (Fig 3.10a) in dark periods. Also, this dark contact promoted the photoactivity in a subsequent photocatalytic *E. coli* inactivation test done under visible light (Fig. 3.10b). For that reason, it is possible to suggest that during dark inactivation of *E. coli* the bacteria's outer membrane may act as electron donors regenerating the Ag^0 species needed for a further photoactivation and

production of ROS under visible light. This suggests that under dark periods, it is possible to regenerate the photoactivity of the Ag-TiO_2 photocatalyst lost by action of the UV irradiation. Probably, these suggested electron transferring processes may cause the oxidation of *E. coli*'s cell wall perhaps explaining its inactivation under dark.

3.5. Conclusions

TiO_2 was effectively modified using the hydrothermal synthesis to insert Ag in its structure. The presence of Ag successfully promoted the photocatalytic inactivation of *E. coli* in water under visible (Vis) light irradiation. Either light source; ultraviolet (UV) or Vis, used to evaluate the photocatalytic activity of the samples induced chemical transformations of the Ag particles in TiO_2 that directly affect the photocatalytic activity towards *E. coli* inactivation. UV pre-irradiation led to a total decrease of photoactivity in a subsequent visible light photocatalytic *E. coli* inactivation test. Such feature was related to the oxidation of Ag particles and the reduction of Ti^{4+} species in TiO_2, thus, reducing the beneficial interaction between Ag^0 and TiO_2, which seems to be responsible of the photoactivity under Vis irradiation. In addition, Ag oxidation decreases the photooxidation activity of the TiO_2 towards the photodegradation of dichloroacetic acid due to the consumption of holes to form Ag^+/Ag^{2+} species during UV irradiation.

Vis promoted the interaction between Ag^0 and TiO_2 in the fresh Ag-TiO_2 sample led to the formation of singlet oxygen and hydroxyl radical as determined by EPR spin trapping experiments using the spin trapping probe TMP-OH, such reactive oxygen species were responsible of total disinfection of water contaminated with high concentrations of the model biologic contaminant *E. coli* within short times and low irradiation powers.

Furthermore, post-irradiation events suggested that increased Ag oxidized states content potentiates the bacteriostatic action of Ag-TiO_2 in dark periods leading to *E. coli* inactivation due to the increase in Ag oxidized states content. But also, it was observed

that in-dark contact of the oxidized Ag-TiO_2 and *E. coli* possibly “bioregenerates” the photocatalyst promoting Vis light photoactivity lost under UV irradiation.

References

[1] O. Carp, C.L. Huisman, A. Reller, *Photoinduced reactivity of titanium dioxide*, Prog. Solid State Chem., 32 (2004) 33-177.

[2] J.M. Herrman, *Heterogeneous photocatalysis: fundamentals and applications to the removal of various types of aqueous pollutants*, Catal. Today, 53 (1999) 115-129.

[3] C.A. Castro-López, A. Centeno, S.A. Giraldo, *Fe modified TiO_2 photocatalysts for the oxidative degradation of reclacitrant water contaminants*, Catal. Today, 2010, doi:10.1016/j.cattod.2010.04.050

[4] J. Kiwi, C. Pulgarín, P. Peringer, M. Gratzel, *Beneficial effects of heterogeneous photocatalysis on the biodegradation of anthraquinone sulfonate observed in water-treatment*, New J. Chem., 17 (1993) 487-494.

[5] M.K. Seery, R. George, P. Floris, S.C. Pillai, *Silver doped titanium dioxide nanomaterials for enhanced visible light photocatalysis*, J. Photochem. Photobiol. A: Chem., 189 (2007) 258-263.

[6] K. Awazu, M. Fujimaki, C. Rockstuhl, J. Tominaga, H. Murakami, Y. Ohki, T. Watanabe, *A plasmonic photocatalyst consisting of silver nanoparticles embedded in titanium dioxide*, J. Am. Chem. Soc., 130 (2008) 1676-1680.

[7] B. Xin, L. Jing., Z. Ren, B. Wang, H. Fu, *Effects of simultaneously doped and deposited Ag on the photocatalytic activity and surface states of TiO_2*, J. Phys. Chem. B, 109 (2005) 2805-2809.

[8] O. Akhavan, E. Ghaderi, *Self-accumulated Ag nanoparticles on mesoporous TiO_2 thin film with high bactericidal activities*, Surf. Coat. Technol., 204 (2010) 3676-3683.

[9] J. Ye, N. Verellen, W.V. Roy, L. Lagae, G. Maes, G. Borghs, P.V. Dorpe, *Plasmonic modes of metallic semishells in a polymer film*, ACS Nano, 4 (2010) 1457-1464.

[10] A. Zielinska, E. Kowalska, J.W. Sobczak, I. Lacka, M. Gazda, B. Ohtani, J. Hupka, A. Zaleska, *Silver-doped TiO_2 prepared by microemulsion method: Surface properties, bio- and photoactivity*, Sep. Purif. Technol., 72 (2010) 309-318.

[11] D.R. Monteiro, L.F. Gorup, A.S. Takamiya, A.C. Ruvollo, E. Rodrigues, D. Barros, *The growing interest of materials that prevent microbial adhesion: antimicrobial effect of medical devices containing silver*, Int. J. Antimicrob. Agents, 34 (2009) 103-110.

[12] T. Yuranova, A.G. Rincon, C. Pulgarin, D. Laub, N. Xantopoulos, H. J. Mathieu, J. Kiwi, *Performance and characterization of Ag-cotton and Ag-TiO_2 loaded textiles during the abatement of E. coli*,. J. Photochem. Photobiol. A: Chem., 181 (2006) 363-369.

[13] H. Zhang, G. Wang, D. Chen, X. Lv, J. Li, *Tuning photoelectrochemical performances of Ag-TiO_2 nanocomposites via reduction/oxidation of Ag*, Chem. Mater., 20 (2008) 6543-6549.

[14] K. Kawahara, K. Suzuki, Y. Ohko, T. Tatsuma, *Electron transport in silver-semiconductor nanocomposite films exhibiting multicolor photochromism*, Phys. Chem. Chem. Phys., 7 (2005) 3851-3855.

[15] H.M. Gong, S. Xiao, X.R. Su, J.B. Hang, Q.Q. Wang, *Photochromism and two-photon luminescence of Ag-TiO_2 granular composite films activated by near infrared ps/fs pulses*, Optics Express, 15 (2007) 13925-13929.

[16] M.C. Biesinger, L.W. Lau, A.R. Gerson, R.S. Smart, *Resolving surface chemical states in XPS analysis of first row transition metals oxides and hydroxides: Sc, Ti, V, Cu and Zn*, Appl. Surf. Sci., 2010, doi:10.1016/j.apsusc.2010.07.086.

[17] Y.E. Nesmelov, D.D. Thomas, *Multibore sample cell increases EPR sensitivity for aqueous samples*, J. Mag. Reson., 178 (2006) 318-324.

[18] R. Romand, M. Roubin, J.P. Deloume, *ESCA studies of some copper and silver selenides*, J. Electron Spectrosc. Relat. Phenom. 13 (1978) 229-242.

[19] B. Xin, Z. Ren, H. Hu, X. Zhang, C. Dong, K. Shi, L. Jing, H. Fu, *Photocatalytic activity and interfacial carrier transfer of Ag-TiO_2 nanoparticle film*, Appl. Surf. Sci., 252 (2005) 2050-2055.

[20] Z.Y. Huang, G. Mills, B. Hajek, *Spontaneous formation of silver particles in basic 2-propanol*, J. Phys. Chem., 97 (1993) 11542-11550.

[21] V.K. Kaushik, *XPS core level spectra and Auger parameters for some silver compounds*, J. Electron Spectrosc. Relat. Phemon., 56 (1991) 273-277.

[22] O. Akhavan, *Lasting antibacterial activities of Ag-TiO_2/Ag/a-TiO_2 nanocomposite thin film photocatalysts under solar light irradiation*, J. Colloid Interf. Sci. 336 (2009) 117-124.

[23] F. Werfel, O. Brümmer, *Corundum structure oxides studied by XPS*, Phys. Scr., 28 (1983) 92-96.

[24] Y. Wang, N. Herron, *Nanometer-sized semiconductor clusters: materials synthesis, quantum size effects, and photophysical properties*, J. Phys. Chem., 95 (1991) 525-532.

[25] A. Babapour, O. Akhavan, A.Z. Moshfegh, *Physical characteristics of heat-treated nano-silvers dispersed in sol-gel silica matrix*, Nanotech., 17 (2006) 763-771.

[26] R. Konaka, E. Kasahara, W.C. Dunlap, *Ultraviolet irradiation of titanium dioxide in aqueous dispersion generates singlet oxygen*, Redox Rep., 6 (2001) 319-325.

[27] J.A. Rengifo-Herrera, K. Pierzchala, A. Sienkiewicz, *Abatement of organics and Escherichia coli by N,S co-doped TiO_2 under UV and visible light. Implications of the formation of singlet oxygen ($^1O_2$) under visible light*, Appl. Catal. B: Env., 88 (2009) 398-406.

[28] A. Sienkiewicz, B. Vileno, K. Pierzchala, M. Czuba, P.R. Marcoux, A. Graczyc, P.G. Fajer, L. Forró, *Oxidative stress-mediated protein conformation changes: ESR study of spin labeled Staphylococal nuclease*, J. Phys. Cond. Mat., 19 (2007) 1-13.

[29] K. Sato, K. Takeshita, J.I. Ueda, T. Ozawa, *Two reaction sites of a spin label, TEMPOL (4-Hydroxy-2,2,6,6-tetramethylpiperidine-N-oxyl), with hydroxil radical*, J. Pharm. Sci., 92 (2003) 275-280.

[30] P.K. Robertson, L.A. Lawton, B.J. Cornish, M. Jaspars, *Processes influencing the destruction of microcystin-LR by TiO_2 photocatalysis*, J. Photochem. Photobiol. A: Chem., 116 (1998) 215-219.

[31] C.S. Salazar, R.L. Romero, C.A. Martin, A.E. Cassano, *Photocataytic intrinsic reaction kinetics I: Mineralization of dichloroacetic acid*, Chem. Eng. Sci., 60 (2005) 5240-5254.

[32] R. Enriquez, P. Pichat, *Different net effect of TiO_2 sintering temperature on the potocataytic removal rates of 4-chlorophenol, 4-cholorobenzoic acid and dichloroacetic acid in water*, J. Environ. Sci. Health A, 41 (2006) 955-966.

[33] A. Romanyuk, P. Oelhafen, *Formation and electronic structure of TiO_2-Ag interface*, Sol. Energy Mater. Sol. Cells, 91 (2007) 1051-1054.

[34] Y. Zhang, K. Aslan, M.J. Previte, C.D. Geddes, *Metal-enhanced singlet oxygen generation: A consequence of plasmon enhanced triplet yields*, J. Fluoresc., 17 (2007) 345-349.

[35] N.V. Shcherbakov, A.N. Emel'yanov, E.V. Khaula, A.N. Il'ichev, M.V. Vishnetskaya, Y.N. Rufov, *Photo- and thermogeneration of singlet oxygen by the metal ions deposited on Al_2O_3 and SiO_2*, Russ. J. Phys. Chem., 80 (2006) 918-922.

[36] S. Xu, J. Shen, S. Chen, M. Zhang, T. Shen, *Active oxygen species ($^1O_2$, $O_2^{\bullet-}$) generation in the system of TiO_2 colloid sensitized by hypocrellin B*, J. Photochem. Photobiol. B: Biol., 67 (2002) 64-70.

[37] A.N. Romanov, Y.N. Rufov, V. Korchak, *Thermal generation of singlet oxygen ($^1\Delta_g O_2$) on ZSM-5 zeolite*, Mendeleev Commun., 10 (2000) 116-117.

[38] T.A. Dahl, Aquatic and Surface Photochemistry, First ed., CRC Press, Boca Raton, 1994.

[39] T.A. Dahl, *Direct exposure of mammalian cells to pure exogenous singlet oxygen ($^1\Delta_g O_2$)*, Photochem. Photobiol., 57 (1993) 248-254

[40] Z.Y. Cheng, Y.Z. Li, *What is responsible for the initiating chemistry of iron mediated lipid peroxidation: an update*, Chem. Rev., 107 (2007) 748-466.

[41] K. Hirakawa, T. Hirano, *Singlet oxygen generation photocatalyzed by TiO_2 particles and its contribution to biomolecule damage*, Chem. Letters, 35 (2006) 832-833.

[42] T. Okuno, H. Kawai, T. Hasegawa, H. Ueno, *Enhancement of hydroxil radical formation from superoxide anion radical in the presence of organic selenium compounds*, J. Health Sci., 47 (2001) 240-247.

4. Effect of transition metals on the TiO_2's photocatalytic and bacteriostatic activities

As previously presented, there is a latent discussion towards the action of metals inserted in the TiO_2's matrix. 25 years ago Mizushima *et al.* [1] proposed that metal iron impurities can trap e^- decreasing recombination, and thus, increasing the photoactivity of TiO_2. However, the paradigm of transition metal doping in TiO_2 photocatalysis is being replaced by a new generation of researchers pointing to the paradigm of plasmonics in photocatalysis, in which metal nanoparticles interact with visible light promoting photocatalytic enhancement by electronic transitions from the metal particles conduction band (CB) to the TiO_2 CB [2].

Analysis of the results, presented so far in this thesis, proportionate relevant information about the mechanisms of photoexcitation and activity of the TiO_2 modified with Fe and Ag. Diffusive reflectance spectroscopy (DRS) studies showed that Fe and Ag modifications induce different spectral responses in TiO_2, such as the induced absorption in the visible region. DRS spectrum is formed by absorption of the material causing electron transitions form a lower energy state to a higher one. Thus, important information to understand the action of the metal impurities in the electronic structure of the photocatalyst and their effect on the photoactivity can be obtained from such spectra.

Spectral analyses of Fe-TiO_2 materials, observed in Figs. 1.2 and 2.3, showed that Fe modification decreases the E_g of the TiO_2; even so, it promotes the recombination of the TiO_2's photogenerated e^- - h^+ pair. On the other hand, Ag did not change the slope decay of the absorption threshold of the TiO_2; thus indicating no reduction of the E_g. Nonetheless, Ag did enhanced TiO_2's photoactivity under visible light irradiation as observed in chapter 3.

Electronic structures and semiconductor features can be analyzed in order to go further in the understanding of the different spectral behaviors of Ag and Fe modified TiO_2 photocatalysts for photocatalytic applications, such as the *E. coli* photoinactivation and the photodegradation of azo dyes.

Fig. 4.1 shows a schematic energy spectrum in a metal versus a semiconductor. Filled and empty circles represent full and empty quantum states, two per level corresponding to the two spin orientations, as in an atom.

Fig. 4.1 Energy diagram of the electronic structures in metals and semiconductors.

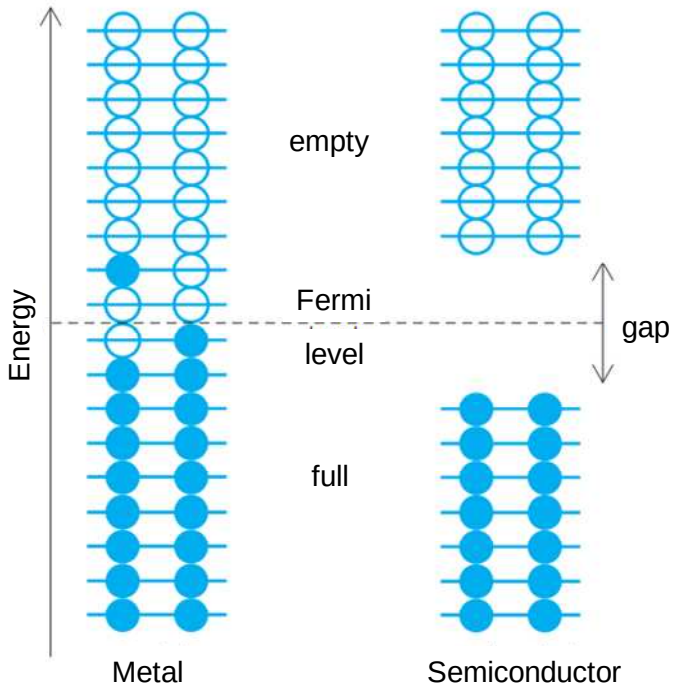

Source: The author.

Energy levels are infinitesimally close except at the Fermi level[4] of a semiconductor, which lies in the E_g, where there are no quantum states. The metal states are shown

[4] The *Fermi Energy* often denoted E_f or *chemical potential* in semiconductor physics is the energy at which there would be a fifty percent chance of finding an electron, if all energy levels were allowed.

with a filled state above the Fermi level and a vacant state, or hole, below the Fermi level, as it would happen under normal conditions at room temperature without light excitation. Semiconductors are likely to have a few excitations due to energy absorption. In such a non-excited state the conductivity would be close to zero. Therefore, in the context of conductivity and energy spectrum it is possible to explain the difference in photoexcitation and photoactivity mechanisms of the TiO_2 based photocatalyst modified with Fe and Ag.

Fig. 4.2 shows the proposed electron transitions occurring during UV-Vis irradiation of the Fe-TiO_2 and Ag-TiO_2 photocatalysts. It is well known that near UV promotes the transition of electrons form the VB to the CB of TiO_2. This first transition is observed for both irradiated materials and is responsible of the major absorption band observed in DRS analyses (Figs. 2.3 and 3.3) under irradiation between 280 to 380 nm.

In addition, for the Fe-TiO_2 photocatalyst, two more e^- transitions may explain the change in the TiO_2's DRS spectra promoted by the presence of Fe (Fig. 2.3). A second transition could occur from the new Fe^{3+} state or the Fe_2O_3's VB to the CB of TiO_2 surpassing the energy level of the CB of the Fe_2O_3. This transition requires light of lower energy level since the VB of the Fe_2O_3 is energetically located above the VB of the TiO_2. A general scheme of the configuration of the Fe-TiO_2 semiconductor is presented in Fig. 2.8. This process explains the decrease in the energy bandgap observed in DRS analyses of Fe-TiO_2 materials in chapters 1 and 2.

Furthermore, the increase in Fe concentration could have increased the Vis light absorption by more e^- transitions, thus, explaining the E_g decay due to the increased concentration of Fe. Finally, the third transition requires the lowest energy to promote electron transitions between d orbitals in Fe atoms giving rise to the shoulder-like peak in the DRS spectra (chapter 2).

Nevertheless, the experienced obtained in the development of metal modified TiO_2 in this thesis indicate that not all the electron transitions imply an increase of the photoactivity. In this case, Fe ionic states may act as a bridge for recombination of the electron-hole pair (chapter 3 and [3]); process even faster than their transfer to the reaction media for redox reactions to form reactive oxygen species (ROS) or induce direct oxidation [4].

Fig. 4.2 Energy diagram of the proposed electron transitions occurring during UV-Vis irradiation of the M-TiO_2 photocatalyst. M = Fe or Ag.

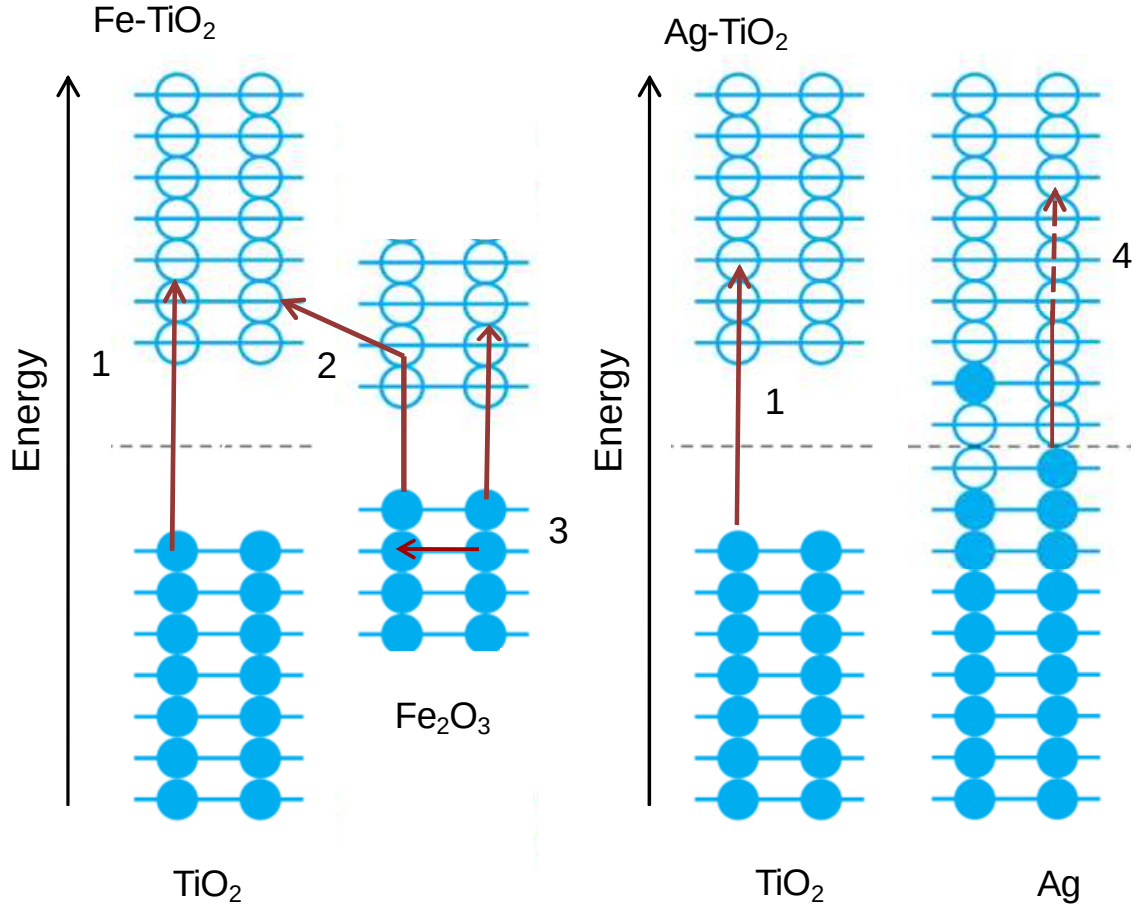

Source: The author.

In addition, promoted electrons to higher energy levels with lower energy requirements (transitions 2 and 3), may recombinate easier than those promoted in UV absorption

(transition 1) due to the tendency to return to their initial energy state and stabilize charges. Hence, electrons involved in transitions 2 and 3 have a reduced chance to participate in redox reactions in addition to the inhibition due to promoted recombinations.

Though, it was confirmed that the Fe^{3+}/Fe_2O_3-TiO_2 configuration enhances the electron acceptance from a sensitizing dye thus promoting photoactivity. This Fe promoted process is possible due to the new allowed energy state of Fe_2O_3 in Fe-TiO_2 which is lower than the TiO_2 CB; this is the CB of Fe_2O_3.

On the other hand, it was found a different and special configuration for the Ag-TiO_2 material. In this case, surface Ag particles are observed to be partially oxidized in XPS analyses of chapter 3. Moreover, a surface plasmon resonance effect (SPR) was observed for such Ag particles. In metal nanoparticles with sizes smaller than the wavelength of the incident light, as well as the optical penetration depth, all atoms in the particle can be collectively excited. Hence, this collective oscillations resonate with light and are therefore detectable as a pronounce absorption band in the visible or UV part of the spectrum [5]. Silver exhibits a particularly strong size-dependent optical response in the visible spectral range (1.8 to 3 eV) [5]. Therefore, these electrons are excited by an electromagnetic resonance (SPR effect) induced by absorption of Vis light. This effect promotes electrons to higher energy states than those observed for Fe_2O_3 due to absorption of light with low energy, and are represented as the fourth transition in Fig. 4.2. Consequently, photoactivity enhancement is observed when this SPR promoted electron is transferred to TiO_2. This assumption is in agreement to the proposed interaction between Ag^0 and TiO_2 (proposed in chapter 3) as responsible of such photoactivity enhancement.

Consequently, in our case it was possible to attribute the Ag-TiO_2 photoactivity to e^- transitions from the collective oscillations of the metallic particles to the TiO_2 CB. Probably, the injected electron may be located at different states in the TiO_2 CB thus

promoting the formation of singlet oxygen (-0.98 eV; $O_2/^1O_2$ [6]) and superoxide radical (-0.51 eV; $O_2/O_2^{\bullet-}$ [7]).

In addition, it was observed decay in photoactivity for the Ag-TiO_2 towards the photodegradation of dichloroacetic under UV irradiation (chapter 3), where Ag is not photoactivated. This process is due, not to the Ag ionic species, but to the Ag^0 species acting as electron donors to stabilize the TiO_2's photoproduced holes. Therefore, the metallic species were oxidized decreasing photoactivity.

Fe did not formed metallic species in the TiO_2 surface when inserted during hydrothermal synthesis. Probably, the oxidation state Fe^{3+}, from the salt precursor: $Fe(NO_3)_3$, was not reduced during the synthesis as it was possible with Ag^+, from $AgNO_3$, to form Ag^0. Thus, as increasing the oxidized state of the metal is more difficult to form metallic species in the surface of the photocatalyst and the formation of junction semiconductors is possible decreasing photoactivity by the increased recombination. Hence, transitions metals of groups I and II are suitable candidates to form such metallic species in the TiO_2's surface; indeed, these metals can be SPR excited under visible light irradiation [5, 8, 9].

In addition, transition metals, such as Au, Ag, and Cu are used in the manufacture of high value added products such as devices for antimicrobial applications due to their toxicity [10]. These metals, biocompatible with the outer membrane of microorganisms, cause a disruption of the respiratory chain and metabolism processes leading to the imminent cell death [10, 11]. This behavior was observed using Ag modified TiO_2 photocatalysts in dark contact with *E. coli*. The increased content of the Ag oxidized states on the Ag-TiO_2's surface was proved to be responsible of the decay in bacteria concentration in dark periods.

Additional experience with Cu loaded textiles (not reported here but available for lecture in [12][5]) showed that the oxidation states of Cu, such as Cu^{3+}, Cu^{2+}, and Cu^{+} are involved in the inactivation of bacteria in dark periods, as observed in *E. coli* deactivation tests and XPS analyses. Hence, photocatalyst loaded with transition metal ions present a bacteriostatic activity as an added value for the inactivation of microorganisms.

Research highlights

It is important to remark the contribution of this thesis to the knowledge of photocatalysts taking into account the presented analyses of the results of the modifications of TiO_2 using Ag and Fe and its effect on the photoactivity. First of all, it was proposed mechanisms of light activation and photoactivity of the TiO_2 when modified with Fe and Ag towards the photodegradation of Or-II and *the E. coli* photoinactivation, respectively. These mechanisms are new insights in the photocatalytic performance of the Fe and Ag modified photocatalysts, indeed, the details of charge transitions, indirectly analyzed using several photochemical reactions under irradiation of different light sources; has been not reported in literature until the results of this thesis were published.

Moreover, as far of our knowledge goes, the production of singlet oxygen and hydroxyl radical, had not been observed for suspensions of TiO_2 irradiated with visible light. Therefore, this thesis presents evidence of an effective increase of the TiO_2 light response into the visible spectrum using transition metals inserted in its matrix.

And finally, the results of the bacteriostatic activity of the metals inserted in to the TiO_2 matrix, and other metals such as Cu, not only corroborates the current literature reports of their bactericide properties, but indeed, contributes to the general knowledge of these materials applied to the photocatalytic disinfection of water.

[5] doi:10.1016/j.jphotochem.2010.06.030

Engineering of TiO_2 based photocatalyst for the photocatalytic inactivation of *E. coli* in water

The photocatalytic water disinfection process is determined by the oxidative action in the homogeneous phase of ROS species produced in the photocatalyst's surface. Therefore, in order to enhance TiO_2's photoactivity it is necessary to: i) increase the production of ROS, and, ii) promote the formation of ROS with longer half-life times and effective oxidative potential. ROS, such as, $^{\bullet}OH$, $HO_2^{\bullet}$, and $O_2^{\bullet-}$, produced in TiO_2 UV irradiation [4], have the potential to induce the lipid peroxidation that leads to the disruption of the wall's structural integrity with further lysis and death. In addition to the observed reactive species, singlet oxygen has a longer half-life time, as discussed in chapter 4, thus promoting photooxidation. Oxidative damage effects, of both $^{\bullet}OH$ and $^1O_2$, among the photoproduced ROS, are neither possible to be recovered by the regeneration process of the bacteria, nor to be stopped by the self-defense enzymatic mechanisms, such as, the catalase and peroxidase enzymatic systems, giving protection towards $HO_2^{\bullet}$ and $O_2^{\bullet-}$, attacks respectively.

To accomplish the purpose, TiO_2 can be modified inserting metallic particles with optical spectral response in the visible region (400 - 800 nm) that induce the formation of $^{\bullet}OH$ and $^1O_2$. Hydrothermal synthesis is a suggested route to form metal particles on the TiO_2's surface with such optical characteristics. One proposed metal is silver because of its interesting SPR that generates electronic interaction with TiO_2. Other metals could enhance photoactivity due to their SPR effect in the Vis region, such as, gold [8] and platinum [9].

In addition, the concentration of the modifying metal can be tailored to achieve the maximum photoactivity without surpassing the concentration in which the formation of recombination centers is promoted.

Finally, since the metal-hydrothermally modified TiO_2 is extremely sensitive to light irradiation, materials should be kept in suitable containers protected from day light due to deactivation processes, in which, the metallic active species are oxidized by the photogenerated holes in TiO_2. As observed here, regeneration processes are possible when promoting a reduction of the oxidized surface; nevertheless, such processes need further investigations. Moreover, transition metal ions were found to be bacteriostaticly active in dark periods. Such performance can be exploited to increase the oxidation potential of the photocatalyst towards the inactivation of microorganisms in water.

General Conclusion

It is possible to increase the TiO_2 photocatalytic activity using transition metals, sensitive to visible light irradiation, located in their metallic state on the surface of the photocatalyst and that may promote electron transitions to the TiO_2. Such transitions promote the formation of more ROS species with higher quality for oxidation processes, such as $^{\bullet}OH$ and $^1O_2$, leading to a faster inactivation of microorganisms in water.

References

[1] K. Mizushima, M. Tanaka, S. Lida, *Energy levels of iron group impurities in TiO_2*, J. Phys. Soc. Jpn., 32 (1972) 1519-1524.

[2] P. Zolotavin, E. Permenova, O. Sarkisov, V. Nadtochenko, R. Azouani, P. Portes, K. Chhor, A. Kanaev, *Two-photon luminescence enhancement of silver nanoclusters photodeposited onto mesoporous TiO_2 film*, Chem. Phys., Lett. 457 (2008) 342-346.

[3] B. Xin, Z. Ren, P. Wang, J. Liu, L. Jing, H. Fu, *Study on the mechanisms of photoinduced carriers separation and recombination for the Fe^{3+}-TiO_2 photocatalysts*, Appl. Surf. Sci., 253 (2007) 4390-4395.

[4] O. Carp, C.L. Huisman, A. Reller*, Photoinduced reactivity of titanium dioxide*, Prog. Solid State Chem. 32 (2004) 33-177.

[5] G. Ritchie, E. Burstein, R.B. Stephens, *Optical Phenomena at a silver surface submicroscopic bumps*, J. Opt. Soc. Am. B, 2 (1985) 544-551.

[6] C. Schweitzer, R. Schmidt, *Physical mechanics of generation and deactivation of singlet oxygen*, Chem. Rev., 103 (2003) 1685-1757.

[7] M. Gratzel, *Energy resources through photochemistry and catalysis*, First ed., Academic Press Inc., New York, 1983.

[8] T.A. El-Brolossy, T. Abdallah, M.B. Mohamed, S. Abdallah, K. Easawi, S. Negm, H. Talaat, *Shape and size dependence of the surface plasmon resonance of gold nanoparticles studied by photoacoustic technique*, Eur. Phys. J. Special Topics, 153 (2008) 361-364.

[9] R.C. Johnson, J. Li, J.T. Hupp, G.C. Schatz, *Hyper-Rayleigh scattering studies of silver, copper, and platinum nanoparticle suspensions*, Chem. Phys. Lett., 356 (2002) 534-540.

[10] D.R. Monteiro, L.F. Gorup, A.S. Takamiya, A.C. Ruvollo, E. Rodrigues, D. Barros, *The growing interest of materials that prevent microbial adhesion: antimicrobial effect of medical devices containing silver*, Int. J. Antimicrob. Agents, 34 (2009) 103-110.

[11] K.B. Holt, A.J. Bard, *Interaction of siler (I) with the respiraorio chain of Escherichia coli: an electrochemical and scanning electorchemical microscopy stuy of the antimicrobial mechanism of micromolar* Ag^{+}, Biochem., 44 (2005) 13214-13223.

[12] C.A. Castro, R. Sanjines, C. Pulgarin, P. Osorio, S.A. Giraldo, J. Kiwi, *Structure-reactvity relations for DC-magnetron sputtered Cu-layers during E. coli inactivation in the dark and under light*, J. Photochem. Photobiol. A: Chem., 2010, doi:10.1016/j.jphotochem.2010.06.030.

Publications

Peer reviewed journals

- *Evaluación de la degradación fotocatalítica de E. coli con TiO_2 modificado en sistemas tipo SODIS*.
  Camilo A. Castro, Alba Arámbula, Aristóbulo Centeno, Sonia A. Giraldo
  Información Tecnológica, 20 (2009) 29-36.

- *Fe-modified TiO_2 photocatalysts for the oxidative degradation of recalcitrant water contaminants*.
  C.A. Castro-López, A. Centeno, S.A. Giraldo
  Catalysis Today, 157 (2010) 119-124.

- *Effect of the synthesis variables on the TiO_2's photocatalytic activity towards the degradation of water pollutants.*
  Camilo Andrés Castro López, Sonia Reyes, Aristóbulo Centeno, Sonia Azucena Giraldo.
  Accpeted for publication in: Revista Facultad de Ingenería de la Universidad de Antioquia, 2010.

- *Structure-reactivity relations for DC magnetron sputteres Cu-layers during E. coli inactivation in the dark and under light*.
  C.Castro, R. Sanjines, C. Pulgarin, P. Osorio, S.A. Giraldo, J. Kiwi
  Journal of Photochemistry and Photobiology A: Chemistry, 216 (2010) 295-302.

- *Role of silver in the mechanisms of light excitation and Ag-TiO_2 performance towards the photoinactivation of E. coli in water*.
  Camilo A. Castro, Paula Osorio, Andrzej Sienckiewicz, Cesar Pulgarin, Aristóbulo Centeno, Sonia A. Giraldo.
  Submitted to Applied Catalysis B: Environmental. Manuscript number: APCAT-D-10-00960

- *Iron promotion of the TiO_2 photosensitization process towards the photocatalytic oxidation of azo dyes under solar-simulated light irradiation*.
  Camilo A. Castro, Aristóbulo Centeno, Sonia A. Giraldo.
  In preparation for submision in: Colloids and Surfaces A: Physicochemical and Egineering Aspects.

- *Estudio cinético de la desinfección foocatalítica de agua contaminada con E. coli: Efecto de la concentración del fotocatalizador y la potencia de irradiación*.
  Andrea L. Moreno, Camilo A. Castro, Aristóbulo Centeno, Sonia A. Giraldo.
  Submitted to. Información Tecnológica.

- *Influencia de la composición química del agua sobre su desinfección fotocatalítica.*
  Carlos Romero, Oscar Salazar, Camilo A. Castro, Aristóbulo Centeno, Sonia A. Giraldo.
  Submmitted to: U.D.C.A. Actualidad y Divulgación Científica

Scientific Events

Oral presentations

- *Efectos causados por tratamientos fotocatalíticos con TiO_2 sobre la E. coli.*
  Camilo A. Castro, Andrea Moreno, Alba L. Arámbula, Giovanna Rincón, Aristóbulo Centeno, Sonia A. Giraldo.
  II Simposio Latinoamericano de Procesos Avanzados de Oxidación y sus combinaciones con otros procesos (II SILAPAO), 27-28 de Noviembre de 2008, Medellín, Colombia.

- *Fijación de TiO_2 sobre polietilentereftalato y polietileno lineal de baja densidad y su evaluación en la degradación fotocatalítica de Orange II*.
  Camilo A. Castro, Elizabeth Rueda, Alexander Diaz, Aristóbulo Centeno, Sonia A. Giraldo.
  II Silapao, November 27-28, 2008, Medellín, Colombia.

- *An efficient Fe modified TiO_2 photocatalyst for the oxidative degradation of recalcitrant water contaminants*.
  C.A. Castro, A. Centeno, S.A. Giraldo
  6th World Congress on Oxidation Catalysis (6^{th} WCOC), July 5 -10, 2009, Lille, France.

- *Evaluación del efecto de las varables de síntesis de TiO_2 en fase líquida sobre su fotoactividad.*
  Sonia Reyes, Camilo Castro, Aristóbulo Centeno, Sonia A. Giraldo.
  VI Simposio Colombiano de Catálisis, October 28-30, 2009, Medellín, Colombia.

- *Implicaciones de la fotooxidación de azo colorantes frente a la del fenol cuando se utiliza TiO_2 dopado y codopado con Fe y/o Ag como fotocatalizador*.
  Castro Camilo, Centeno Aristóbulo, Giraldo Sonia A.
  XXII Congreso Iberoamericano de Catálisis (XXII CICAT), September 5-10, 2010, Viña del Mar, Chile.

Poster communications

- *Evaluación de la degradación heliofotocatalítica de Escherichia coli con TiO_2 modificado en sistemas tipo SODIS*.
  Castro L. Camilo, Centeno Aristóbulo, Arámbula Alba L., Giraldo Sonia A.
  XXI Simposio Iberoamericano de Catálisis (XXI SICAT), June 22-27, 2008, Málaga, Spain.

- *Development of heliophotocatalytic technologies for the production of drinkable water.*
  Castro Camilo, Centeno Aristóbulo, Pulgarín Cesar, Giraldo Sonia A.
  EPFL-UNESCO Chair International Scientific Conference on Technologies for Development, February 8-10, 2010, Lausanne, Switzerland.

- *Influencia de los iones $(HCO_3)^-$, Cl^-, $(SO_4)^{2-}$, $(HPO_4)^{2-}$ sobre la desinfección fotocatalítica de agua.*
  Carlos F. Romero, Oscar M. Salazar, Camilo A. Castro, Aristóbulo Centeno, Sonia A. Giraldo.
  XXII CICAT, September 5-10, 2010, Viña del Mar, Chile.